Enzyme and Directed Evolution Technologies

For Nerve Agent Neutralisation

by Luis Briseño-Roa

Medical Research Council

Centre for Protein Engineering.

Supervisor: Professor Sir Alan R. Fersht, FRS

A dissertation submitted to the University of Cambridge in Candidature for the degree of Doctor of Philosophy

Gonville and Caius College, Cambridge,
July 2005.

To my parents Cristina and Luis,

to my sister Julieta

Declaration of Originality

This dissertation is the result of my own work and does not include material from collaboration unless specifically stated.

This thesis has not been submitted, and is not currently being submitted, for any other degree or qualification at any academic institution.

In accordance with the Copyright, Design and Patents Act, 1988, copyright ownership is retained by me.

Luis Briseño-Roa

Cambridge, July 2005.

Abstract

Owing to the magnitude of the utilisation of organophosphorus (OPs) insecticides and the possibility of using OPs nerve agents (NA) against civilian populations, the research and development of enzymes involved in the biotransformation and detoxification of OPs has attracted considerable attention in recent years.

A number of enzymes have been identified that can catalyse the hydrolysis of OPs, including nerve agents. Two of the best characterised are *Pseudomonas diminuta* phosphotriesterase (PTE) and PON1, a mammalian member of the Serum paraoxonase (PONs) family. These enzymes have excellent catalytic properties towards some OPs, but relatively poor activities against others. It has been possible to alter PTE substrate specificity by rational site-mutagenesis, but with little improvements on the wild-type rates. A more successful approach has been the application of directed-evolution strategies.

The aim of the present work has been to create variants of PTE with an increased catalytic efficiency towards OPs nerve agents. To this end, a directed-evolution platform was developed to enable screening for organophosphatase activity. This methodology relies on the screening of *Escherichia coli* colonies transformed with PTE-variant libraries.

Twelve fluorogenic NA analogues, with a 3-chloro-7-hydroxy-4-methylcoumarin leaving group, were tested for suitability as substrates for PTEs and PON1. Included in this series were analogues of the pesticides Paraoxon and Parathion, and the chemical warfare agents DFP, Dimefox, Tabun, Sarin, Cyclosarin, Soman, VX, and Russian-VX . These chemical surrogates have a similar structure but do not share the same physico-chemical properties as the nerve agents themselves.

The directed evolution platform developed and used consisted of two parts. First, partially lysed *Escherichia coli* colonies were screened using the fluorogenic nerve agents analogues as probes. Second, the selected (positive) clones were grown in microplates filled with liquid medium, and their organophosphatase activity was measured *in vivo.*

Several gene libraries were synthesised in each of which four codons of the residues forming PTE's substrate binding site were selectively randomised. The PTE

variant S5a was used as template for the libraries, as it expresses at 20-fold higher level than the wild type, in bacterial hosts, while retaining its kinetic properties for the *wild-type* substrate, Paraoxon. These libraries were screened using analogues of Russian-VX and Parathion as probes; approximately 10^6 clones were screened in total. The twenty most active variants, as determined *in vivo*, were expressed, purified, and their kinetic parameters for Paraoxon and the NA analogues were determined.

PTE-S5a itself hydrolysed 8/VX, 9/Sarin and 10/Russian-VX analogues between 2.5 and 3.5 times more readily than PTE-wt. In contrast, towards 11/Soman and 12/Cyclosarin analogues its activity, was only 70% of that of the wild type enzyme.

Three of the selected clones, PTE -A (I106T), C (I106L), and H (I106T/F132V/S308A/Y309W), exhibited a higher k_{cat} than PTE-S5a towards Paraoxon. The latter exhibited a 5-fold increased in its turnover rate (31,016 s^{-1}); this rate is higher than that of the *in vitro* evolved PTE-H5 (26,294 s^{-1}).

PTE variants A (I106T), C (I106L), D (I106A/F132G), E (I106V/F132L), and F (I106L/F132lG) exhibited between 2 and 4-fold increases in their k_{cat}/K_M towards the Paraoxon analogue relative to PTE-S5a. Variants Q (G60V/I106L/ S308G), S (G60V/I106M/L303E/S308E), and T(G60V/I106S/L303P/S308G) showed between 2 and 14-fold improvements in their activities towards Russian-VX, Soman and Cyclosarin analogues. The selectivity for this latter group towards phosphonate NA analogues increased up to 10^7-fold, relative to the wild type PTE.

Each PTE monomer binds two divalent transition metal ions via a cluster of four histidines (His-55, His-57, His-201 and His-230) and one aspartate (Asp-301). In addition, the two metal ions are linked together by a carbamate functional group, formed by the carboxylation of the ε-amino group of Lys-169 and a water (or hydroxide ion) from the solvent. A case study is presented in which using both site-directed mutagenesis and directed evolution strategies, the possibility of replacing the carboxylated lysine (Lys-169) by any other residue was assessed.

To understand the significance of the Great Recitation … one must have lived at Fez, a city of learning which seems to have been constructed around the schools…when one is pronounced ready for the Great Recitation by the schoolmaster, one immediately passes from childhood to man's estate, from anonymity to fame.

Amin Maalouf, 1986. Leo The African.

Acknowledgements

The words in this dissertation are entirely my responsibility, nevertheless the insights and ideas belong mostly to other people. I would like to acknowledge those who so generously shared their thoughts and experience with me, not only regarding this dissertation but all through my training at the MRC Centre for Protein Engineering.

My supervisor Sir Alan R. Fersht, for his unconditional support and advice; Dr. Andrew Griffiths (MRC Laboratory of Molecular Biology), who patiently guided me through the thorny subject of directed evolution. Caroline Blair for thoroughly proof-reading this thesis. Dr. Zoryana Oliynick, whose suggestions contributed to the setting up the screening system. Dr. Tobias Janowitz for the fruitful discussion. Dr. Nuria Sanchez-Puig for her precious advice on protein purification. Dr. Pia Sondergeld for her patient support and reliability. Dr. Richard Weinberg, for the inspiring explanations on chemical mechanisms, protein purification, and wine tasting. Mrs. Linda Judd for preparing the media and plates. Dr. Andreas Joerger for his guidance regarding the crystallisation studies.

The Gates Cambridge Trust and the Overseas Research Student award scheme for their financial support.

Dr. Christopher M. Timperley from the Defence Science and Technology Laboratory (Porton Down, UK), for supplying the fluorogenic analogues and his invaluable advice on the chemistry of organophosphorus compounds.

Dr. Bernard Kelly, Dr. Jeremy Agresti, and Dr. Richard Williams (Griff's crew); for their generous help during the library construct and emulsion selections. Dr. Dan Tawfik, for providing the mammalian serum paraoxonases (PON), and his crew from the Weizmann Institute (Israel): Dr. Leonid Gaydukov for his help and advice during the PON purification, Cintia Roodveldt for her insights into bacterial selection and for finding PTE variant S5a, and Dr. Stephen Gould for his precious insights into

bacterial selection. Luis Olguin (Dept. of Biochemistry, University of Cambridge) for his advice on bacterial selection.

Dr. Stacey Rutledge for proof-reading this thesis, and helpful discussions. Fiona Sait for proof-reaing this thesis. Dr Fiona Townsley for helpful discussions. Dr. Giovanni Settanni for his help with the statistical analysis. Dr. Dimitry Veprintsev for designing and providing the software used in the data analysis. Dr. Stephan Rüdiger and Dr. Mark Allen for their help and advice on the protein purification. Dr. Stefano Gianni and Dr. Per Jemth for sharing the secrets of the pre-steady state kinetics trade. Dr. Chris Johnson for his help with physicochemical measurements and instrumentation. Dr. Trevor Rutherford, Dr. Heather Petoh and Dr. Jose Perez Candillas for their patient explanations of NMR. Past and present members of the Centre for Protein Engineering (UK): Tony, Charo, Sebastian, Roberto, Sue, Satoshi, Hwee Ching, Grace, Jade, Charles, Tim, Neil, Clara, Ugo. Paula Murphy and Andrew Northrop, for their friendly and efficient help.

Prof. Francis H. Arnold, Dr. Alexey Murzin, and Prof. Simon Conway-Morris; for their insight into the fields of directed evolution, protein structure, and natural evolution.

I would like to thank again Fernando Díaz de la Serna, for his kind support and words advice. All the members of the families Briseño and Roa for their kind support.

I would like to take the opportunity to thank my friends for their support during the last years: Maruxa, Carlos, Roberta, Omar, Silvia, Elsa, David, Thomas, Nathalie, José Antonio, Anna Laura, Elena, Garret, Natalia, Ignacio, Silvia, Orla, Alejandra, Kristin, Enrico, Casandra, Alejandro, members of the former 5 Westland Terrace community, present and past members of Darwin College basketball team, and members of the Gates Student Council 2002 – 2003, in particular to Dr. Rob Perrons. Also to Victor Manuel, Maika, Gabriel, Lorenza, Juan, Carlos, Isabel, Bárbara, Liliana, Javier. To my life-long friends Santiago, Andrés, and Jaime for their precious support and advice.

Katia for her caring support.

I am most grateful to my sister Julieta. Her courage and support permeate every word that has been written in this dissertation. Gracias por todo mi Julis!

I will never be eloquent enough to express how much I owe my parents. In particular, during the time I have spent in Cambridge, their support and altruism has been overwhelming, despite the sometimes seemingly abysmal distance that physically separated us. Gracias *má*! gracias *chif*!

Finally, I thank myself, for enduring and pushing this work through.

Cambridge, UK.

Table of Contents

Abstract iv
Acknowledgements vii
Table of Contents x
Chapter 1 Introduction 1
1.1 Enzymes 1
1.1.1 Enzyme structure 2
1.1.2 Enzyme kinetics 4
1.1.3 Enzyme engineering 10
1.2 Organophosphorus Compounds (OPs) 14
1.2.1 OPs structure 14
1.2.2 OPs as nerve agents (NAs) 14
1.2.3 NA legislation and NA attacks 18
1.2.4 Organophosphatases 19
1.3 Phosphotriesterase *Pseudomonas diminuta* (PTE) 19
1.3.1 Structure of PTE 20
1.3.2 PTE metal binding site 21
1.3.3 PTE reaction mechanism 23
1.3.4 PTE Substrate binding site 23
1.3.5 Biotechnological applications of PTE 27
1.4 Serum Paraoxonases (PONs) 28
1.4.1 Structure and mechanisms of PON1 29
1.4.2 Directed evolution of PON1 substrate selectivity 30
1.5 General aim 30
Chapter 2 Materials and Methods 32
2.1 Microbiology 32
2.1.1 Materials 32
2.1.2 Methods 34
2.2 DNA Biochemistry (Molecular Biology) 39
2.2.1 Materials 39
2.2.2 Methods 45
2.3 Protein Biochemistry 51

2.3.1 Materials 51
2.3.2 Methods 53
2.4 Organophosphorus (OP) chemistry 59
2.4.1 Safety Measures 59
2.4.2 Materials 59
2.4.3 Methods 60
2.5 Bioinformatics 60
2.5.1 Materials 61
Chapter 3 Hydrolysis of Fluorogenic Nerve Agents Analogues by Organophosphatases 62
3.1 Introduction 62
3.2 Results 63
3.2.1 Protein production, purification, and quantification 63
3.2.2 k_{cat} and K_M for Paraoxon 65
3.2.3 k_{cat} / K_M for nerve agents analogues 66
3.3 Discussion 68
Chapter 4 Screening Platform for Organophosphatases Using Fluorogenic Substrates 71
4.1 Introduction 71
4.2 Results 72
4.2.1 Colony fluorescence 72
4.2.2 Quantification of Activity 77
4.3 Discussion 79
Chapter 5 Selection using Nerve Agent Analogues as Probes 82
5.1 Introduction 82
5.1.1 Neutralisation of NAs 82
5.1.2 Enzyme promiscuity 83
5.1.3 Classification of NA Analogues 83
5.2 Results 84
5.2.1 Library design 84
5.2.2 Library Construction 86
5.2.3 Screening using 10/Russian-VX and 2/Parathion analogues 92
5.2.4 Determination of kinetic parameters 95

5.3 Discussion 104
5.3.1 Library construction bias 104
5.3.2 Screening 104
5.3.3 Kinetic properties of PTE-S5a 105
5.3.4 Kinetic parameters of the selected PTE variants 105
5.3.5 Activity towards Nerve Agents 108
5.3.6 Relationship between selectivity and activity 109
5.3.7 Improvements in activity relative to PTE-wt 109
5.3.8 Changes in the activity towards wild-type substrate 109
Chapter 6 Replacement of Lys-169 in PTE Metal Binding Site 111
6.1 Introduction 111
6.1.1 Metal binding via carboxylated lysines 111
6.1.2 Protein Homologue to PTE from *Escherichia coli* (ePHP) 112
6.2 Results 114
6.2.1 PTE-like family multiple alignment 114
6.2.2 Design of point mutants 116
6.2.3 Construction of mutants by directed mutagenesis. 116
6.2.4 Determination of activity *in vivo* 117
6.2.5 Refolding 119
6.2.6 Library design 120
6.2.7 Library construction 121
6.2.8 Library screening 123
6.2.9 Metal binding mutants purification 126
6.2.10 Metal binding variants k_{cat} and K_M towards Paraoxon 126
6.3 Discussion 127
6.3.1 PTE-like family 127
6.3.2 Replacement of Lys*169 by Glu 128
6.3.3 Selection of libraries 128
Conclusions and Future Work 130
Conclusions 130
Future Work 131
Supplementary Information 133
References 141

Chapter 1 Introduction

1.1 Enzymes

In nature, enzymes are responsible for catalysing and controlling most of the chemical reactions involved in the biological metabolism. Their spectacular efficiency and versatility has allowed life to permeate into almost every microenvironment on the planet. Two examples of enzymes, occurring in the nature today, can be used to highlight their importance in life processes.

The neurotransmitter, acetylcholine, spontaneously degrades to its constituents, acetate and choline, over approximately 3 years ($t_{1/2}$) [1]. In the presence of the enzyme, acetylcholine esterase (AchE), the same reaction takes place in less that 0.1 milliseconds (Harel, Schalk et al. 1993). This 10^9-fold acceleration, permits careful control of the size and duration of the postsynaptic potential in the synaptic clefts.

Pyrococcus furiosus is a hyperthermophile that inhabits continental and submarine hydrothermal systems worldwide, where it growths (optimally) at high temperatures (100 °C) and pressures (3 bar) (Lloyd 1999). *P. furiosus* citrate synthase (CS), an enzyme that synthesises citrate from oxaloacetate and acetyl-CoA in the Tricarboxylic acid cycle, is structurally identical to the CS isolated from an Antarctic bacterium DS2-3R (Russell, Ferguson et al. 1997) (Russell, Gerike et al. 1998). This implies that both enzymes share the same ancestor capable of adapting to two extreme thermal conditions (Arnold, Wintrode et al. 2001).

AchE highlights the impressive catalytic power of enzymes; *P. furiosus* CS, their adaptability. Precisely because of these properties, amongst others, there is a great deal of interest in enzyme-derived technology.

1 Time at which half of the reaction has proceeded.

1.1.1 Enzyme structure

Enzymes are proteins [2] and, as such, linear polymers of amino acids linked by peptide bonds into a specific sequence. The peptide bonds are formed via a dehydration synthesis reaction between the carboxy group of the first amino acid (C'_i) with the amino group of the second amino acid (N_{i+1}). There are twenty amino acid in the standard repertoire of the cell, and given subsequent post-translational modifications (phosphorylation, methylation, glycosylation, etc.), and addition of cofactors and prosthetic groups (metal ions, flavin, riboflavins, heme groups, etc.), enzymes have approximately 200 chemical groups available to be use by enzymes (Smith 2000); it has been conservatively estimated that in eukaryotes more than ten distinct mature protein molecule species are generated from every genetically encoded polypeptide chain (Kent 2004).

Although it has been found that some functional proteins [3] lack folded structure under physiological conditions (Tompa 2002), the polypeptide chains of all known active enzymes exhibit a well defined structure. This structure is reached by the folding of the polypeptide chain in what can be roughly describe as a hierarchical folding assembly. The primary structure, or assembly, is defined by the amino acid sequence itself, without regard to any of its possible spatial arrangements.

1.1.1.1 Secondary structure

To define the secondary structure it is necessary to review the nature of the peptide bond. The polypeptide chain has three degrees of freedom per residue (dihedral angles): the twist about the $N_i - C^{\alpha}_i$ bond axis (ϕ), that about the $C^{\alpha}_i - C'_i$ axis (ψ), and the one about $C'_i - N_{i+1}$, the peptide bond (ω). The peptide bond however, is effectively planar given the significant delocalisation of the lone pair of electrons of the nitrogen onto the carbonyl oxygen. This partial double-bonded character allows only values of $\omega = 0°$ (*cis*) or $180°$ (*trans*), with a 75 – 90 kJ/mol (18 – 21 kcal/mol) energy barrier between the two configurations. Owing to steric hindrance, the *trans*

2 Those constituted by RNA, or mixture of both, can be classified as riboenzymes.

3 The role of these natively unfolded proteins involves regulatory activities without intrinsic enzymatic properties.

conformation is much more populated than the *cis* (999:1). This holds true for all residues except proline, for which the ratio can be as high as 7:3. Steric restrictions also apply to ϕ and ψ angles; the conformation space that is accessible to ϕ and ψ, can be represented by a two-coordinate vector (ϕ, ψ) known as Ramachandran space.

Secondary structure then, refers to the arrangements of the polypeptide chain into a relatively regular hydrogen bonded structures, which maps to specific regions of the Ramachandran space. There are mainly two such structures: the α-helix (– 57, – 47) in which the C_i=O group makes a hydrogen bond with N_{i+4}H, the C=O groups lying parallel to the axis of the helix and the side chains of pointing away from it; and β-sheet (–119, +113), in which parallel or antiparallel extended polypeptide chains make hydrogen bonds between the C=O groups of one and NH of the other. The side chains in this case, alternate on opposite sides of the sheet. There are a few other secondary structures such as loops and 3_{10}-helices that will not be described here (Fersht 1999).

1.1.1.2 Supersecondary structure

The next level in the structural hierarchy are the motifs, or supersecondary structures, these being common combinations of regions of secondary stucture. Classic units of supersecondary structure include the β-β unit, two antiparallel strands connected by a hairpin; and the β-α-β unit, two parallel strands separated by an antiparallel alpha-helix, with 2 hairpins connecting the three secondary structures. Further *up* in the hierarchy are the domains. These are independent units of folding that frequently have discrete biological function in their own right (DNA-binding homeodomains).

1.1.1.3 Tertiary and Quaternary Structure

Tertiary structure can be defined as the three-dimensional configuration of the entire folded polypeptide chain. This results from interactions between residues, secondary structured regions, motifs, and domains separated prior to the folding process. Quaternary structure refers to the spatial arrangement of the subunits composed of different polypeptide chains (Branden and Tooze 1991).

1.1.1.4 The α/β-barrel fold

The canonical α/β-barrel fold is defined by a close ring of eight parallel β-strands surrounded by eight α-helices (Reardon and Farber 1995). The active sites of all α/β-barrel enzymes are at the C-terminal end of the barrel, and are formed by residues of the eight loops connecting each β-strand with the α-helix following it (β/α loops) (Wierenga 2001). Besides their key role in catalysis, the β/α loops are important in forming hetero-oligomeric structures (Pujadas and Palau; 1999). In fact, most of the known α/β-barrel enzymes form quaternary structures.

Electrostatic calculations have highlighted a common, distinctive electrostatic field pattern determined predominantly by the backbone atoms, which generates a positive potential at the C-terminal end of the barrel near the active site region (Raychaudhuri, Younas et al. 1997). This correlates with the known preference of α/β-barrel enzymes for negatively charged substrates, in particular phosphate-containing molecules (Copley and Bork 2000).

The α/β-barrel fold is one of the most common in enzymes, with about 10% of structurally characterised proteins containing at least one domain with this fold (Gerlt and Raushel 2003). It is seen in many different enzyme families, catalysing completely unrelated reactions (Hegyi and Gerstein 1999). Because the α/β-barrel fold was first described in triosephosphate isomerase (TIM), it is also referred to as the TIM barrel fold (Banner, Bloomer et al.; 1975).

Proteins with α/β-barrel structures are very stable, and are, therefore, suitable for protein engineering studies (Luger, Hommel et al. 1989; Mainfroid, Goraj et al. 1993; Tanaka, Kimura et al. 1994; Lang, Thoma et al. 2000; Silverman, Balakrishnan et al. 2001).

1.1.2 Enzyme kinetics

Chemists have been studying rates of reactions, and the factors that control them, since the middle of the 19th century. Measuring the rate of fermentation of sucrose in the presence of yeast, the British chemist, Adrian John Brown, found that the reaction

rate was independent of the amount of substrate present (Brown 1892). He suggested that this could be explained if the invertase [4] molecules present in yeast formed a complex with the sucrose (Brown 1902; Laidler 1997).

1.1.2.1 Michaelis-Menten model

Leonor Michaelis and his assistant Maud Leonora Menten observed that the effect noticed by Brown was only present at high concentrations of substrate, whereas at low concentrations the rate became proportional to the concentration of substrate (Michaelis and Menten 1913; Laidler 1997). To explain this phenomenon, the kinetic consequences of the enzyme-substrate complex were considered in the model

$$E + S \xleftrightarrow{K_M} ES \xrightarrow{k_{cat}} E + P \qquad \textbf{Scheme 1}$$

where E, S and P are the enzyme, substrate, and product molecules respectively.

Assuming that the first step exists in a rapid and reversible equilibrium,

$$K_M = \frac{[E][S]}{[ES]} \qquad \textbf{- 1}$$

that the chemical process occurs in the second step,

$$v = k_{cat}[ES] \qquad \textbf{- 2}$$

and that the total enzyme concentration remains constant,

$$[E]_O = [E] + [ES] \qquad \textbf{- 3}$$

the Michaelis-Menten model can be describe with the following expression

4 Now known as β-fructofuranosidase.

$$v = \frac{[E]_O[S]k_{cat}}{K_M + [S]} \qquad \textbf{- 4}$$

Other assumptions to be considered are that the concentration of enzyme is negligible compared with that of the substrate ([E] << [S]), that the reaction is measured before the concentration of product becomes significant ([P] ≈ 0) and that the substrate has not been appreciably depleted ([S] = $[S]_O$).

In a Michaelis-Menten system, the velocity is at a maximum (V_{max}) when all the enzyme is in complex with the substrate ([ES] ≈ $[E]_O$). From here it can be inferred that

$$\text{if } v = ½\, V_{max} \Rightarrow [S] = K_M \qquad \textbf{- 5}$$

consequently, if [S] << K_M

$$v = \frac{k_{cat}}{K_M}[E]_O[S] \qquad \textbf{- 6}$$

This equation describes the linear correlation between k_{cat}/K_M and [S], given a fixed amount of enzyme. Since most of the enzyme is free of substrate molecules ($[E]_O \approx$ [E]), equation 6 can be rewritten as

$$v = \frac{k_{cat}}{K_M}[E][S] \qquad \textbf{- 7}$$

an expression that defines the velocity in terms of free enzyme and free substrate. In this case, k_{cat}/K_M emerges as an apparent second-order rate constant.

1.1.2.2 Extending Michaelis-Menten to Briggs-Haldane

The Michaelis-Menten mechanism assumes that there is a thermodynamic equilibrium between the enzyme-substrate complex and the free enzyme and substrate. A more accurate description of the same processes was proposed by the scheme

$$E + S \underset{k_{-1}}{\overset{k_1}{\rightleftharpoons}} ES \xrightarrow{k_2} E + P$$ **Scheme 2**

where Michaelis-Menten conditions hold whenever $k_2 << k_{-1}$. This model and its kinetic expression was first proposed by G. E. Briggs and J. B. S. Haldane (Briggs and Haldane 1925). The Briggs-Haldane model assumes that the enzyme-substrate complex is not in equilibrium but in a dynamic steady state.

$$\frac{d[ES]}{dt} = 0 = k_1[E][S] - k_2[ES] - k_{-1}[ES] \quad \textbf{- 8}$$

thus

$$[E] = \frac{k_1}{k_{-1} + k_2}\frac{[ES]}{[S]} \quad \textbf{- 9}$$

Using equation 3 and since

$$v = k_2[ES] \quad \textbf{- 10}$$

the initial velocity would be given by

$$v = \frac{[E]_O[S]k_2}{(\frac{k_{-1} + k_2}{k_1}) + [S]} \quad \textbf{- 11}$$

This equation has the same form as equation 4, but in this case the K_M is constituted by the microscopic constants (k_1, k_{-1} and k_2), and k_{cat} is equivalent to the microscopic constant k_2.

1.1.2.3 Enzymatic meaning of k_{cat} and K_M

In the Michaelis-Menten model, k_{cat} represents the rate of substrate conversion to product. When this model is further extended to that of Briggs-Haldane, the k_{cat}

appears as an apparent rate, function of the first order constants [5]. In either case, k_{cat}, is also known as *turnover number*, or *rate*, and represents the number of substrate molecules converted to products per unit of time per active site.

Similarly, while according to Michaelis-Menten, K_M is the true dissociation constant of the enzyme-substrate complex, it becomes an apparent parameter, function of the microscopic constants k_1, k_{-1} and k_2 under a Briggs-Halden regime. Typically, K_M, also known as *Michaelis*, or *dissociation constant*, is interpreted as the overall dissociation constant of all enzyme-bound species.

1.1.2.4 k_{cat} / K_M and enzyme selectivity

When two substrates (*i* and *j*) compete for same enzyme (E),

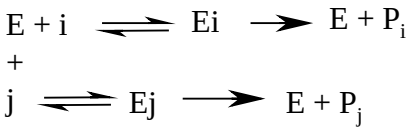

Scheme 3

the ratio of the reaction rates can be rapidly deduced using equation 6

$$\frac{v_i}{v_j} = \frac{(k_{cat} / K_M)_i [i]}{(k_{cat} / K_M)_j [j]} \qquad \textbf{- 12}$$

From this equation it follows that the enzyme's specificity between two competing substrates, is determined by a ratio of k_{cat}/K_M, and not by K_M alone. Thus, the *selectivity* [6] of an enzyme E towards the substrate *i*, relative to the substrate *j*, can be defined as the ratio of the respective k_{cat}/ K_M constants.

$$S^E_{i,j} = \frac{(k_{cat} / K_M)_i}{(k_{cat} / K_M)_j} \qquad \textbf{- 13}$$

5 In more complex models, k_{cat} becomes function of more than one microscopic parameter.

6 In this work the term selectivity constant has been chosen as k_{cat}/K_M by itself has previously referred as specificity constant.

In a steady state regime, from equation 11, it can be seen that

$$\frac{k_{cat}}{K_M} = \frac{k_2 k_1}{k_{-1} + k_2} \qquad \textbf{- 14}$$

and given that

$$\frac{k_2 k_1}{k_{-1} + k_2} \leq k_1 \qquad \textbf{- 15}$$

the parameter k_{cat}/K_M cannot exceed the enzyme-substrate encounter rate (k_1). In a bimolecular free diffusion system, the theoretical limit of k_1 is $10^8 - 10^9$ s^{-1} M^{-1}. In addition, if

$$k_{-1} << k_2 \quad \Rightarrow \frac{k_{cat}}{K_M} = k_1 \qquad \textbf{- 16}$$

k_{cat}/K_M becomes the true microscopic rate constant of the enzyme-substrate encounter. It is worth mentioning that when k_{cat}/K_M is limited by the enzyme-substrate encounter, Briggs-Haldane rather than Michaelis-Menten kinetics are obeyed.

A comprehensive dissection of the kinetic models presented in the previous sections can be found in Fersht (Fersht 1999).

1.1.2.5 Maximum rate

In equation 7, the velocity of reaction is referred to in terms of the k_{cat}/K_M, the free enzyme and the free substrate. Thus, the velocity will reach its maximum by maximising either k_{cat}/K_M or [E]. It has been mentioned, that k_{cat}/K_M is limited by the rate of enzyme-substrate encounter, implying that once this limit has been reached, increase in velocity can only be achieved by an increase in the free form of the enzyme, and thus the K_M (Fersht 1974).

1.1.3 Enzyme engineering

The manipulation of enzymes has been indispensable to our understanding of the catalytic/binding mechanisms in naturally occurring enzymes, and is prerequisite if they are to be adapted for medical and industrial applications.

It is possible to extensively modify the structure of enzymes, through the manipulation of their coding genes. For example, site directed mutagenesis easily allows mutation of one residue to another (Farber and Petsko 1990); several error-prone-PCR methods allow the incorporation of random mutations while carefully controlling their nature (transitions and/or transversion) and rate (Cadwell and Joyce 1994; Zaccolo, Williams et al. 1996); and it is possible to shuffle genes [7] in a homology dependent (Stemmer 1994) or independent fashion (Voigt, Martinez et al. 2002; Hiraga and Arnold 2003; Bittker, Le et al. 2004). Recent engineering of the genetic code has allowed non-natural amino acids to be incorporated into the primary structure of enzymes (Chin and Magliery in preparation). To complement these genetic manipulation techniques, a myrad of others have been developed in order to produce, extract and purify engineered enzymes (Higgins and Hames 1999; Hardin 2001).

In spite of the technical feasibility of completely reshaping existing enzymes, most of the changes that can be effected are likely to be functionally deleterious (Taddei, Radman et al. 1997). This is mainly due to enzymes' marginal stability (Taverna and Goldstein 2002) and their complexity [8]. In recent years, these two hurdles have been overcome with relative success by combinatorial engineering also known as directed evolution.

1.1.3.1 Directed evolution

It is possible to (re)design enzymes by implementing a Darwinian evolutionary algorithm of iterative rounds of mutation and selection (Zhao and Arnold 1997;

7 It has even been possible to shuffle complete genomes (Zhan and Perry et al, 2002).

8 Assuming an average protein length of 200 amino acids, there can be 20^{200} different protein sequences, a number that is much greater than, for example, the number of electrons in our (physical) Universe (estimated to be around 6^{79}) (Herztog T, personal communication).

Arnold 1998). Typically, the diversity is generated at gene level by any of the methods previously described (section 1.1.3), and is followed by selection of the desired new protein functional features. Whereas natural evolution measures the fitness of variants by their ability to leave viable offspring, directed evolution experiments depend on the availability of appropriate screens for the identification of the desired variants. To be precise, the availability of a screening or selection method is the most common technically limiting factor for the application of directed evolution strategies.

Directed evolution has been successfully applied to enzymes, to enhance overall performance (Castle, Siehl et al. 2004), to alter substrate specificity (Glieder, Farinas et al. 2002; Meyer, Schmid et al. 2002) and enantioselectivity (May, Nguyen et al. 2000), to improve thermal stability (Gonzalez-Blasco, Sanz-Aparicio et al. 2000; Merz, Yee et al. 2000), and a tad of other features (Martineau, Jones et al. 1998; Naki, Paech et al. 1998; Proba, Worn et al. 1998).

1.1.3.1.1 0Genotype ↔ Phenotype correspondence

Within an organism, several structural traits are under constant pressure to maintain a certain level of functionality. All these components should be physically linked together in order to be (naturally) selected as a single unit, and therefore be evolutionarily stable.

A canonical classification of the cellular machinery uses Genotype to refer to the genetic load upon which mutation takes place (namely DNA); and the Phenotype, in which the functional features are *seen* by the selective forces (namely proteins) [9]. In nature, the biunivocal correlation between the Genotype and Phenotype is created by the cellular transcription and translation machinery, and the compartmentalisation afforded by the cell membrane (Scheme 4)

9 This idea can be traced back to A. Weismann (1834–1914), further rephrased in molecular terms by F. Crick (1916–2004) in his central dogma of molecular biology (Maynard-Smith 1998)(Crick, 1970; Thieffry and Sarkar 1998).

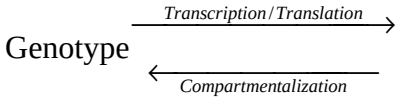

Scheme 4

In directed evolution experiments, the Genotype is linked to the Phenotype by borrowing the cellular transcription and translation machinery, either by transforming cells or by cell-free transcription/translation cocktails. The reverse correlation, can be obtained by several methods. Depending on how Phenotype is linked to Genotype, directed evolution selections can be broadly classified into three categories (Griffths and Tawfik 2000).

1.1.3.1.1.1 *In vivo* selection

In vivo selection strategies make use of the existing cell apparatus. The cell is thereby used as a compartment within which proteins are expressed and perform their catalytic duties, and which will ensure the propagation of the gene encoding the desired protein by means of cellular replication. One way of doing this is to use an auxotrophic strain (Joerger, Mayer et al. 2003) or to link the activity of the protein to be evolved to the survival of the cell (Zaccolo, Williams et al. 1996).

Even though *in vivo* systems have been used with some success because of their methodological simplicity, they have inherent limitations. Firstly, only those functions that can be linked to cell survival can be selected for. Secondly, because *in vivo* selection takes place in the presence of a large genetic background (the genome of the host cell) the cell may be able to provide solutions to its survival problem, like expression levels, which do not necessarily involve the introduced mutant protein [10]. Finally, with *in vivo* strategies, it is difficult to select for enzymes with low activity, since a certain threshold of activity might be necessary to guarantee survival.

10 Following the first rule on directed evolution experiments: 'You get what you select for' (Schmidt-Dannert and Arnold, 1999).

1.1.3.1.1.2 *In vivo-vitro* selection

In vivo-vitro strategies, broadly speaking, include a combination of *in vivo* and *in vitro* steps throughout the selection process. Two of these strategies have been broadly used in the last years: phage display and colorimetric/fluorimetric assays. In phage display the protein of interest is fused to a phage-coat protein, which results in the display of one or more copies of the fusion protein on the surface of filamentous bacteriophage. Molecules are selected by affinity panning on immobilised substrates, and the resulting phage are mixed with bacteria to produce progeny phage for subsequent rounds of panning (Rader and Barbas 1997). Colorimetric/fluorimetric assays consist in utilising bacteria or other host to translate and express the target protein, while using chromogenic/fluorogenic products either to screen colonies of bacteria or using Flourescence Activated Cell Sorting (FACS) to sort repertoires of genes or bacteria compartmentalised in double emulsions (Bernath, Hai et al. 2004).

Because *in vivo-vitro* selections contains an *in vivo* step, the maximum library size is limited by the transformation/transfection limit of the organism involved (for yeast, $10^7 – 10^8$ cells/μg DNA and for *E. coli*, $10^6 – 10^7$ cells/μg DNA). In addition to limiting the library size, the *in vivo* step may apply only for evolving enzymes that do not interfere substantially with cellular metabolism and can be distinguished from the background of other cell processes.

1.1.3.1.1.3 *In vitro* selection

Two main groups of *in vitro* selection technology can be distinguished. The first group makes use of a physical link between messenger RNA (mRNA) and nascent polypeptide, during translation, to couple genotype and phenotype (Martineau, Jones et al. 1998). The second group imitates the compartmentalisation of living cells by performing translation and selection within a water-in-oil emulsion (Tawfik and Griffiths 1998) (Griffiths and Tawfik 2003).

By contrast with *in vivo* selections, *in vitro* display technologies can handle libraries with up to 10^{14} members, depending on the scale of the *in vitro* translation used. This increases the diversity of sequences and thus improves the likelihood that a successful mutant will be isolated. Furthermore, not all sequences express well in

bacteria, as folding, transport, membrane insertion and complex formation provide significant *in vivo* selection pressures against certain proteins and scaffolds. These pressures are likely to be significantly reduced *in vitro*, where efficient translation is the only requirement. The main drawback of this kind of strategy is that these methods can be fairly complicated.

1.2 Organophosphorus Compounds (OPs)

1.2.1 OPs structure

OPs are esters or thiol derivatives of phosphoric, phosphinic, or phosphoramidic acids.

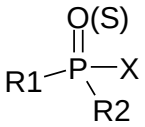

Scheme 5

Normally, R1 and R2 groups are aryl or alkyl moieties that bind to the phosphorus atom either directly (phosphinates), via an oxygen or sulphur atom (phosphates or phosphothioates respectively) [11], or a NH_2 group (phosphoramidates). The X group may be any of a broad range of halogens, aliphatic, aromatic or heterocyclic groups, which bind the phosphorus centre via an oxygen or sulphur atoms. The X group is referred to "leaving group" because it becomes separated when the OP is hydrolysed. As shown in Scheme 5, the double bonded atom may be either oxygen (oxon form) or sulphur (thio form). The chemistry of OPs can be found in Fest (Fest and Schmidt 1973).

1.2.2 OPs as nerve agents (NAs)

OPs have been extensively used in the last fifty years as helminthicides, ascaricides, nematocides, and to a lesser degree as fungicides and herbicides (Sultatos 1994). In addition to their application in agriculture, and given their toxicity to humans, OPs have been manufactured as poisonous nerve agents (NAs) for use in chemical warfare.

11 When both a phosphinate and phosphate/phosphothioate are present, the resulting compound is known as a phosphonate.

Among lethal chemical warfare agents, the nerve agents (NAs) have had a dominant role since their toxicity to humans was discovered in the early 1930's. The discovery of the pesticide Dimefox occurred around the time of the development of the first NA Tabun, which was developed as a weapon but not used during the Second World War (Figure 1). Diisopropyl fluorophosphate (DFP) was investigated as a potential nerve gas in the same period (Black and Harrison 1996), while the development of the more potent NAs Sarin, Soman and Cyclosarin, followed later (Timperley 2000). By the late-1950s, more toxic NAs with a different structure were being synthesised, including VX and its isomer Russian-VX (Bell, Murrell et al. 2001).

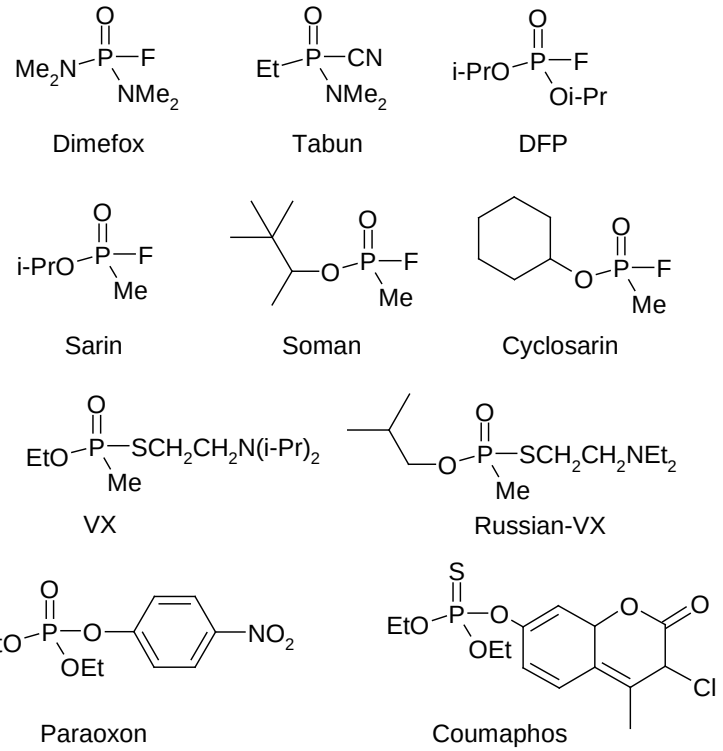

Figure 1. Structures of the main known military nerve gases, their prototypes dimefox and diisopropyl fluorophosphate (DFP), and the pesticides Paraoxon and Coumaphos.

1.2.2.1 Physico-chemical properties of NAs

Under standard conditions (25 °C and 0.1 MPa), all known nerve agents are in liquid form, and exhibit a range of water and organic solvent solubility, volatility and toxicity.

NAs are commonly divided in G- and V-type [12] according to their volatility. G-type nerve agents evaporate quickly (5 – 20 x 10^3 mg m^{-3} at 25 °C), while V-type agents are much less volatile (~ 10 mg m^{-3} at 25 °C) and therefore persist in liquid form for longer. Sarin and Soman, also known as GB and GD respectively, belong to the first group while VX and Russian-VX are included in the latter (and therefore normally used as contact poisons).

In their gas phase, NAs are about 5 to 10 times denser than air and non-flammable below 80 – 160 °C. Tabun and Soman have a slightly fruity and camphor-like odours respectively [13] (ATSDR 2002).

1.2.2.2 Toxicological properties of NAs

OPs vary in toxicity from practically non-toxic chemicals like malathion to extremely toxic such as VX and Russian-VX [14]. To be precise, NAs are those OPs that strongly inhibit acetylcholinesterase (AchE) (see section 1.2.2.3).

NAs are internalised by inhalation, skin contact and ingestion. Their toxicity was determined experimentally using animal models, and the values obtained correlated with those from *in vitro* inhibition assays of AchE in humans (Bajgar 2004).

Upon inhalation, the estimated LD_{50} [15] concentration for humans ranges from 10 mg min m^{-3} for VX to 400 mg min m^{-3} for Tabun. Vapours are not absorbed through the skin (ATSDR 2002). A study of the clinical aspects of percutaneous poisoning by VX has showed that the toxicity varies widely between the anatomical regions exposed. Application on the ventral surface of the ear of anaesthetised

12 "G" stands for German and "V" for venom.

13 Odour does not provide adequate warning.

14 Actually, Russian-VX is repeatedly cited as one of the most toxic man-made compounds known.

15 Dose that is lethal to 50% of the exposed population.

domestic swine (150 μg kg^{-1}), caused death after 30 – 60 minutes; however, when VX was applied on the epigastrium death did not necessarily followed (after 6 hours) (Duncan, Brown et al. 2002; Lundy 2004).

For intramuscular injection, the LD_{50} ranges from 10 to 80 μg kg^{-1} in rats and 4 to 150 μg kg^{-1} in humans. Subcutaneous administration of Russian-VX and Cyclosarin in guinea pigs have been reported to have an LD_{50} of 11.3 and 60 μg kg^{-1} respectively (Chang, Hoffman et al. 2002; Briseño-Roa, Hill et al. 2004). Given the persistence of some NAs, intoxication by ingestion is possible. In rats the LD_{50} by oral administration ranges from 0.1 to 10 mg kg^{-1}. In humans, the data is scarce but the values appear to be around 1 to 10 mg kg^{-1}.

1.2.2.3 Inhibition of acetylcholinesterase by OPs

OP compounds inhibit acetylcholinesterase (AChE) (Timperley, Sellers et al. 2001), an enzyme that controls nerve impulse transmission by hydrolysing acetylcholine to acetic acid and choline [16]. Hydrolysis of acetylcholine by AChE involves an active-site serine residue initiating a nucleophilic attack on the carbonyl carbon of acetylcholine to form a covalent acetyl-acyl-enzyme intermediate, concurrent with the release of free choline from the active site. The free enzyme is regenerated in a second step *via* a hydrolytic attack by water and the release of acetate. NAs mimic the natural substrate of AChE: they phosphylate the active site serine residue, releasing either a cyanide, fluoride or *N*,*N*-dialkylaminoethanethiolate group. This first step is fast, however the regeneration of the free enzyme through the nucleophilic attack by water is extremely slow; thus, a phosphorylated AChE unable to hydrolyse acetylcholine is generated (Tõugu 2001).

1.2.2.4 Effects of NAs

NAs alter the cholinergic synaptic transmission at neuroeffector junctions. The function of both muscarinic and nicotinic receptors is altered in the autonomic,

16 The term “nerve agent” is misleading, as their affect synaptic transmission rather than neural structures, *per se*.

skeletal myoneural, and Central Nervous systems. Muscarinic effects include hypersecretion of salivary, lachrymal, sweat and bronchial glands; bronchi narrowing, nausea, vomiting, diarrhoea, and slow heart rate. Nicotinic effects include skeletal muscle twitching, cramping and weakness; rapid heart rate and high blood pressure. Effects in the Central Nervous System include irritability, nervousness, fatigue, insomnia, memory loss, impaired judgment, slurred speech, and depression.

During exposures to low levels of NAs, a combination of the previously described effects are presented. Exposures to high levels of NAs cause, within minutes, loss of consciousness, convulsions, flaccid paralysis, copious secretions, apnoea, and death. Death follows by respiratory arrest due to NAs nicotinic effect in the respiratory system.

The human liver contains enzymes capable of detoxifying both thion and oxon OPs, such as glutathiones-S-transferases, monooxygenases and paraoxonases. In mammals, any oxon OPs that escapes hepatic detoxification can be subsequently inactivated in the blood by serum paraoxonases. The protection given by such enzymes is rapidly saturated under acute exposure to NAs (Mackness, Durrington et al. 1998).

Atropine, pralidoxime chloride, pyridostigmine are the typical battery of compounds used in prophylaxis against OPs poisoning (Bajgar 2004). After acute exposure, recovery is achieved after three or so months, when AChE is almost completely regenerated (Gunderson, Lehmann et al. 1992; ATSDR 2002).

1.2.3 NA legislation and NA attacks

The Chemical Weapons Convention (CWC), which entered into force on 29 April 1997, is the first arms control treaty which seeks to introduce a verifiable ban on an entire class of weapons of mass destruction. The CWC bans the possession and use of chemical weapons, controls the chemicals that are used to produce them, and requires total destruction of any CW stockpiles (OPCW 2005). It is administered by the Organisation for the Prohibition of Chemical Weapons (OPCW), which is based in The Hague, Netherlands. As from 25 May 2005, OPCW counts with 168 State Parties, comprising 95% of the world's population, and 98% of its chemical industry (OPCW 2005).

Two of the best documented cases of attacks employing NAs (Sarin) occurred in Japan in the mid 1990's. The first one occurred in Matsumoto, Nagano Prefecture, in 1994, where seven people were killed and around 150 injured (Morita, Yanagisawa et al. 1995; Okudera 2002). The second attack occurred a year later in the Tokyo subway system, in which twelve people were killed and around 6000 officially reported injured (Nagao, Takatori et al. 1997). The sect AUM Shinrikyo was indicted for both attacks.

Commercially available OPs, mainly used as pesticides in agriculture, have been reported in professional, suicidal and accidental intoxications. According to the World Health Organisation, more than one million serious poisonings with OP insecticides occur worldwide every year (Jeyaratnam 1990).

1.2.4 Organophosphatases

A number of enzymes have been identified which can catalyse the hydrolysis of OPs. Three of the best characterised are the phosphotriesterase (PTE) from *Pseudomonas diminuta* (Raushel and Holden 2000), the organophosphorus acid anhydrolase (OPAA) from *Alteromonas* sp. (DeFrank and Cheng 1991), and PON1, a member of the mamalian Serum Paraoxonase (PONs) family (Mackness, Durrington et al. 1998). A review of other organophosphatases can be found in Vilanova (Vilanova and Sogorb 1999).

1.3 Phosphotriesterase *Pseudomonas diminuta* (PTE)

Organophosphatase activity was first identified in *Flavobacterium sp*. (ATCC 27551) from samples taken from a Philippino rice paddy, which had been extensively treated with the organophosphate diazinon as insecticide (Sethunathan and Yoshida 1973). Three years later, a strain of the free-living soil bacterium, *Pseudomonas diminuta*, was reported to have the ability to hydrolyse the organophosphotriester parathion (Munnecke 1976; Chaudry, Ali et al. 1988). The genes responsible for these activities

were isolated from extrachromosomal plasmids and turned out to have identical sequences. The "organophosphate degradation" gene was named *opd* and its polypeptide product is widely known as Phosphotriesterase (PTE) (Mulbry, Karns et al. 1986; Harper, McDaniel et al. 1988; McDaniel, Harper et al. 1988; Mulbry and Karns 1989)

PTE has been expressed in several organisms and presents an approximate molecular weight of 35 kDa (339-residues) (Dumas, Caldwell et al. 1989; Phillips, Xin et al. 1990; Dave, Lauriano et al. 1994). PTE has no known natural substrate, however, is capable of hydrolysing man-made organophosphorus compounds with a spectacular efficiency. With its best substrate, the insecticide Paraoxon, a k_{cat} and k_{cat}/K_M of 10^3 s^{-1} and 10^8 s^{-1} M^{-1} respectively have been reported (Omburo, Kuo et al. 1992). This k_{cat}/K_M value is close to the theoretical limit imposed by the diffusion-controlled encounter of the enzyme and substrate (see section 1.1.2.4). It has been shown experimentally that with leaving groups holding a $pK_a < 7.0$, the reactions rates are indeed limited by diffusion (Caldwell, Newcomb et al. 1991).

1.3.1 Structure of PTE

With recombinant material obtained by expressing *opd* in *E. coli*, several structures of PTE have been solved (Benning, Kuo et al. 1994; Benning, Kuo et al. 1995; Vanhooke, Benning et al. 1996; Buchbinder, Stephenson et al. 1998; Benning, Hong et al. 2000; Benning, Shim et al. 2001). PTE crystallised in a homodimeric form, each monomer exhibiting a distinctive distorted eight stranded α/β-barrel fold with two metal transition ions bound in the C'- terminus of the β-sheet core (Figure 2). According to the SCOP structural classification, PTE belongs to the metal-dependent hydrolase superfamily, also referred as amidohydrolase elsewhere (Murzin, Brenner et al. 1995; Holm and Sander 1997). Other members of the same superfamily include *Klebsiella aerogenes* urease and *Mus musculus* adenosine deaminase (Wilson, Rudolph et al. 1991; Jabri, Carr et al. 1995).

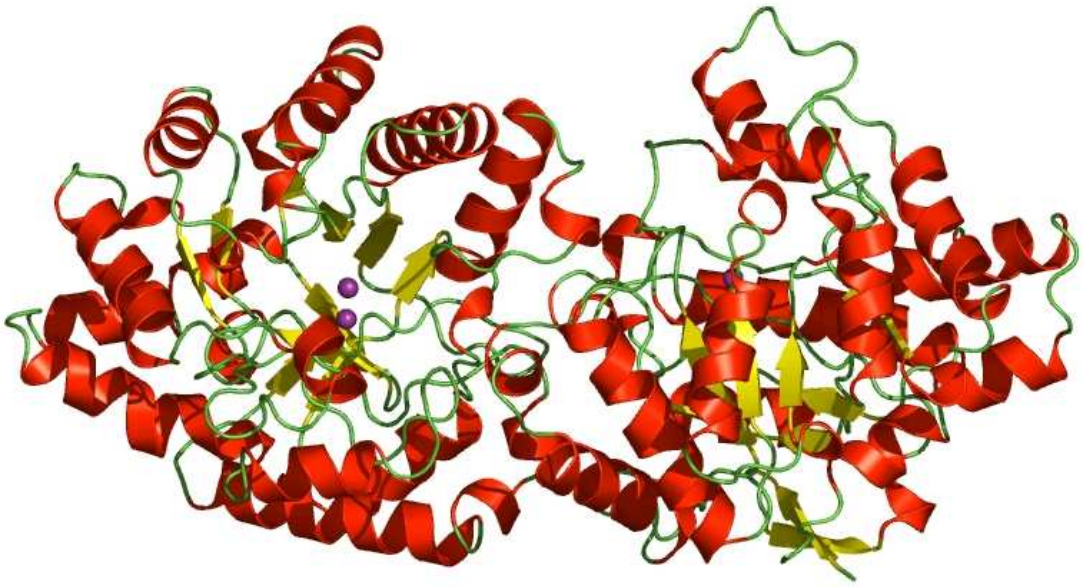

Figure 2. **Structure of the *Pseudomonas diminuta* phosphotriesterase (PTE).** PTE is an active homodimer [17] that possesses a distorted α/β barrel fold which binds two transition metal ions (purple spheres) – Zn(II) in this particular structure (1HZY, (Benning, 1994)).

1.3.2 PTE metal binding site

It has been established by NMR, crystallography and mutagenesis studies, that each PTE monomer binds two divalent transition metal ions via a cluster of four histidines (His-55, His-57, His-201 and His-230) and one aspartate (Asp-301) (Omburo, Mullins et al. 1993; Chae, Omburo et al. 1995). In addition, the two metal ions are linked together by a carbamate functional group, formed by the carboxylation of the ε-amino group of Lys-169 and a water (or hydroxide ion) from the solvent (see section 6.1.1).

17 The notion of PTE as an active homodimer is supported by gel filtration and folding data (Grimsely and Scholtz et al, 1997).

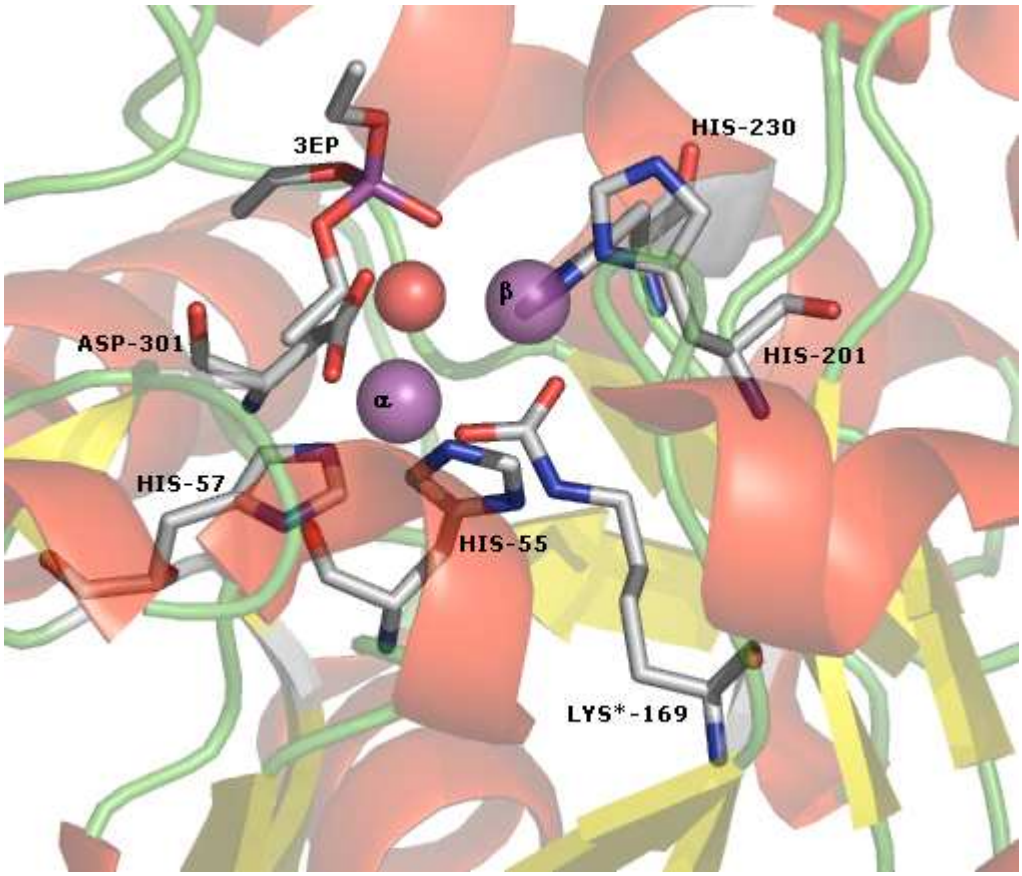

Figure 3. Cluster of residues involved in PTE metal and substrate binding. The two Zn(II) ions (purple spheres) are coordinated to the protein by four histidines (His-55, His-57, His-201 and His-230) and one aspartate (Asp-301). The two binding positions are not symmetrical. The α ion is buried deeper into the structure, while the β ion plays a more active role in the catalytic mechanism (section 1.3.3). The ions are linked together by a carboxylated lysine (Lys*-169) [18] and a water/hydroxyl molecule (red). The latter is bonded and activated by the metals, providing the nucleophilic attack necessary for the reaction to occur. In this particular structure (1ewy)(Benning, Hong et al. 2000), PTE was crystallised with the substrate analogue, triethylphosphate (3EP).

The more deeply buried ion (α) is coordinated through the side chains of Asp-301 (O^{δ}), His-55 ($N^{\varepsilon 2}$), His-57 ($N^{\varepsilon 2}$), Lys*-169 [18] ($O^{\theta 1}$), and a molecule of water in a trigonal bipiramidal arrangement. The more exposed ion (β) is bound through the His-201 ($N^{\delta 1}$), His-230 ($N^{\delta 1}$), Lys*-169 ($O^{\theta 2}$), and the molecule of water in distorted octahedral geometry.

18 * refers to the carboxylation modification.

The two Zn(II) ions found in the naturally occurring protein, can be replaced with Cd(II), Ni(II), Co(II), and Mn(II) ions without significant loss of enzymatic activity (Omburo, Kuo et al. 1992).

1.3.3 PTE reaction mechanism

PTE catalyses the hydrolysis of phosphotriesters (E.C. 3.1.8.1) [19] via an S_2N mechanism with a net stereo inversion in the phosphorous centre (Lewis, Donarski et al. 1988) (Figure 4). A more detailed mechanism has been recently proposed, but will not be considered here (Aubert, Li et al. 2004).

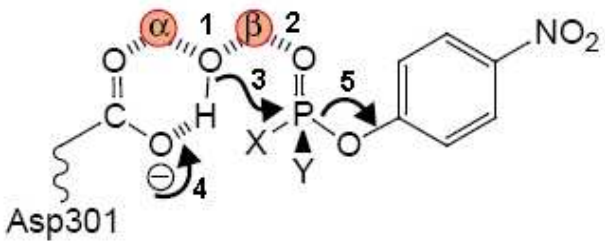

Figure 4. A simple working model for the PTE enzymatic reaction mechanism is shown in scheme 6. It involves (1) the ionisation of a metal-bound water molecule; (2) the polarisation of the phosphoryl-oxygen bond of the substrate by the β-metal; (3) the nucleophylic attack by the ionised-water molecule and the phosphorus centre, (4) assisted by proton abstraction from Asp-301, and resulting in the (5) weakening of the ester bond of the leaving group (Raushel and Holden 2000).

1.3.4 PTE Substrate binding site

As briefly mentioned before, PTE can catalyse the hydrolysis of the NAs sarin, VX and several other OPs compounds; however, the catalytic efficiency of PTE on NAs is 10^3 to 10^5-fold lower than for Paraoxon (Table 1).

19 Nomenclature Committee of the International Union of Biochemistry and Molecular Biology.

Table 1. Catalytic efficiencies of human BChE(G117H), PON1(Q191) and PTE. Data from (Dumas, Durst et al. 1990; Lockridge, Blong et al. 1997; Rastogi, DeFrank et al. 1997; Hong and Raushel 1999; Josse, Lockridge et al. 2001). The 'catalytic efficiencies' of BChE with Sarin and VX are k_{cat}/K_d values.

	k_{cat} / K_M (s^{-1} M^{-1})		
	BChE (G117H)	**PON1 (Q191)**	**PTE**
Paraoxon	1.8×10^2	1.1×10^4	6.2×10^7
Sarin	0.6	1.5×10^4	8.0×10^4
Soman	ND	4.7×10^4	9.6×10^3
VX	2.2	ND	6.9×10^2

Following studies of the three-dimensional structure of PTE with the non-hydrolysable substrate analogue diethyl 4-methylbenzyl phosphonate (Vanhooke, Benning et al. 1996), it became clear that the PTE binding site can be roughly dissected into three binding pockets, namely *small*, *large* and *leaving group* (Chen-Goodspeed, Sogorb et al. 2001). As this first classification does not fully reflect the structural aspects of the substrate, in the present work these regions were renamed *Pro-R*, *Pro-S* and *Entrance* respectively (Figure 5).

The Pro-*R* pocket is defined by the residues Gly-60, Ile-106, Leu-303 and Ser-308, which bind the arm of the inhibitor that points towards the interface between monomers (pro-*R*). Similarly, the Pro-*S* pocket, defined by His-254, His-257, Leu-271, and Met-317, binds the arm of the inhibitor which points away from the binuclear centre towards the solvent (pro-*S*). Lastly, the *Entrance* pocket is defined by the residues Trp-131, Phe-132, Phe-360, and Tyr-309, which create the *septum* between the binding site and the solvent.

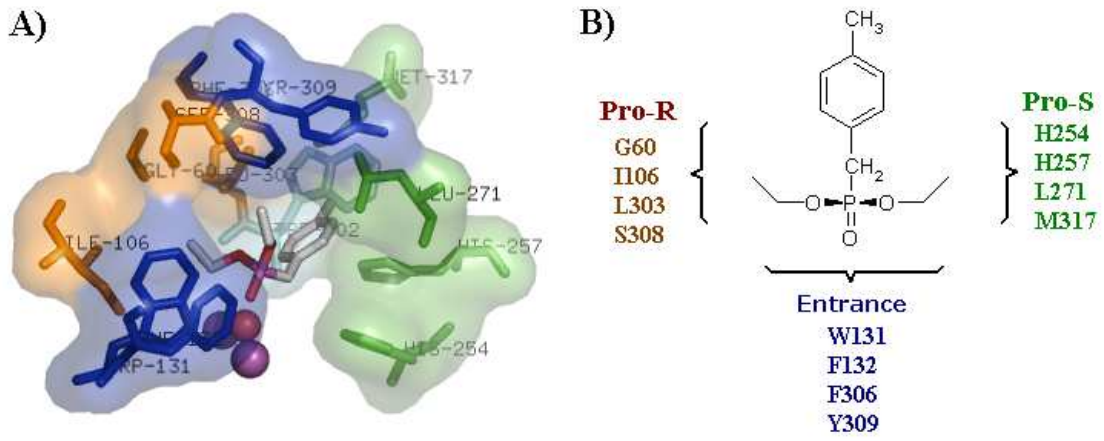

Figure 5. PTE binding pocket dissection. A) PTE co-crystallised with Zn(II) and the inhibitor diethyl-4-methylbenzyl phosphate (DMP) (Vanhooke, Benning et al. 1996). The residues conforming three different pockets are shown in different colours, Pro-*R* (in orange), Pro-*S* (in green), and *Entrance* (in blue). B) Diagram of the approximate localisation of the different pockets in relation with DMP.

1.3.4.1 Engineering of PTE by rational design

Alterations of the substrate-binding cavity of PTE have shown that it is possible to manipulate its substrate selectivity (Table 2). Mutations have been reported which yield improvements in fluoronophosphatase and phosphodiesterase activity in PTE (Watkins, Mahoney et al. 1997; Shim, Hong et al. 1998).

Shifts of the selectivity towards NAs and their analogues have been also described. A PTE variant with a 33% increase in rate of VX hydrolysis compared to wild type has been reported (Gopal, Rastogi et al. 2000). Two other mutants have been isolated with an increased k_{cat}/K_M of 17-fold and 31-fold for NPPMP (Soman analogue) and Demeton S respectively (diSioudi, Grimsley et al. 1999).

A variant PTE with reversed stereoselectivity on phosphotriester substrates was also found to have reversed stereospecificity for chiral Sarin analogues, hydrolysing the S_P-enantiomer 10 times more efficiently than the R_P-enantiomer (Chen-Goodspeed, Sogorb et al. 2001; Li, Lum et al. 2001). This is of particular interest as wild-type PTE hydrolyses analogues of the more toxic S_P-enantiomer of Sarin ten times more slowly than the R_P-enantiomer. In fact, most major NAs (including Sarin, Soman and VX) are racemic mixtures whose individual enantiomers exhibit substantial differences in toxicity.

Table 2. PTE variants obtained by rational design.

Substrate Nickname	Substrate Structure	Substrate Name	k_{cat}/K_M ($s^{-1}M^{-1}$) wildtype	PTE Mutant	k_{cat}/K_M relative to wt	*Reference*
DFP	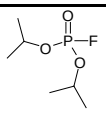	Diisopropyl fluorophosphate	1 [a]	F132H/F306H	10[b]	(Watkins, Mahoney et al. 1997)
Phosphodiester	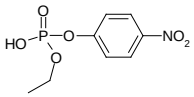	Ethyl-4-nitrophenyl phosphate	0.16 x 10^1	M317K	7	(Shim, Hong et al. 1998)
NPPMP (Soman Analogue)	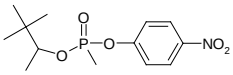	*O*-pinacolyl-4-nitrophenyl methylphosphonate	1.4 x 10^4	H254R/H257L	17	(diSioudi, Grimsley et al. 1999)
Demeton S (VX Analogue)	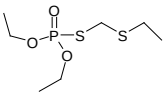	*O,O*-diethyl-*S*-2-ethylthioethyl phosphorothioate	8.7 x 10^2	H254R/H257L	31	(diSioudi, Grimsley et al. 1999)
VX	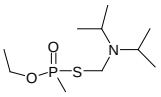	*O*-ethyl-*S*-2-Diisopropylaminoethyl methylphosphonothioate	1 [a]	L136Y	1.3 [c]	(Gopal, Rastogi et al. 2000)
S_P-MENP	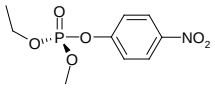	S_P -methylethyl-4-nitrophenyl phosphate	8.7 (33) x 10^6	G60A	3 (1.6)	(Chen-Goodspeed, Sogorb et al. 2001)
R_P-MFNP	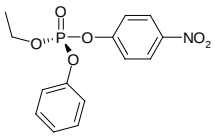	R_P -ethylphenyl-4-nitrophenyl phosphate	3.7 (40) x 10^6	I106G/F132G/ H257Y/S308G	48 (1.5)	(Chen-Goodspeed, Sogorb et al. 2001)
S_P-Sarin Analogue	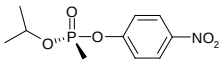	S_P-*O*-isopropyl-4-nitrophenyl methylphosphonate	4.1 (45) x 10^5	I106A/F132A/ H257Y	7 (0.16)	(Li, Lum et al. 2001)
S_PR_C-Soman Analogue	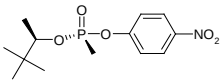	S_PR_C-*O*-pinacolyl-4-nitrophenyl methylphosphonate	3.8 (360) x 10^2	I106A/F132A/ H257Y	24 (0.08)	(Li, Lum et al. 2001)

a. relative units; **b.** k_{cat} values ; **c.** apparent rate; racemic mixture values are showed in parenthesis.

1.3.4.2 Engineering of PTE by Directed Evolution

It has also been possible to successfully alter PTE substrate selectivity by applying directed evolution techniques (Table 3).

From a relatively small library of 400 mutated PTE genes, a variant with a ~1000-fold increase in k_{cat}/K_M towards the most toxic stereoisomer (S_P S_C) of a chromogenic analogue of Soman has been identified (Hill, Li et al. 2003). Using a

strategy based on *in vitro* compartmentalisation (IVC) of genes in aqueous microdroplets in water-in-oil emulsions, and starting from a library of ~10^7 genes, it was possible to select a PTE variant with an even faster turnover rate for Paraoxon than wild type PTE (Griffiths and Tawfik 2003). More recently, using a 2-naphylacetate/Fast Red-coupled screening on a bacterial colonies, it was possible to isolate variants with a 10 and 150-fold selectivity improvement towards 2-naphylacetate and Carboxyflourescein diacetate, respectively (Aharoni, Gaidukov et al. 2005).

Table 3. PTE variants obtained by directed evolution.

Substrate Nickname	**Substrate Structure**	**Substrate Name**	k_{cat}/K_M ($s^{-1}M^{-1}$) wildtype	**PTE Mutant**	k_{cat}/K_M **relative to wt**	***Reference***
SpSc-Soman Analogue	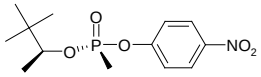	S_PS_C-*o*-pinacolyl-4-nitrophenyl methylphosphonate	~2 x 10^1	H254G/H257W/L303T	~1000 ([a])	(Hill, Li et al. 2003)
Paraoxon	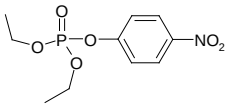	Diethyl-4-nitrophenyl phosphate	7.6 x 10^7	I106T/F132L	4 [b]	(Griffiths and Tawfik 2003)
2NA	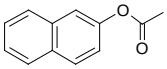	2-naphtylacetate	4.8 x 10^2	H254R/F306C/P342A	10.4	(Aharoni, Gaidukov et al. 2005)
CFDA	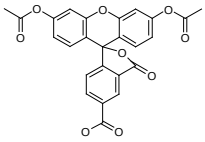	Carboxyflourescein diacetate	5.2 x 10^2	H254R/F306C/P342A	155.8	(Aharoni, Gaidukov et al. 2005)

a. no data available for racemic mixture; **b.** k_{cat} value.

1.3.5 Biotechnological applications of PTE

Overall, organophosphatases that efficiently hydrolyse NAs could have several potential applications, in decontamination of areas exposed to chemical warfare agents (LeJeune, Wild et al. 1998; Love, Vance et al. 2004), destruction of NA stockpiles (LeJeune, Mesiano et al. 1997), "active' fabrics and filter elements for personal protection (Richins, Mulchandani et al. 2000) (Gill and Ballesteros 2000), and sensors for CW agents (Mulchandani, Chen et al. 2001). It could also be attractive to use

enzymes which hydrolyse NAs for medical treatment of individuals exposed, or at risk of exposure, to CW agents. For instance, if it were possible to engineer a variant PTEs which hydrolysed a NA as efficiently as it hydrolyses Paraoxon (k_{cat} / K_M), it is estimated that just 2.5 kg of enzyme, immobilised within a polyurethane foam matrix, might be sufficient to degrade 30,000 tons of nerve agent in one year (LeJeune, Mesiano et al. 1997).

1.4 Serum Paraoxonases (PONs)

The family of serum paraoxonases (PONs) encompasses three genes that share between 60 to 70% identity (*pon1, pon2, pon3*). PONs have attracted considerable attention, not only due to they role in OPs detoxification, but also given their role in preventing atherosclerosis (Lusis 2000; Durrington, Mackness et al. 2001).

PON1 is a protein of 354 amino acids (with a molecular mass of 43 kDa) that catalyses the hydrolysis of a broad range of esters and lactones (E.C. 3.1.8.1)[19] in a calcium-dependent manner (La Du 1992). PON1 is also capable of catalysing, although at much lower rates, the hydrolysis of various OPs, including NAs like Sarin and Soman (Draganov and La Du 2004). It is highly conserved in mammals, but absent in fish, birds and arthropods. PON1 is almost exclusively located on the high-density-lipoprotein particles, and its level of activity in the blood appears to correlate to an individual's susceptibility to pollutants, insecticides and atherosclerosis (Smolen, Eckerson et al. 1991).

Human PON1 is rather unstable and it is difficult to produce enough quantities to carryout crystallographic studies. Family shuffling of four mammalian PON1 genes [20] and screening for esterolytic activity led to the isolation of variants (rePON1s) with high expression yields in *E. coli* (Aharoni, Gaidukov et al. 2004). rePON1s turned out to bear 75 to 91% identity with wild-type rabbit PON1, and had enzymatic properties essentially identical to those of human PON1.

Compared to PON1, relatively little is known about PON3 (Draganov and La Du 2004). PON3 is mostly expressed in the liver and at low levels in the kidney and

20 Human, rabbit, mouse, and rat genes.

blood serum. PON3s were only recently purified and characterised from human and rabbit sera (Draganov Stentson 2000). They were found to hydrolyse a wide variety of esterase and lactones but not Paraoxon. PON3 appears to have an enhanced ability to protect low-density-lipoproteins from oxidation relative to PON1. Rabbit PON3 (RabPON3) was readily expressed in *E. coli*, and like the PON3 isolated from sera, this recombinant protein showed little paraoxonase activity. After three rounds of shuffling and screening of wild-type PON3s, clones with greatly increase rates of both 2-naphtylacetate (20-fold) and paraoxon (240-fold) hydrolysis were isolated (Aharoni, Gaidukov et al. 2004).

Almost nothing is known about PON2. PON2 is not detectable in plasma but is expressed widely in a number of tissues including brain, liver, kidney, and testis, and may have multiple mRNA forms. Dihydrocoumarin is the only substrate so far reported for PON2 (Draganov and La Du 2004).

1.4.1 Structure and mechanisms of PON1

PON1 (rePON1-G2E3) is a six-bladed β- propeller, each blade containing four strands. In its core, two calcium atoms separated by 7.4 Å are bonded in the centre of the propeller. The lower one (Ca2) most probably helps to stabilise the whole structure, while it has been proposed that the higher one (Ca1) stabilises the oxyanionic moieties, generated as intermediates during the hydrolysis process (Harel, Aharoni et al. 2004).

The postulated catalytic site includes Ca1, the His-His catalytic dyad (His-115 and His-134), and the phosphate donated by the mother liquor. The first step of the mechanism involves deprotonation of a water molecule by the His-His dyad to generate an hydroxide anion. The activated water attacks the ester carbonyl (assuming a 2-naphthylacetate as substrate), producing an oxyanionic tetrahedral intermediate stabilised by the Ca1 atom. The intermediate breaks down to an acetate ion and either phenol or 2-naphtol.

1.4.2 Directed evolution of PON1 substrate selectivity

As mentioned before, PON1 is known to catalyse the hydrolysis of aromatic and aliphatic lactones like dihidroxycoumarin, 2-Coumaronon and homocisteine thiolactone (Billecke, Draganov et al. 2000; Aharoni, Gaidukov et al. 2004); organophosphates like Paraoxon, Chlorpyrifos, sarin, and soman (Davies, Richter et al. 1996); and aromatic esters like phenylacelate and 2-naphtyl acetate (Smolen, Eckerson et al. 1991). Aiming to increase the activity towards different substrates, gene libraries of rePON1 were prepared by random mutagenesis and cloned in bacterial cells. Colonies on agar plates were screen with several different substrates representing each of the substrate reaction types catalysed by PONs. The best clones were shuffled and the process iterated. Using this technique, it is was possible to isolate mutants with higher (16 to 46 times) activities towards specific compounds (Harel, Aharoni et al. 2004; Aharoni, Gaidukov et al. 2005).

1.5 General aim

Owing to the extensive use of organophosphorus (OPs) insecticides and the possibility of using OPs nerve agents (NAs) against civil populations (sections 1.2.2 and 1.2.3), the research and development of enzymes involved in the biotransformation and detoxification of OPs has attracted considerate attention in recent years.

A number of enzymes have been identified which can catalyse the hydrolysis of OPs, including nerve agents (section 1.2.4). Two of the best characterised are *Pseudomonas diminuta* phosphotriesterase (PTE) (section 1.3) and PON1, a mammalian member of the Serum paraoxonase (PON) family (section 1.4). These enzymes have excellent catalytic properties towards some OPs, but relatively poor against others. It has been possible to alter PTE substrate selectivity by rational site-mutagenesis, but with little improvements on the wild type rates (section 1.3.4.1). A more successful approach has been the application of directed evolution strategies (sections 1.1.3.1 and 1.3.4.2).

The aim of the present work was to develop variants of PTE with an increased catalytic efficiency towards OPs nerve agents. To this end, a directed evolution

platform was developed to enable screening for organphosphatase activity. This method relies in the use of fluorogenic NA analogues as probes.

Chapter 2 refers to the material and methods utilised throughout the present work; Chapter 3 describes kinetics studies on PTE and PON1 using the fluorogenic NA analogues as substrates, while the platform itself is described in detail in Chapter 4. Chapter 5 reports the isolation of PTE variants with increased activity towards Russian-XV and Cyclosarin NA analogues. Chapter 6 describes the possibility of replacing the metal binding carboxylated Lys-169 of PTE by any other residue while restaining enzymatic activity. Finally, the conclusions and future work are discussed.

Chapter 2 Materials and Methods

Objects large and small have secret, vicious lives of their own… manifestly focused on making man's life sheer misery.

Fred Vargas, 2001. Have Mercy on Us All

The material and methods presented here are organised in five sections. **(2.1) Microbiology**, which includes all the manipulations of bacteria (*Escherichia coli* strains), from electroporation to plasmid DNA extraction and sonication. **(2.2) DNA Biochemistry**, focusing mainly on different aspects of DNA synthesis and its manipulation: Polymerase Chain Reactions (PCRs), cloning, vector engineering, and constructions of libraries. **(2.3) Protein Biochemistry**, ranging from protein extraction and purification from crude bacterial lysates to the biochemical characterisation of the product. **(2.4) Organophosphorus Chemistry**, which describes the methods and safety measures taken while manipulating organophosphates compounds. And, **(2.5) Bioinformatics,** which refers to the software used in the manipulation of protein and DNA sequences, protein visualisation and imaging.

2.1 Microbiology

2.1.1 Materials

Ampicillin sodium salt and isopropyl -β-D-thiogalactoside (IPTG) were from Melford Laboratories Ltd. (Chelsworth, UK). Bacto-tryptone and Bacto-yeast extract and Tryptone were from Biogene Ltd. (Kimolton, UK). Antifoam 204 was from Sigma (St. Louis, MO, USA). α-lactose, D(+)-Glucose, Zinc Chloride, and the remaining

buffers were from BDH (Poole, UK). BugBuster™ was from Novagen (Lutterworth, UK). PROTRAN Nitrocellulose Transfer membrane (pore size 0.45 μm) was from Schleicher & Schuell BioScience Inc (Dassel, Germany). 384-well microplates and pin replicators were purchased from Genetix (Hampshire, UK). Deionised water was obtained using a Millipore Milli-Q Gradient system (Gloucestershire, UK).

2.1.1.1 Bacterial strains

E. coli DH5α was used for standard DNA manipulation procedures. *E. coli* C41 was used as expression strain in all protein preparations. *E. coli* MC1061 was used and prepared for library cloning (high electroporation yield). *E. coli* XL-1 Blue strain was used for cloning point mutations.

Table 4. Genotype annotations of *Escherichia coli* strains.

***Escherichia coli* Strains**	**Genotype**
C41 (Miroux and Walker 1996)	BL21(DE3) variant, no genotype available.
BL21(DE3) (Studier, Rosenberg et al. 1990) (Novagene)	F^- *ompT* $hsdS_b(r_B^- m_B^-)$ *gal [dcm][Ion] (DE3)**
DH5α (ATCC)	F^- *supE44 hsdR17 recA1 gyrA96 endA1 thi-1 relA1 deoR* λ^-
MC1061 (Casadaban and Cohen 1980)	F^- *araD139* Δ*(lac-leu)7696 galE15 galK16* Δ*(lac)X74 rpsL(*Str^r*) hsdR2(*$r_k^- m_k^+$*) mcrA mcrB1*
XL1-Blue (Bullock, Fernandez et al. 1987) (Stratagene)	F^- *proA*$^+$*B*$^+$ *lacI*^{q}Δ*(lacZ)M15::Tn10 recA1 endA1 gyrA96(*Nal^r*) thi-1 hsdR17(*$r_k^- m_k^+$*) supE44 relA1 lac*

* a λ prophage carrying the T7 RNA polymerase gene

All the bacterial stocks were kept at –80 °C in 10% (v/v) Glycerol after being flash-frozen in liquid nitrogen. Any Medium or glassware that had come in direct contact with bacteria were disinfected with iodine solution.

2.1.1.2 Buffers and media

Table 5. Recipes for Microbiological Buffers and Media

Name	Recipe
2x TY Medium	1.5 % (w/v) Bacto- tryptone, 1.0 % (w/v) Bacto-yeast extract, 0.5 % (w/v) NaCl. Stored at 4 °C
2x TY Agar	2xTY Media, 1.5 % (w/v) agar
1000x Ampicillin stock solution	100 mg ml^{-1} ampicillin (Na-Salt) in mH_2O[a], 0.22 μm filtered. Stored at –20 °C.
1000x IPTG stock solution	1M in mH_2O, 0.22 μm filtered. Stored at –20 °C.
Expression Media	2xTY, 100 μg ml^{-1} Ampicillin. Stored at 4 °C.
Growth Medium	2xTY, 1.0% (w/v) D(+)-Glucose, 100ug ml^{-1} Ampicillin. Stored at 4 °C.
Induction Medium	2xTY, 1mM IPTG, 100 μg ml^{-1} Ampicillin, 1mM $ZnCl_2$. Stored at 4 °C.
Agar Growth Medium	Growth Medium, 1.5 % (w/v) agar
Agar Induction Medium	Induction Medium (no Zinc), 1.5 % (w/v) agar
20x NPS stock solution	100mM PO_4, 25mM SO_4, 100mM Na, 50mM K. Add in sequence to beaker, and stir. pH should be ~6.75.
50x 5052 stock solution	0.5% (v/v) Glycerol, 0.05% (w/v) D(+)-Glucose, 0.2% (w/v) α-lactose. Add in sequence to beaker, and stir. α-lactose takes ~1hr to be dissolved.
Autoinduction Medium	2xTY, 1mM $MgSO_4$, 1x5052, 1xNPS, 0.5% (v/v) Antifoam 204, 1mM $ZnCl_2$.

a. Deionised water (Millipore).

2.1.2 Methods

2.1.2.1 Preparation of electrocompetent cells

Freshly thawed defrosted cells were streaked onto a 2xTY plate, and incubated at 37 °C for 16 hrs. 10 ml of 2xTY Medium (in 50 ml polypropylene tube) were inoculated with one colony and incubated at 37 °C and shaking at 250 rpm for 16 hrs. Sterile one litre *Erlen-Meyer* flasks containing 250 ml 2xTY were inoculated with 2.5 ml from this overnight culture. The culture was grown at 30 °C with shaking at 250 rpm until it reached an OD_{600nm} of ~ 0.7. The culture was then transferred to autoclaved and

prechilled 0.5 L spin bottles and incubated on ice for 30 minutes. Cells were harvested by spinning at 4000 rpm for 30 minutes. The resulting cell pellet was suspended in the original volume of ice-cold filter-sterilised mH_2O and respun. Cells were then resuspended in 40 ml of ice-cold filter-sterilised mH_2O, transfered to ice-chilled 50 ml-polypropylene tubes and incubated for 30 minutes in ice. Pellets were spun at 4000 rpm in a pre-chilled bench centrifuge at 4 °C for 20 minutes. Cells pellets were washed once in 40 ml of 10% (v/v) glycerol in mH_2O following the same procedure. Lastly, pellets were resuspended in 20 ml (for standard use) or 2 ml (for library transformations) of 10% (v/v) glycerol in mH_2O, aliquoted (100 µl) and dispensed into prechilled biofreeze vials, flash frozen and stored at – 80 °C.

2.1.2.2 Transformation by electroporation

Electroporation involves the application of a transient high voltage electrical field to a mixture of cells and plasmid DNA, thereby enabling DNA to pass through the cell membrane and be retained (Fiedler and Wirth 1988). Electro-competent cells were thawed on ice before transformation. 50 µl of these cells and 1 µl of DNA were mixed in a pre-chilled 2 mm path-length electroporation cuvette (EQUIBIO). Electroporation was performed using BioRad Gene PulserTM II Apparatus at 2.5 kV voltage, 200 Ω resistance, 25 µFD capacitance. 1 ml of 2xTY was added immediately and cells were incubated at 37 °C for 20-50 minutes before spreading onto plates containing Growth Medium.

2.1.2.3 Plasmid DNA extraction

5 ml of Growth Medium inoculated with one colony of *E.coli* MC1061 or C41, were left growing overnight (ordinarily ~16 hrs) at 37 °C, shaking at 250 rpm. Plasmid DNA were extracted and prepared using the Qiagen Miniprep Spin Kit according to the manufacturer's instructions.

2.1.2.4 Determination of cell numbers

The approximated number of bacteria in a solution was calculated with the formula $N_{cells/\ ml} = 0.1\ OD_{600nm} \times 10^8$ (using a path-length of 1 cm). When necessary, dilutions were done to ensure a OD_{600nm} reading values between 0.1 and 1.

2.1.2.5 Bacterial-fluorescence screening

2.1.2.5.1 Library Plasmid DNA production

100 µl of *E. coli* MC1061 cells (7.8 $x10^8$ cells ml^{-1}) were transformed (section 2.1.2.2). with 9 – 12 µg (total) of ligated library DNA (section 2.2.2.10.3). After recovering at 37 °C for 20 – 25 minutes, the cells were plated in pre-dried 23x23 cm Agar Growth Medium plates and incubated 37 °C for 16 hrs. The bacterial lawn (~ 10^7 cfus) obtained was scraped and washed from the plate with ~50ml of 2xTY medium, and homogenised (section 2.1.2.3).

2.1.2.5.2 First Round

2.1.2.5.2.1 Plate preparation

50 µl of *E. coli* C41 Cells (2.1 $x10^9$ cells ml^{-1}) were transformed (section 2.1.2.2) with 100-180 ng of library plasmid DNA. After recovering at 37 °C for 20 – 25 minutes, the cells were plated in pre-dried 23x23 cm Agar Growth Medium plates, covered with a 22x22 cm PROTRAN Nitrocellulose Membrane, and incubated 37 °C for 14 hrs. The number and distribution of cfus obtained were tightly controlled, ranging ~5000 per plate. Membranes were carefully detached and inversely placed over 23x23 cm plates containing Agar Induction Medium. The plates were incubated at room temperature for 20 – 24 hrs.

2.1.2.5.2.2 Top agar/ substrate addition

25 ml of Top-Agarose Activity formulation (0.5 % (w/v) Agarose, 2x BugBuster, 50mM HEPES pH 8.5) (per plate) was prepared and equilibrated at 45 °C for 30 minutes. Substrate was added to a final concentration of 50 µM, mixed, and finally

poured over a plate that resulted from process in previous section; this being carried out in the chemical fume hood. Plates were illuminated from above with a 365nm-UV lamp (230V, 50Hz, SYNGENE). Pictures were taken at different time intervals with a Geneflash system (Syngene) using a standard cut-off glass filter ($T_{50\%}$ = 418nm). Positive colonies were picked with sterile wooden toothpicks, not later than 5 minutes after adding the top agar, and transferred to Petri plate containing Agar Growth Medium (spreading them with a L-shape disposable spreader). The plates were incubated at 37 °C for 16 hrs.

2.1.2.5.3 Second round

2.1.2.5.3.1 Preparation of 384-well microplates

384-well microplates were filled with 50 µl Growth Medium (*Stock Plates*), 4 – 16 colonies from each Petri plate were transferred (one per well) and incubated at 37 °C for 16hrs. Large volume 384-well microplates were filled with 40 µl of Induction Medium (*Assay Plates*), into which the Stock Plates were replicated using 348-pin disposable plate replicators. The Assay Plates were incubated at 37 °C for 16 – 36 hrs, and Stock Plates were kept at 4 °C.

2.1.2.5.3.2 Assaying 384-well microplates

The AU_{600nm} (pathlength of ~0.5 cm) of Assay Plates was measured using a SpectraMAX 190 Microplate spectrometer (Molecular Devices). Using a Multidrop 384 (Labsystems), 40 µl of 50mM HEPES pH 8.5, 2x BugBuster, 2% (v/v) DMF, and 10 µM substrate, were dispensed into the plates. The apparition of product was immediately measured following the change in fluorescence (emission = 355nm, excitation = 460nm, cut-off = 455nm) with a SpectraMAX GeminiXS Microplate spectrofluorimeter (Molecular Devices).

2.1.2.6 Growth of bacteria and harvest for protein expression

Exact expression conditions, such as induction temperature and duration, were varied in specific cases in order to maximise production of soluble protein, however all protocols used the same following general guidelines.

2.1.2.6.1 IPTG induction

3 ml of Growth Medium was inoculated with one colony of freshly transformed *E. coli* C41 and incubated at 37 °C and 250 rpm overnight. One litre of Expression Medium was inoculated with 3 ml of the overnight preinocule. The flask was incubated at 37 °C with shaking at 240 rpm. Protein expression was typically induced with 0.1 – 1 mM IPTG and 1mM $ZnCl_2$ when the culture reached at OD_{600nm} of 0.6 – 0.8. After induction the temperature was drop to 18 °C and left growing for further 36 hrs. Cells were harvested at 15 krpm for 20 minutes in a Sorvall® RC 3B pre-cooled to 4 °C. The cell pellet was stored at -20 °C if purification was not started the same day.

2.1.2.6.2 α-lactose induction (Autoinduction)

3 ml of Growth Medium was inoculated with one cfu of freshly transformed *E. coli* C41 and incubated at 37 °C and 250 rpm overnight. One litre of Autoinduction Medium were inoculated with 3 ml of the overnight preinocule. The flasks were incubated at 37 °C, shaking at 240 rpm. The temperature was drop after 10 – 12 hrs to 25 °C for a further 16 – 24 hrs. Cells were harvested at 4000 rpm for 20 minutes in a Sorvall® RC 3B pre-cooled at 4 °C. The cell pellet was stored at - 20 °C if purification was not started the same day.

2.1.2.7 Cell Lysis

2.1.2.7.1 Sonication

Cell pellets (from 1 – 3 litres of medium) were resuspended in 40 ml of Ni-Lysis Buffer or 50mM HEPES pH 8.5 (see section 2.3.1.1), transferred to 50 ml polypropylene tubes, and chilled in ice for 10 minutes. The sonication was performed

on ice, power 8 of a Sonicator XL (Misonik Incorporated) for a total of 3 minutes, typically with 10 seconds on and with 30 seconds off.

2.1.2.7.2 Detergent Lysis

Whenever low volumes (0.1 – 1 ml) of soluble fractions were needed, a chemical treatment was used to obtained soluble fractions. 1 ml of bacterial culture was transferred to a clean 1.5 microtube and spun in a bench microcentrifuge for 1 minute at 13,000 rpm. The pellet obtained was resuspended in 0.2 ml of Bugbuster™ (Stratagene). The reaction mix was vortexed for 1 minute and incubated at room temperature before being spun for 1 minute at 13,000 rpm. The supernant, i.e. crude soluble fraction, was transfered to a clean microtube.

2.2 DNA Biochemistry (Molecular Biology)

2.2.1 Materials

All enzymes and corresponding buffers were from New England BioLabs (Beverly, MA, USA) apart from Turbo*Pfu* polymerase which was from Stratagen (La Jolla, CA, USA), Super*Taq* polymerase from HT Biotechnology Ltd. (Cambridge, UK) , and BpiI from Fermentas Inc. (Hanover, USA). DNA Miniprep, PCR Purification and Gel Extraction kits were purchased from QIAGEN (Hilden, Germany). Hyperladder I DNA marker was from Bioline Ltd. (London, UK). Ampicillin and isopropyl -β-D-thiogalactoside (IPTG) were from Melford Laboratories Ltd. (Chelsworth, UK). Ultrapure deoxynucleotides (dNTP) were from Amersham Biosciences UK Limited (Little Chalfont, UK). Hi-Pure Low EEO Agarose was from Biogene Ltd. (Kimolton, UK).

2.2.1.1 Oligonucleotides

Oligonucleotides were ordered from TAGN Ltd. (Newcastle, UK) or were produced at the MRC Laboratory of Molecular Biology (Cambridge, UK). Those to be used in

point and indel mutagenesis, and library construction were ordered HPLC (reverse phase) purified.

2.2.1.1.1.1 Sequencing

P020404C 5′-GGTCGTCAGACTGTCGATGAAGCC-3′

P020404D 5′-CGCCAGGGTTTTCCCAGTCACGAC-3′

PTE-1 5′-GGCGACCCCCTTTCAGGA-3′

PTE-2 5′-CTGTGACCAATACAAACC-3′

T7Rev 5′-TAATACGACTCACTATAGGG-3′

T7For 5′-TAATACGACTCACTATAGGG-3′

Table 6. Primer used for DNA sequencing.

Primer Code	Binding Site
P020404C	pMAL vector (5'end)
P020404D	pMAL vector (3'end)
PTE-1	*opd* gene
PTE-2	*opd* gene
T7Rev	T7 Terminator
T7For	T7 Promotor

2.2.1.1.1.2 Cloning

P020404A 5′-GGATTTCAGAATTCTACAAAGATGACGATGATA-3′

P020404B 5′-AAGCTTGCCTGCAGTTATTACGCATAATCCGGC-3′

P220404-A 5′-GGAGATATACCATGGACTACAAAGATGACG-3′

P220404-B 5′-GCTGCAGAGCTCTTATTACGCATAATCCGG-3′

P020604-B 5′-GGTAGAATTCTTATTAACCGCCGGTACCTGACGC-3′

P040804A 5′-CAAGGATCCATCACCAACAGCGGCGATCGG-3′

LMB2-1 5′- CAGGCGCCATTCGCCATT –3′

LMB2-2 5′- CAGGCTGCGCAACTGTTG –3′

LMB2-3 5′- GGAAGGGCGATCGGTGCG –3′

LMB2-4 5′- GGCCTCTTCGCTATTACG –3′

LMB2-5 5′- CCAGCTGGCGAAAGGGGG –3′

LMB2-6 5′- ATGTGCTGCAAGGCGATT –3′

LMB2-7 5′- AAGTTGGGTAACGCCAGG –3′

LMB2-8 5′- GTTTTCCCAGTCACGACG –3′

LMB2-9 5′- GTAAAACGACGGCCAGT –3′

PIVB-1 5′- AGAAATTGCATCAACGC –3′

PIVB-2 5′- CGAGAACGGGTGCGCAT –3′

PIVB-3 5′- GCGGTCGGACAGTGCTC –3′

PIVB-4 5′- ACTGGGCGGCGGCCAAA –3′

PIVB-5 5′- GTAGCGAAGCGAGCAGG –3′

PIVB-6 5′- GTCGATAGTGGCTCCAA –3′

PIVB-7 5′- GTCGCCATGATCGCGTA –3′

PIVB-8 5′- TCCACAGGACGGGTGTG –3′

PIVB-9 5′- GGAACTATATCCGGATA –3′

Table 7. Primers used in the cloning of *opd* genes.

Primer Code	Restriction Site	Gene	Localisation	Vector
P220404-A	NcoI	*ivp*	For	pIVEX
P220404-B	SacI	*ivp*	Rev	pIVEX
P020604-B	EcoRI	*opd*	For	pHLT
P040804-A	BamHI	*opd*	Rev	pHLT
P220404-A	NcoI	*ivp*	For	pTrc99a
P220404-B	SacI	*ivp*	Rev	pTrc99a

2.2.1.1.1.3 Site Directed Mutagenesis

P230704-C 5′-AATGACTGGACGTTCGGGTTT-3′

P230704-D 5′-AAACCCGAACGTCCAGTCATT-3′

P290704-A 5′-AGGGCGGGCATTATCCTGGCCTCCGGAACCACAGGCAAGGCGACC-3′

P290704-B 5′-GGTCGCCTTGCCTGTGGTTCCGGAGGCCAGGATAATGCCCGCCCT-3′

P290704-C 5′-AGGGCGGGCATTATCCTCTGCGCGGCAACCACAGGCAAGGCGACC-3′

P290704-D 5′-GGTCGCCTTGCCTGTGGTTGCCGCGCAGAGGATAATGCCCGCCCT-3′

P290704-E 5′-AGGGCGGGCATTATCAAGGTCGGCGGCACCACAGGCAAGGCGACC-3′

P290704-F 5′-GGTCGCCTTGCCTGTGGTGCCGCCGACCTTGATAATGCCCGCCCT-3′

P040804-D 5′-GGTCTAGACGGGATCCCGTGGAGTGCGATTGG-3′

P040804-E 5′-CCAATCGCACTCCACGGGATCCCGTCTAGACC-3′

P270804-A 5′-AGGGCGGGCATTATCGAGAGCGGGACCACAGGCAAGGCGACC-3′

P270804-B 5′-GGTCGCCTTGCCTGTGGTCCCGCTCTCGATAATGCCCGCCCT-3′

P290804-E 5′-AGGGCGGGCATTATCAAGGTCGGCGGCACCACAGGCAAGGCGACC-3′

P290804-F 5′-GGTCGCCTTGCCTGTGGTGCCGCCGACCTTGATAATGCCCGCCCT-3′

Table 8. Primer used in the construction of point mutations.

Primer Code	Modified Residues
P230704-C	L303T(for)
P230704-D	L303T(rev)
P290704-A	K169LA, V170S, A171G (for)
P290704-B	K169LA, V170S, A171G (rev)
P290704-C	K169LC, V170A (for)
P290704-D	K169LC, V170A (rev)
P290704-E	K169KV, V170G, A171G (for)
P290704-F	K169KV, V170G, A171G (rev)
P040804-D	H254G/H257W (for)
P040804-E	H254G/H257W (rev)
P270804-A	K169E, V170S, A171G (for)
P270704-B	K169E, V170S, A171G (rev)
P270804-C	K169R, V170V, A171H (for)
P270804-D	K169R, V170V, A171H (rev)

2.2.1.1.1.4 Libraries

2.2.1.1.1.4.1 Binding pocket

P010704A 5′-CTCGCAACTGAAGACTTGCACATCTGCNNSAGCTCGGCAGGA-3′

P010704B 5′-CTCGCAACTGAAGACTTGTGCTCGTGAGTCAGTGTGAA-3′

P010704C 5′-CTCGCAACTGAAGACTTACCGGCTTGTGGNNSGACCCGCCACTT-3′

P010704D 5′-CTCGCAACTGAAGACTTACCGGCTTGNNSNNSGACCCGCCACTT-3′

P010704E 5′-CTCGCAACTGAAGACTTCGGTCGCCGCCACGATATGAA-3′

P010704F 5′-CTCGCAACTGAAGACTTTCTTCTAGACCAATCGCACTSNNCGGGATSNNGTCTAGACC-′3

P010704G 5′-CTCGCAACTGAAGACTTAAGATAATGCGAGTGCATCAGCCNNSCTGGGCATCCGT-3′

P010704H 5′-CTCGCAACTGAAGACTTGAATGACTGGCTGTTCGGGTTTTCGNNSNNSGTCACCAACATC-3′

P010704I 5′-CTCGCAACTGAAGACTTGAATGACTGGNNSTTCGGGTTTTCGNNSTATGTCACCAACATC-3′

P010704J 5′-CTCGCAACTGAAGACTTGAATGACTGGCTGTTCGGGNNSTCGAGCNNSGTCACCAACATC-3′

P010704K 5′-CTCGCAACTGAAGACTTATTCGAAACGAGGATTTGTTT-3′

P171004 5′-CTCGCAACTGAAGACTTATCATGGACGTGNNSGATAGCGTGAAC-3′

P010704M 5′-CTCGCAACTGAAGACTTTGATGTTGGTGACATAGCTCG-3′

P090804-A 5′-CTCGCAACTGAAGACTTCGACTTTCGATNNSGGTCGCGACGTC-3′

P090804-B 5′-CTCGCAACTGAAGACTTGTCGACACATCGACAATCGTT-3′

Table 9. Primer used in the construction of substrate binding libraries

Primer Code	Residues Targeted
P010704A	G60
P010704C	F132
P010704D	W131, F132
P010704F	H254, H257
P010704G	L271 (Rev)
P010704H	S308, Y309
P010704I	L303, S308
P010704J	F306, Y309
P171004	M317
P090804-A	I106

2.2.1.1.1.4.2 Metal Binding

P050302A 5′-GTCCTCGCAACTGAAGACTTTTAGGGCGGGCATTATCNNSNNSGSAACCACAGGCAAG-3′
P050302B 5′-GTCCTCGCAACTGAAGACTTTTAGGGCGGGCATTATCNNSNNSNNSACCACAGGCAAG-3′
P050302C 5′-GTCCTCGCAACTGAAGACTTTTAGGGCGGGCATTATCGSAGAGVYYGSAACCACAGGCAAG-3′
P050302D 5′-GTCCTCGCAACTGAAGACTTTTAGGGCGGGCATTATCNNSGAGNNSGSAACCACAGGCAAG-3′
P050302E 5′-GTCCTCGCAACTGAAGACTTTTAGGGCGGGCATTATCNNSNNSNNSGSAACCACAGGCAAG-3′
P210302GBO 5′-GTCCTCGCAACTGAAGACTTCTAATTCCGGTGTCTTCGATGCCATATTG-3'
P180404A 5′-CTCGCAACTGAAGACTTCGATGTGTCGNNSTTCGATATCGGT-3′
P210704-A 5′-CTCGCAACTGAAGACTTATCGACAATCGTTCGCACGCC-3′
P180404C 5′-CTCGCAACTGAAGACTTTCGTGGCGNNSACCGGCTTGTGG-3′
P210704-B 5′-CTCGCAACTGAAGACTTACGATATGAACGTCGGCA-3′

Table 10. Primer used in the construction of metal binding libraries

Primer Code	Residues Targeted
P050302A	K169*a*, V170*a*, A171*b*
P050302B	K169*a*, V170*a*, A171*a*
P050302C	K169*b*E, V170*c* A171*b*
P050302D	K169*a*E, V170*a*, A171*b*
P050302E	K169*aa*, V170*a*, A171*b*
P210302GBO	Rev(K169, V170, A171)

2.2.1.2 Buffers and Solutions

Table 11. Recipes for DNA Biochemistry Buffers and Media

Name	Recipe
6x Agarose gel loading buffer	40 % (w/v) sucrose, 0.25 % (w/v) bromophenol blue
10x TBE buffer	890 mM Tris-base, 890 mM boric acid, 20 mM EDTA (pH 8.0)
2x W+B solution	10 mM Tris HCl pH 7.4, 1 mM EDTA, 2M NaCl
PCR Buffer (no $MgCl_2$).	10 mM Tris HCl, 01% Triton X-100, 50 mM KCl
20x dNTPs stock solution	5mM each dNTP
10x T4 Ligase Buffer stock solution	20 ul aliquots stored at –20 °C.

2.2.1.3 Vectors

2.2.1.3.1 pIVEX 2.6a (Roche)

The pIVEX 2.6a vector is designed for high-level expression of HA-tagged proteins in the cell free RTS *E. coli* system. The vectors contain all regulatory elements necessary for *in vitro* expression based on a combination of T7 RNA polymerase and prokaryotic cell lysates. The introduction of a N-terminal Flag (Chiang and Roeder 1993) and a C-terminal HA-tag (Field, Nikawa et al. 1988) provides a rapid method of detecting and purifying proteins of interest. The vector provides a ribosome-binding site and confers resistance to 100 μg ml^{-1} ampicillin. pIVEX 2.6a contains binding sequences for series of nested primers: the LMB2, LMB3 and PIVB series.

All the constructs cloned in pIVEX bear a N-terminal Flag and a C-terminal HA tag.

2.2.1.3.2 pTrc 99A (Amersham Pharmacia Biotech)

p*Trc* 99A is a derivative of the pKK233-2 expression vector which has a strong *trc* promoter and a strong *rrn*B transcription termination signal downstream. The vector provides a ribosome-binding site and confers resistance to 100 μg ml^{-1} ampicillin.

2.2.1.3.3 pHLT

pHLT is a homonym for a pRSET-A-derived (Novagene) vector designed for high-level protein expression and purification from cloned genes in T7 promoter supportive *E. coli* strains (Dodd, Allen et al. 2004). The DNA inserts are positioned downstream and in frame with a sequence that encodes a 6xHis Tag followed by the hypersoluble Lipoyl Domain. When the polypeptide product is produced a Tobacco Etch Virus (TEV) protease cleavage recognition sequence (Polayes, Goldstein et al. 1994) is encoded between the Lipoyl Domain and the target. The vector provides a ribosome-binding site and confers resistance to 100 μg ml^{-1} ampicillin.

2.2.1.3.4 pMAL-c2g (New England Biolabs Inc.)

In pMAL-cg2, the cloned gene is inserted down-stream from the *malE* gene, which encodes maltose-binding protein (MBP). This results in the expression of an MBP-fusion protein, using a *ptac* promoter. Expression from the pMAL vectors has been proven to enhance the solubility of proteins expressed in *E. coli* (Kapust and Waugh 1999).

2.2.2 Methods

2.2.2.1 Polymerase Chain Reaction (PCR)

DNA was amplified and manipulated using the Polymerase Chain Reaction (PCR). Standard amplifications were carried out in final a volume of 50μl, typically containing: 5 – 50ng of template DNA, 12.5 mmoles of each dNTP, 25 pmoles of each primer, 5 units of Super*Taq* polymerase or 5 units of *Pfu* Turbo polymerase. In most cases, the thermal cycling was carried out on a DNA Engine PTC-200 Peltier Thermal Cycler (MJ Research) using the following program: 94°C for 3 minutes (step1); 94 °C for 1 minute (step2); 50 °C for 1 minute (step3); 72 °C for 1 minute (step4); repetition of steps 2 to 4 for 25 cycles; and 72 °C for 5 minutes. The reaction mix was then kept at 4 °C or –20 °C until needed.

PCR products were confirmed by DNA Electrophoresis (section 2.2.2.4).

2.2.2.1.1 PCR using DNA/beads as templates (bPCR)

Once the DNA-biotin had been purified and bound to streptavidin beads (section 2.2.2.8), bPCRs were carried out in final a volume of 200 µl, with 10 µl of DNA/beads, 50 mmoles of each dNTP, 100 pmoles of each primer, and 20 units of Super*Taq* polymerase, with the following thermal cycle: 94°C for 3 minutes (step1); 94 °C for 1 minute (step2); 50 °C for 1 minute (step3); 72 °C for 1 minute (step4); repetition of step 2 to 4 for 25 cycles; and 72 °C for 5 minutes. The reaction mix was kept at 4 °C or -20 °C until needed.

2.2.2.1.2 Inverse PCR (iPCR)

iPCR amplifications were carried out in final a volume of 50 µl, typically containing: 10 times more DNA template than for standard PCR (50-250 ng), 12.5 mmoles of each dNTP, 25 pmoles of each primer, and 5 units of Turbo*Pfu* polymerase. The thermal cycle was run on a DNA Engine PTC-200 Peltier Thermal Cycler (MJ Research) with the following program: 94 °C for 3 minutes (step1); 94 °C for 1 minute (step2); 50 °C for 1 minute (step3); 72 °C for 7 minute (step4); repetition of step 2 to 4 for 25 cycles; and 72 °C for 7 minutes. The reaction mix was then kept at 4 °C until needed.

2.2.2.2 Restriction endonucleases digestion

Restriction endonucleases were used according to the manufacturer's instructions. Digestions were done in a final volume of 80 µl.

2.2.2.3 DNA ligation for standard cloning

Standard sticky-end ligations were performed using T4 DNA ligase in a final volume of 10 – 30 µl. Typically, 0.6 – 2.5 ng (0.5 – 1.8 pmoles if 1000 bps) of insert and 0.2 – 1 µg of vector were used. Vector to insert ratios ranged from 1:3 to 1:10. Negative

control reactions containing vector DNA only were included. The ligation mixtures were left at room temperature for 2 hrs or overnight at 16 °C. A variation of this protocol was used for ligation of libraries into vectors (see section 2.2.2.10.3).

2.2.2.4 DNA electrophoresis

In order to resolve a mixture of DNA by weight (typically ranging between 0.4 and 5 kbps), the DNA solution was subjected to electrophoresis at a constant current of 100mA in a 1 – 2 % (w/v) agarose, 2 ng/ml ethidium bromide gel made with 1x TBE buffer. Hyperladder I from Bioline was used as DNA molecular weight marker.

2.2.2.5 DNA quantification

Concentrations of plasmid DNA were measured by UV light absorption at 260nm using a Nanodrop (Nanodrop Technologies). 1 OD_{260nm} = 50 μg dsDNA was assumed.

2.2.2.6 DNA Purification by electrophoresis

After standard electrophoresis (section 2.2.2.4), the bands were visualised under UV light and those of correct size were excised, and purified using a Qiagen Gel Extraction Kit according to the manufacturer's instructions.

2.2.2.7 DNA Purification using affinity columns

To remove salt, buffer, and proteins from a solution containing DNA, a Qiagen PCR Purification Kit was used according to the manufacturer's instructions.

2.2.2.8 DNA purification by biotin/streptavidin coupling

2.2.2.8.1 DNA capture on beads

50 µl (500 µg per binding reaction) of M280 Streptavidin Dynabeads (Dynal)[21] were washed twice with 200 µl 2x W+B solution, and resuspended in 50 µl 2x W+B solution. The washed beads were added to each PCR / ligation and transfer to clean 1.5 ml microtubes. The mixture was incubated for 2 hours at 37 °C with a ten second mixing step of 1400 rpm, every minute using, a Thermomixer comfort (Eppendorf).

2.2.2.8.2 Bead washing

Each tube containing the DNA-beads was washed three times with 200 µl 2x W+B solution and twice with 200 µl 1x PCR buffer without $MgCl_2$. The beads were resuspended in 40 µl of 1x PCR buffer with $MgCl_2$ (1.5 mM final concentration).

2.2.2.9 Point-mutants constructions

Complementary primers containing the desired mutation were used in a iPCR with methylated dsDNA as template (plus a non-template control). After competition of the PCR, mixtures were incubated with 1 µl of DpnI at 37 °C for 1 – 3 hrs to remove residual (methylated) parental DNA. 1 µl was used to transform 100 µl of *E. coli* XL1-Blue cells. Plasmid DNA were extracted and sent for sequencing.

2.2.2.10 Construction of libraries

DNA Libraries were constructed using reverse and complementary oligonucleotides bearing a recognition site for the restriction endonuclease BbsI or its isochizomer BpiI (Figure 6). In all library constructions, the pIVEX vector was used as template. pIVEX contains adjacent primer binding regions flanking regions up- and downstream of the cloned gene, allowing the usage of nested primers series; LMB-2, PIVP and LMB-3.

2.2.2.10.1 Construction of single-region libraries

21 100 µl (500 µg) of Dynabeads (3.35 x 10^6 beads) binds ~10 pmoles 1kb DNA (6 x 10^{12} molecules) or 5 pmoles of a 2-4kb dsDNA (3 x 10^{12} molecules). Hence, 50 µl should bind 5 pmoles 1kb dsDNA (3 x 10^{12} molecules).

Using a standard PCR procedure (section 2.2.2.1), DNA fragments were created up- and downstream from the regions to be randomised. Triple biotinylated upstream primers (LMB2 series) were used, resulting in PCR products bearing these probes. After purification with a PCR Purification Kit (Qiagen), the PCR products were incubated with 20U of BbsI or BpiI enzyme in a final volume of 80 µl for 3 hrs at 37 °C. After purification using a PCR Purification Kit (Qiagen), the digested fragments were mixed in equimolar ratios (typically 10 pmoles in 50 µl) and incubated with T4 Ligase for 16hrs at 10 °C (or for 30 hrs at 4 °C). The ligation products were by purified capturing the biotin tags with streptravidin coated beads (section 2.2.2.8). The DNA was recovered and reassembled from the beads with an additional PCR (section 2.2.2.1.1).

Nested primers, both up- and downstream, were used in every PCR step. The final PCR had to be scaled up prior to ligation into the vector, in order to produce sufficient material (~30 µg) for the ligation.

2.2.2.10.2 Construction of multiple-region libraries

For most of the libraries created, more than one region had to be randomised. When two regions needed to be targeted, two consecutive single-region library construction steps (section 2.2.2.10.1) were needed. However, when three regions had to be diversified, several single-region library construction steps were merge to keep the rounds of PCR to a minimum (Figure 7).

2.2.2.10.3 Cloning of libraries into vector

In order to increase the transformation efficiency of libraries into bacteria, ligations of constructed libraries into vectors were performed as follows. Ligations were performed using 2 units T4 DNA ligase in a final volume of 500 µl. Typically, 10 – 35 µg (6 – 24 pmoles if 1000 bps) of insert and 4 – 18 µg of vector were used. Vector to insert ratios were 1:3. The ligation mixtures were left at 10 °C for 16 hrs or at 4 °C for 36 hrs.

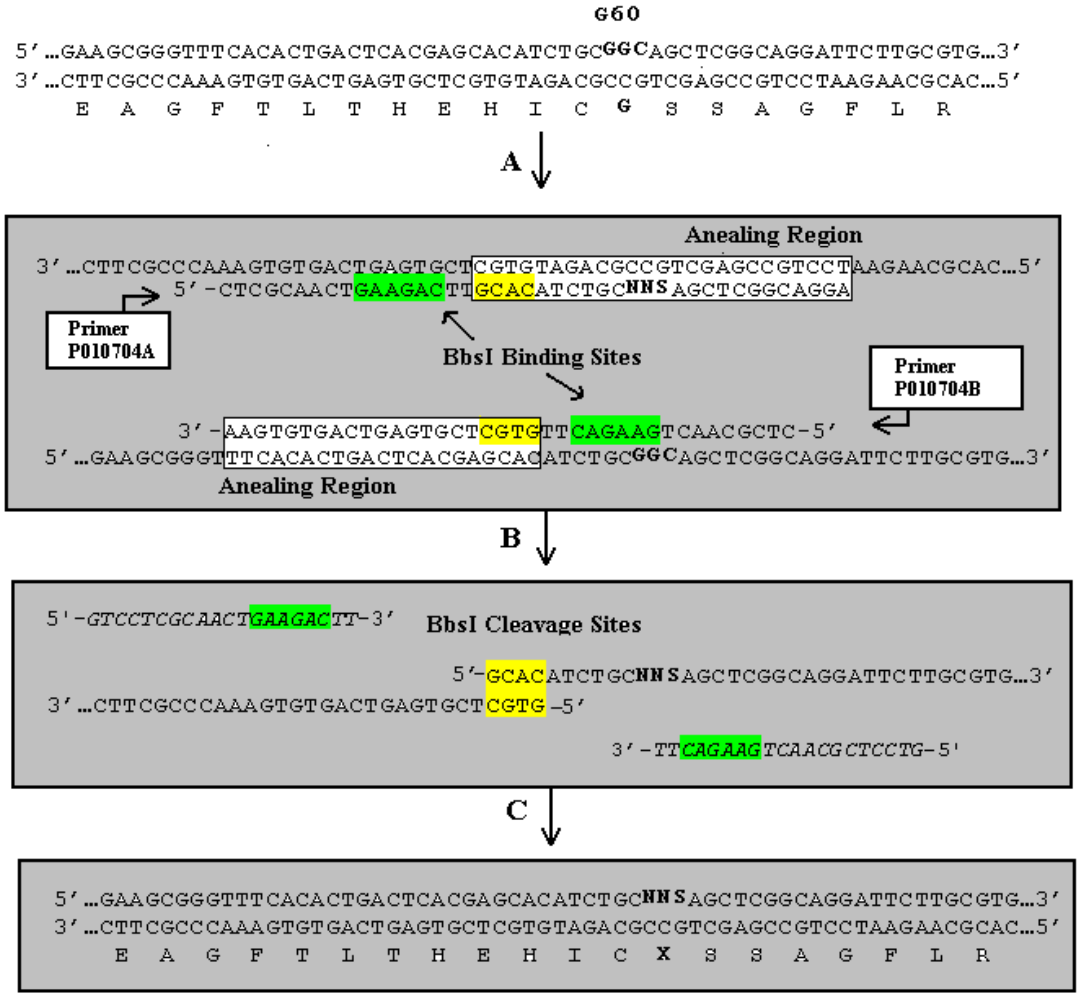

Figure 6. Library construction by ligation of reverse and complementary oligonucleotides. (A) Two sets of primers were designed (P010704A and P010704B) to anneal to adjacent regions near the codons to be modified (in this case G60). These primers contained a BbsI restriction endonuclease recognition site, and one of them (P010704A) consists of mixed oligonucleotide population bearing codon targeted diversity. Using separate PCRs and a set of complementary primers (not shown), two complementary *opd* regions were created. **(B)** By digesting with BbsI, both the creation of sticky-ends (used in a subsequent product ligation), and the removal of the self-adhering endonuclease binding site were ensured. **(C)** A final PCR reassembled and amplified the ligated products, resulting in an *opd* population with targeted diversity.

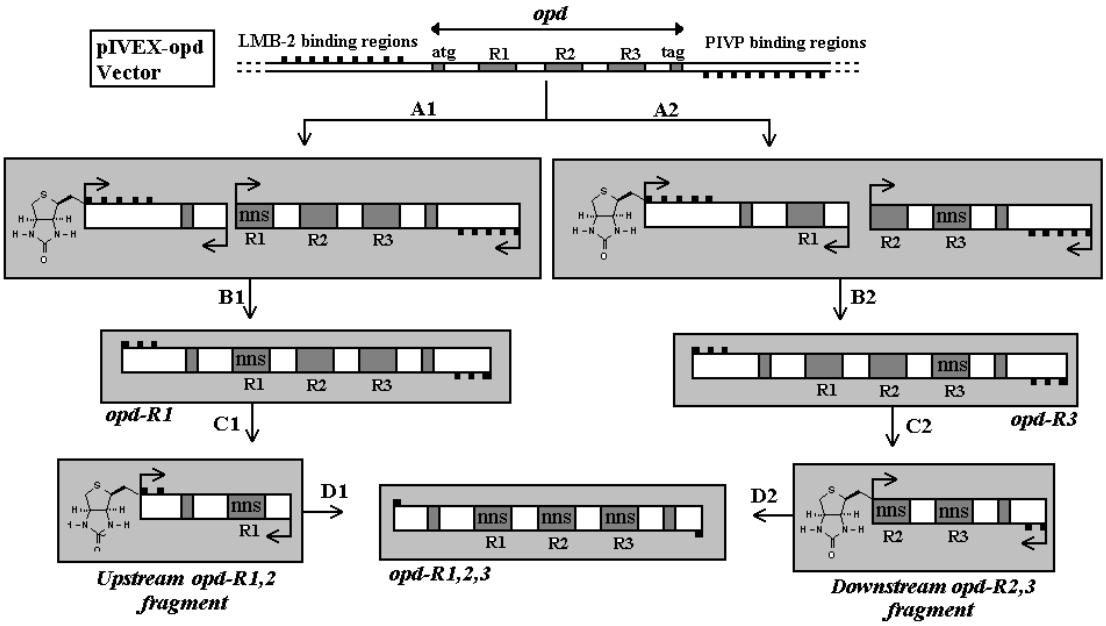

Figure 7. Mutiple-sites library construction. Schematic representation of the vector pIVEX-OPD and the primer binding regions flanking the *opd* gene. R1, R2 and R3 represent three regions to be diversified. Steps A1, B1 and A2, B2 show the two parallel single-region library construction steps (section 2.2.2.10.1) of the R1 and R3 regions. Once these two sets of genes were reassembled, each was used to generate the up- and downstream fragments of R3 the same manner as used for construction of the single-region libraries.

2.2.2.11 DNA sequencing

Typically, 500 ng of dsDNA were sent to MRC Geneservice (Hinxton, UK) or Lark (Lark Technologies Inc.). Whenever necessary, 100 pmoles of primers were included (Table 6). (See section 2.5.1.2 for sequence analysis).

2.3 Protein Biochemistry

2.3.1 Materials

Paraoxon, Coumaphos and Protamine sulphate salt were purchased from SIGMA-Aldrich (Dorset, UK). Dimethylformamide (DMF), Calcium Chloride ($CaCl_2$), Zinc Chloride ($ZnCl_2$), Phosphate Buffers, Imidazole, Sodium Chloride and Sodium Sulphate from BDH Laboratory Supplies (Leicester, UK). Ampicillin sodium salt,

isopropyl β-D-thiogalactoside (IPTG), N-2-Hydroxyethyl piperazine N'-2-2ethanesulfonic acid sodium salt (HEPES sodium salt), and Dithiothreitol (DTT) from Melford Laboratories (Chelsworth, UK). N-2-hydroxyethyl piperazine N'-2-2ethanesulfonic acid (HEPES) and Sodium Chloride (NaCl) from Fisher Scientific (Loughborough, UK). Centriprep concentrators were from Millipore (Bedford, MA, USA). Minisart HighFlow filters were from Sartorius (Gottingen, Germany). Dialysis membranes came from Spectrum (Houston, TX, USA), Novex pre-casted gels, and MES buffer were from Invitrogen (Paisley, UK). Ultra pure Guanidinium hydrochloride was from ICN Biomedicals Inc. (Ohio, USA). Vivas 20 ml Concentrators were from VivaScience (Hanover, Germany). BCA Protein Assay Kit was from Piece (Cramlington, UK).

2.3.1.1 Buffers and Solutions

Table 12. Protein Biochemistry Buffers and Media

Name	Receipt
2x SDS Sample Loading Buffer	10 mM Tris-HCl pH 6.8, 10 % (v/v) glycerol, 2.5% (w/v) SDS, 5% (v/v) 2-mercaptoethanol and 0.001% (w/v) bromophenol blue
Coomassie Blue Staining Solution	50 % (v/v) ethanol, 10 % (v/v) acetic acid, 0.2 % (w/v) Coomassie Blue R250
Destaining Solution	25 % (v/v) ethanol, 10 % (v/v) acetic acid
Ni-Lysis Buffer	50 mM Potassium phosphate (KP_i), 300 mM NaCl, 10 mM Imidazole pH=8.0
Ni-Elution Buffer	50 mM Potassium phosphate (KP_i), 300 mM NaCl, 250 mM Imidazole pH=8.0
Inclusion Body Resuspension Buffer	50 mM HEPES pH=8.0
Inclusion Body Isolation Buffer	50 mM HEPES pH=8.0, 500 mM NaCl, 1% (v/v) Triton X-100 pH=8.0
Inclusion Body Denaturation Buffer	6 M GdmHCl, 50 mM HEPES pH =8.0, 500 mM NaCl, 1 mM 2-mercaptoethanol, 50 μM $ZnCl_2$
Refolding Buffer	50 mM HEPES pH =8.0, 5 mM DTT, 50 μM $ZnCl_2$

2.3.2 Methods

2.3.2.1 Protein expression (after Sonication)

The sonicated crude lysates (section 2.1.2.7.1) were centrifuged at 15,000 rpm for 20 minutes using a Sorvall SS34 rotor at 4 °C. The supernatants were filtered using a 0.2 μm Stericup^{TM} disposable vacuum filter device (Millipore), and kept on ice.

2.3.2.2 Protein purification

Two different strategies were used when purifying PTE and its variants. **(1)** Fractionating crude lysates with Protamine and ammonium sulphate salts, followed by gel filtration and anion exchange chromatography. **(2)** Using N-terminal His-tagged constructs with a Nickel-NTA affinity column.

For the purification of PONs, crude lysates were received in ammonium sulphate from Dr. Dan Tawfik [22]. The lysates were further processed, and PONs were batch-purified by Nickel-NTA affinity in batch.

2.3.2.2.1 *Omburo* method

The method describe in Omburo (Omburo, Kuo et al. 1992), was employed to purified PTE and PTE-5 (Chapter 3). The following modifications were included.

2.3.2.2.1.1 Protamine sulphate

Protamine sulphate salt (Grade X, from Salmon) solution was added dropwise, with stirring, at room temperature to a pre-filtered cell crude lysate. Once the desired final concentration was reached 4% (v/v), the mixture was left incubating for a further 30 minutes. The precipitates were removed from the soluble fraction by spinning at 10,000 rpm in a SLA3000 Sorvall rotor at 4 °C.

2.3.2.2.1.2 Ammonium sulphate

Saturated ammonium sulphate solution was added dropwise, with stirring, at room temperature, to the soluble fraction obtained after the protamine sulphate fractionating. The volume of solution of ammonium sulphate needed to reach a final 45% (v/v) concentration (V) was calculated using the formula $V = V_1 (S_2-S_1) (1-S_2)^{-1}$, where S_1 (= 0), S_2 (= 0.45), and V_1 were the initial and final ammonium sulphate concentration, and the initial sample volume, respectively. After all the ammonium sulphate had been added, the mixture was further incubated for an hour. The precipitates were collected from the soluble fraction by spinning at 10 krpm in a SLA3000 Sorvall rotor, and resuspended in 10 ml of ice-cold 50 mM HEPES pH 8.5, 0.2 μm filtered, and kept on ice.

22 Department of Biological Chemistry, The Weizmann Institute of Science, Rehovot 76100, Israel.

2.3.2.2.2 Gel filtration

Using a Pharmacia low pressure system, a 4 – 7 ml preparation was put through a Superdex-75 column (Pharmacia – Pfizer) equilibrated with 50 mM HEPES pH 8.5, 50 mM NaCl. Fractions were analysed by PAGE (section 2.3.2.5.1) and pooled based on absorbance at 280nm and enzymatic activity (hydrolysis of 0.25 mM Paraoxon, as described in section 2.3.2.5.3).

2.3.2.2.3 Perfusion chromatography

Using a Vision ™ WorkStation (Applied Biosystems), the pooled fractions were loaded into POROS ® 20HQ and 20PI Perfusion Chromatography columns in tandem, pre-equilibrated with 50 mM HEPES pH 8.5, and eluted with a linear NaCl gradient of 0 - 400mM over 50 column volumes. The elution buffer was exchanged to 50 mM HEPES pH 8.5, 50 mM NaCl, using Centricon bench centrifuge filters with a 10kDa cutoff. Proteins were quantified and a purity above 90% was verified by PAGE (section 2.3.2.5.1). Aliquots were dispensed, fast frozen in liquid nitrogen, and stored at –80 °C for subsequent use.

2.3.2.2.4 Purification of PONs

PONs cloned into a pET32-trx (Novagen) system were expressed in *E. coli* Origami B DE3 (Novagen). Cell pellets were harvested and resuspended in 50 mM Tris pH=8.0, 1mM $CaCl_2$, 50mM $NaCl_2$, 0.1 mM DTT, and 1μM Pepstatin A (PL Buffer). Cells were lysed by sonication and the recovered supernatant incubated with 0.1% (v/v) Tergitol for 2.5 hrs. The solutions were further fractionated with 55% (w/v) ammonium sulphate, and the pellets stored at 4 °C. Up to this point, the process was by Dr. Leonid Gaidukov in Dr. Dan Tawfik's laboratory [22].

The pellets were resuspended in ice cold PL Buffer with 0.1% (v/v) Tergitol, and dialysed consecutively against PL Buffer and then 50 mM Tris pH=8.0, 1mM $CaCl_2$, 50mM $NaCl_2$, 0.1% (v/v) Tergitol (PA Buffer), at 4 °C. The solutions were incubated with 2 ml Ni-NTA Resin slurry (Qiagene) in 300mM NaCl, 20mM Imidazole, PA Buffer, at 4 °C for 16hrs. The resin was further washed with 300mM NaCl, 35mM Imidazole, PA Buffer and eluted with 150mM Imidazole, PA Buffer. The eluted fractions were dialysed against PA Buffer, supplemented with 0.02% (w/v)

sodium azide, and stored at 4 °C. Proteins were quantified by BCA Protein Assay Kit, and analysed by SDS PAGE.

2.3.2.3 His-Tag affinity method

2.3.2.3.1 First Ni-NTA column

The filtered supernatant, product of autoinduction (section 2.1.2.6.2), were loaded through pumps onto a 25 ml Nickel-NTA (Qiagen) column equilibrated with Lysis Buffer using a Pharmacia low pressure system at a flow rate of 5 ml min^{-1}. The protein was eluted using Ni-Elution Buffer while 8 ml fractions were collected. These fractions were analysed by SDS PAGE and for enzymatic activity (hydrolysis of 0.25 mM Paraoxon). Fractions containing the target construct were pooled (typically ~24 ml total). 1 mg of TEV protease (produced according to manufacturer's specifications) per 50-200 mg of protein was added to samples and dialysed using a Spectra/Por 3 Membrane MWCO=3.5 kDa against 1000x sample volume of Lysis Buffer at 4° C for 16 hrs.

2.3.2.3.2 Second Ni-NTA column

The dialysed samples were 0.2 μm filtered and loaded through pumps onto a 25 ml Nickel-NTA (Qiagen) column equilibrated with Lysis Buffer using a Pharmacia low pressure system at a flow rate of 5 ml min^{-1}. Flowthough fractions were collected and analysed by SDS PAGE and for enzymatic activity (hydrolysis of 0.25 mM Paraoxon). Fractions containing the target construct were pooled, concentrated and buffer exchanged with 50 mM HEPES pH 8.0 using a 20 ml Vivaspin concentrator membrane. The preparation was divided into 1 ml aliquots, flash frozen and stored at -80 °C.

2.3.2.4 Protein Refolding

2.3.2.4.1 Inclusion body preparation

Two litres of *E. coli* C41 / pIVEX-PTE-K169GE (PTE-G1) were grown, induced and harvested as described in section 2.1.2.6.1. Cell pellets were resuspended in 80 ml

Inclusion Bodies Resuspention Buffer, sonicated on ice for 2 minutes (10s on, 30s off) and spun at 15,000 rpm for 20 minutes in a Sorvall® RC 3B cooled to 4 °C. The pellets obtained were resuspended in 50 ml ice cold Inclusion Body Isolation Buffer, sonicated on ice for 2 minutes (10s on, 30s off) and spun at 15,000 rpm for 20 minutes in a Sorvall® RC 3B pre-cooled to 4 °C. These second pellets were resuspended in 50 ml ice cold Inclusion Body Denaturation Buffer, stirred for 60 minutes at room temperature, spun at 15,000 rpm for 20 minutes in a Sorvall® RC 3B, pre-cooled to 4 °C, and filtered using a 0.45 μM Stericup^{TM} disposable vacuum filter device (Millipore).

2.3.2.4.2 Refolding by *Infinite* Dilution

0.5 ml of denatured inclusion bodies was added dropwise, with stirring, to 2 litres of cold Refolding Buffer. After completion, the refolded material was filtered using a 0.45 μM StericupTM disposable vacuum filter device (Millipore) and loaded at a flow of 5 ml min^{-1} onto a Hi-Trap column pre-equilibrated with Refolding Buffer. The column was eluted with 10 ml of Refolding Buffer containing 500 mM NaCl. Loaded, flowthough and eluted fractions were collected and analysed by SDS PAGE.

2.3.2.4.3 Refolding by Dialysis

45 ml of denatured inclusion bodies were dialysed stepwise against 250 ml of Refolding Buffer with 5, 4, 3.5, 2 and 1 M of GdmHCl. Each dialyses step was left to equilibrate for 4 to 8 hours at 4 °C.

2.3.2.5 Protein characterisation

2.3.2.5.1 Polyacrilamide gel electrophoresis (PAGE)

For routine analysis of protein expression and purification, proteins were resolved using Novex NuPAGE pre-cast gels (Novagene) (12% or 4-12% (v/v) Bis-Tris) using MOPS or MES as running buffer. Crude lysates of pIVEX-Δ*opd* cloned into *E. coli* C41 and pTrc-99a-IGPS cloned into DH5a, were used as gel controls whenever cells

lysates were analysed by gel. Gels were stained with Coomassie Blue staining solution for 10 minutes at room temperature before been transferred to destaining solution.

2.3.2.5.2 Protein quantification

2.3.2.5.2.1 Spectrophotometric technique

The concentration of PTE variants was measured spectrophotometrically measuring AU_{280nm}. The molar extinction coefficient at 280nm (ε_{280}) was calculated from its amino acid sequence (Pace, Vajdos et al. 1995): $\varepsilon_{280} = a \cdot \varepsilon_{280}^{Trp} + b \cdot \varepsilon_{280}^{Tyr} + c \cdot \varepsilon_{280}^{Cys}$ where a, b and c are the number or Trp, Tyr and Cys residues in the protein and ε_{280}^{Trp}, ε_{280}^{Tyr}, and ε_{280}^{Cys} are the molar extinction coefficients of Trp, Tyr and Cys respectively.

2.3.2.5.2.2 Colorimetric assay

Given that the detergent used to keep PONs in solution absorbs at 280nm (1% (v/v) Tergitol), PONs were quantified using a bicinchoninic-acid based (BCA) colorimetric assay (PIERCE) (Smith, Krohn et al. 1985). BSA was used to produce a standard curve; it was prepared by 2-fold serial dilutions of a 10mg/ ml stock provided by the manufacturer (AU_{562nm} = 0.61±0.01 mg ml^{-1}). Microplates were used to make endpoint readings at 562nm, with a path of 0.5 cm. Three independent protein measurements were averaged.

2.3.2.5.3 Determination of k_{cat} and K_M (Paraoxon)

The hydrolysis of Paraoxon was followed by the change in absorbance at 405nm using a SpectraMAX 190 Microplate reader (Molecular Devices) at 25 °C. Initial velocities were measured at different final Paraoxon concentrations (typically ranging from 2 nM to 5 mM) with a fixed amount of enzyme. The kinetics parameters k_{cat} and K_M were obtained by plotting substrate concentration versus initial rates. The data was non-linearly fitted to Michaelis-Menten equation ($v / [E_o] = [S] k_{cat} / [S] + K_M$) using Origin™ (Microcal Software Inc).

2.3.2.5.4 Determination of k_{cat} / K_M (Nerve agent analogues)

The hydrolysis of the nerve gas analogues was followed by change in fluorescence at 460 nm (ex. = 355 nm, cutoff = 455 nm) using a SpectraMAX GeminiXS Microplate reader (Molecular Devices) at 25 °C. Initial velocities were measured at five different final substrate concentrations (0.5, 1, 1.5, 2, 2.5 μM) with amounts of enzyme that ensured reliable signal. As [S] << K_M, the k_{cat} / K_M values were obtained by plotting substrate concentration versus initial rates (v / [Eo] ≈ [S] (k_{cat} / K_M). 50 mM HEPES pH 8.0 was used as base buffer, and DMF was present at a final concentration of 1% (v/v) whenever mention.

2.4 Organophosphorus (OP) chemistry

2.4.1 Safety Measures

Manipulation of OP compounds was done in the chemical fume hood. Double Nitrile / Latex gloves, laboratory coat and safety glasses were worn at all times. All the consumables in direct contact with OPs were incubated for 1 – 24 hrs with freshly prepared liquid bleach, before disposal in closed containers as for bioharzard materials. Spills were cleaned with 4M NaOH or liquid bleach, and rinse with an excess of 50% ethanol. Non-disposable consumables were treated with a 70 μM solution of PTE (85% pure) in 50 mM HEPES pH 8.5 for 24 – 48 hrs, before rinsing with an excess of 50% ethanol. It has been reported that organic solvents (isopropanol) have little or no effect on the absorption rate of NAs (VX) (Lundy 2004).

2.4.2 Materials

Coumaphos was obtained from SIGMA-Aldrich (Dorset, UK). 96-half area acrylic UV-transparent plates were from Corning Incorporated (Aberdeen, UK). Dimethylformamide (DMF) and Ethanol was from BDH Laboratory Supplies (Leicester, UK). The nerve agent 3-chloro-7-hydroxy-4-methylcoumarin fluorogenic analogues were synthesised and provided by Dr. Christopher M. Timperley's group at

the Defence Science and Technology Laboratory, Chemical and Biological Defence Sector, Porton Down, Salisbury, Wiltshire, SP4 0JQ, UK.

2.4.3 Methods

2.4.3.1 Quantification

Paraoxon stocks were prepared in 100% (v/v) DMF, and its concentration determined by absorbance at 274 nm (ε_{274} = 8.9 x 10^3 M^{-1} cm^{-1}). For the quantification of the fluorogenic nerve gas analogues, their absorbance at 315nm in 100% (v/v) DMF was averaged from two fold dilutions and compared against a standard curve obtained using commercially available Coumaphos (ε_{315} = 8.9 x 10^3 M^{-1} cm^{-1}) (**Figure 8**). This latter was done by measuring 80 µl samples in 96-half area acrylic UV-transparent plates (Corning) using a SpectraMAX 190 Microplate reader (Molecular Devices) at 25 °C.

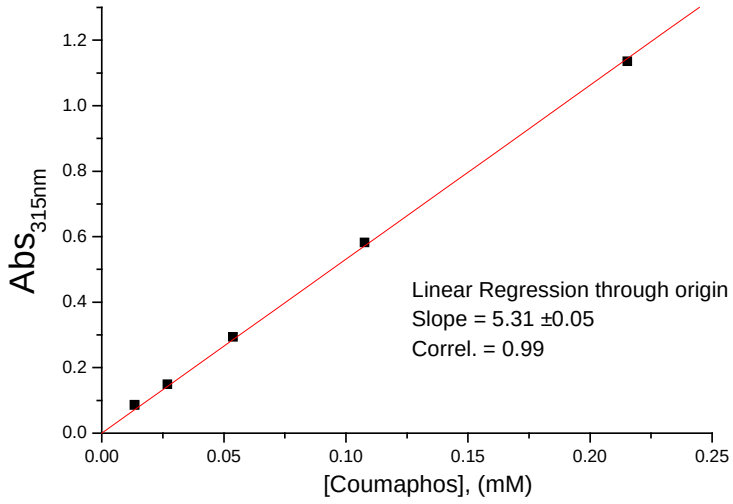

Figure 8. Standard Curve for quantification of nerve gas analogues.

2.5 Bioinformatics

2.5.1 Materials

2.5.1.1 Data Manipulation

Data manipulation was done using Microsoft ® Excel (Microsoft 1999). Non-linear fit and data imaging were done using Origin™ (Microcal Software Inc).

2.5.1.2 DNA and Protein Sequence Manipulation

DNA and Protein sequences were analysed using MacVector™ software (Oxford Molecular) and Microsoft ® Word (Microsoft 1999). For multiple protein sequence alignment, BioEdit Sequence Aligment Editor (Hall 1999) was used and the phylogenetic tree generated by PhiloWin (Galtier and Gouy). Protein genes were retrieved using *Entrez* (National Center for Biotechnology Information). The protein entries in the Entrez search and retrieval system are compiled from a variety of sources, including SwissProt (Swiss Institute of Bioinformatics and The European Bioinformatics Institute), Protein Information Resource (National Biomedical Research Foundation, Georgetown University Medical Center), Protein Research Foundation Protein Research Foundation (JAPAN), RCSB Protein Data Bank, and translations from annotated coding regions in GenBank (NCBI) and Reference Sequence collection (NCBI). A copy of Codon Controller was a gift from Paul H. Dear, MRC-LMB, Cambridge, UK (Dear 1999).

2.5.1.3 Manipulation and Imaging of Protein Structure

Protein structures were manipulated and visualised with Deep View / Swiss-Pdb Viewer v3.7 (Guex, Peitsch et al. 2001) and RasWin v.2.6-ucb (Sayle 1995). Protein images and rendering were generated with PyMOL v0.95. (Delano 2004).

2.5.1.4 Text Manipulation

The present dissertation was typed using Microsoft ® Word (Microsoft 1999).

Chapter 3 Hydrolysis of Fluorogenic Nerve Agents Analogues by Organophosphatases

3.1 Introduction

In this chapter, the testing of 12 fluorogenic nerve agent (NA) analogues, with a 3-chloro-7-hydroxy-4-methylcoumarin leaving group, as suitable substrate for PTEs and PONs is described. Included in this series were the analogues of the pesticides Paraoxon and Parathion, and the chemical warfare agents DFP, Dimefox, Tabun, Sarin, Cyclosarin, Soman, VX, and Russian-VX . These chemical surrogates have a similar structure but do not share the same physico-chemical properties as the nerve agents themselves (Figure 9).

The enzymes employed were PTE-wt, and its variant H5 (I106T/F132L) (Griffiths and Tawfik 2003); a high-yield, soluble PON1, (G3C9 in (Aharoni, 2004) and two variants of the latter, 2.4PC (L69V/S193P/V346A) and 3.2PC (L69V/S138L/S193P/N287D). The departure of the coumarin group allowed acquisition of kinetics data by measurement of fluorescence. The results of this chapter comprised the first step towards the development of a systematic high-throughput screen for PTE variants capable of hydrolysing NAs efficiently.

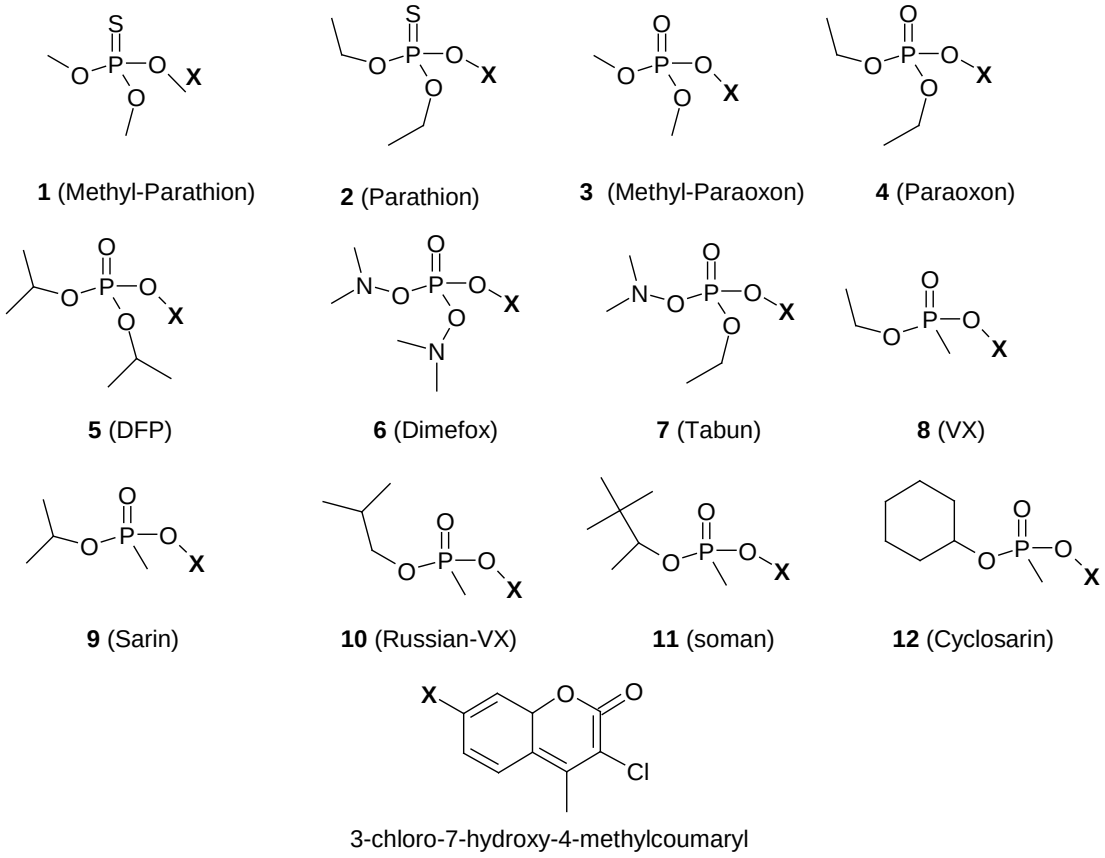

Figure 9. Fluorogenic nerve agent analogues. This set of compounds were synthesised and provided by Dr. Christopher M. Timperley [23]. The name of the parental nerve agent is given in parentheses.

3.2 Results

3.2.1 Protein production, purification, and quantification

3.2.1.1 Bacterial phosphotriesterases: PTE and PTE-H5

E. coli C41 cells were transformed with pIVEX-PTE and pIVEX-PTE-H5 plasmids. Cells were grown, induced, and harvested as described in section 2.1.2.6.1. Cell pellets were sonicated (see section 2.1.2.7.1), and crude lysates of PTE and PTE-H5 recovered (see section 2.3.2.1). PTE and PTE-H5 were purified using protamine and

23 Defense Science and Technology Laboratory, Chemical and Biological Defence Sector, Porton Down, Salisbury, Wiltshire, SP4 0JQ, UK.

ammonium sulphate fractionation, followed by a gel filtration and anion exchange chromatography steps (section 2.3.2.2.1) (Figure 10.A). PTE and PTE-H5 were quantify by absorbance at 280nm (section 2.3.2.5.2.1), while a purity above 95% was verified by PAGE (Figure 10.B). Aliquots were dispensed, fast frozen in liquid nitrogen, and stored at –80 °C for later use.

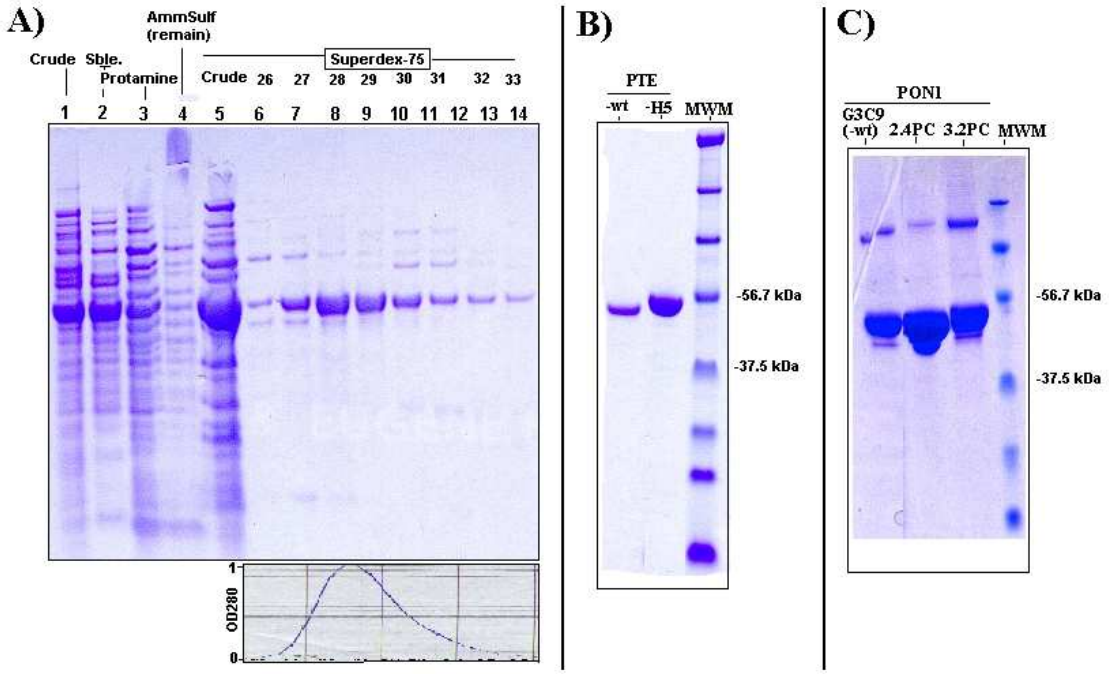

Figure 10 . PTE and PONs aliquots, obtained during purification process, and run on a 12% Bis-Tris SDS-PAGE gel with MOPS Buffer. **(A)** PTE-H5 purification process. Lane 1, crude cell lysate. Lane 2, lysate soluble fraction (after Sonication). Lane 3, Protamine sulphate fractionating. Lane 4, ammonium sulphate soluble fraction (waste). Lane 5, resuspended ammonium sulphate precipitate. Lane 6 to 14, Superdex-75 fractions (with the elution profile in the bottom inset). After the Gel Filtration, the samples were put through two anionic exchange columns, in tandem (not shown). **(B)** PTE and PTE-H5 after purification, **(C)** PONs after purification.

3.2.1.2 Mammalian PONs: PON1-wt, 2.4PC and 3.2PC

PONs crude lysates were received in ammonium sulphate from Dr. Dan Tawfik [22]. The lysates were further processed, and PONs were purified by Nickel-NTA affinity in batch (section 2.3.2.2.4). Purity of ~90% as ensured by PAGE (Figure 10.C). PONs were quantified using BCA Protein Assay Kit (see section 2.3.2.5.2.2).

3.2.2 k_{cat} and K_M for Paraoxon

The NA analogues, have poor aqueous solubility. However, 1% (v/v) dimethylformamide (DMF) in the reaction buffer solubilised enough substrate to allow accurate measurements [24]. To assess the effect of 1% (v/v) DMF on the performance of the enzymes, their kinetics parameters with Paraoxon as substrate were determined in the presence and absence of DMF (Figure 11). As shown in Table 13, 1% (v/v) DMF in the reaction mixture tends to increase the K_M, but not to any significant degree.

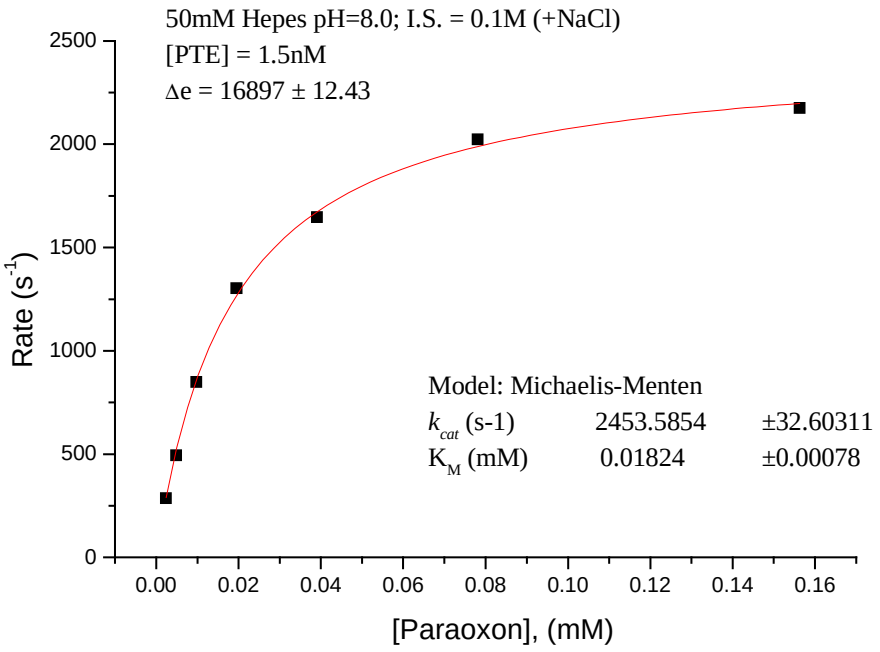

Figure 11. Dependence of PTE activity rate on Paraoxon concentration. The hydrolysis of Paraoxon was followed by the change in absorbance at 405nm at 25 °C. The kinetic parameters, k_{cat} and K_M, were obtained by non-linear fitting to Michaelis-Menten equation (v / [Eo] = [S] k_{cat} / [S] + K_M) (see section 2.3.2.5.3). The reaction was done in 50 mM HEPES pH = 8.0; Ionic Strength = 0.1 M (adjusted with NaCl), with an enzyme concentration of [PTE] = 1.5 nM.

24 up to ~10 μM of Coumaphos.

Table 13. Effect of 1% (v/v) DMF on the kinetics parameters for the hydrolysis of Paraoxon.

Enzyme	DMF (v/v)	k_{cat} (s^{-1})	K_M (mM)	k_{cat}/K_M ($s^{-1}\,M^{-1}$)	$(k_{cat}/K_M)/(k_{cat}/K_M)^{1\%DMF}$
PTE-wt	-	2453 ± 33	0.018 ± 0.001	1.35 (±0.06) x10^8	1.8
	1%	2380 ± 60	0.031 ± 0.002	7.60 (±0.57) x10^7	
PTE-H5	-	9135 ± 272	0.81 ± 0.04	1.12 (±0.06) x10^7	0.6
	1%	9662 ± 156	0.53 ± 0.02	1.82 (±0.08) x10^7	
PON1-*wt*	-	5.12 ± 0.06	0.711 ± 0.027	7.20 (±0.28) x10^3	1.2
	1%	5.23 ± 0.09	0.888 ± 0.042	5.89 (±0.29) x10^3	
2.4PC	-	19.58 ± 0.49	1.124 ± 0.076	1.73 (±0.12) x10^4	1.1
	1%	18.72 ± 0.63	1.142 ± 0.102	1.64 (±0.16) x10^4	
3.2PC	-	10.20 ± 0.09	0.237 ± 0.008	4.30 (±0.15) x10^4	1.1
	1%	10.59 ± 0.08	0.273 ± 0.008	3.88 (±0.12) x10^4	

3.2.3 k_{cat} / K_M for nerve agents analogues

The hydrolysis of the nerve gas analogues was followed by the change in fluorescence at 460nm (excitation = 350nm, cut-off = 455nm) at 25 °C (section 2.3.2.5.4). Initial velocities were measured at 0.5, 1, 1.5, 2, 2.5 μM final substrate concentrations. The amounts of enzyme were empirically determined to ensure a reliable signal. The initial rates obtained were linearly fitted to equation v / [Eo] ≈ [S] (k_{cat} / K_M) (see section 2.3.2.5.4) (Table 14).

Both PTE-wt and PTE-H5 were able to hydrolyse thiono **1**/Methyl-Parathion and **2**/Parathion with the latter being the best substrate for PTE. In general, PTE hydrolyses natural P=O better than unnatural P=S compounds (Horne, Sutherland et al. 2002). However, PTE-wt was found to hydrolyse analogue **2**/Parathion four times more efficiently than **4**/Paraoxon analogue.

Compounds which contained a dimethylamino substituent were hydrolysed poorly: analogues **6**/Dimefox and **7**/Tabun were much less reactive than the rest of the tested analogues.

Table 14. Efficiency of hydrolysis of substrates (k_{cat}/K_M in $s^{-1} M^{-1}$)

Compound	Analogue of	Structure of Analogue	PTE-wt	PTE-H5	PON1-wt	2.4PC	3.2PC
Paraoxon	-	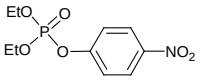	7.6(±0.6) x10^7	1.8(±0.1) x10^7	5.9(±0.29) x10^3	1.6 (±0.2) x10^4	3.9(±0.1) x10^4
1	Methyl-parathion	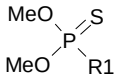	6.5(±0.5) x10^5	6.4(±0.4) x10^3	†	†	†
2	Parathion	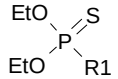	1.1(±0.1) x10^7	2.4(±0.6) x10^5	†	†	†
3	Methyl-paraoxon	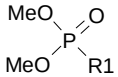	3.6(±0.3) x10^5	3.2(±0.2) x10^2	4.9(±0.3) x10^2	7.8(±0.4) x10^2	1.8(±0.1) x10^3
4	Paraoxon	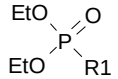	2.7(±0.3) x10^6	3.0(±0.2) x10^5	5.3(±0.2) x10^2	1.8(±0.1) x10^3	6.24(±0.1) x10^4
5	DFP	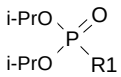	2.2(±0.2) x10^5	6.8(±0.4) x10^4	†	1.32(±0.1) x10^2	2.1(±0.1) x10^1
6	Dimefox	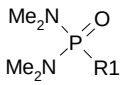	0.094 (±0.012)	†	†	†	†
7	Tabun	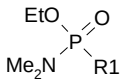	1.2(±0.1) x10^3	16(±2)	4.28(±0.1)	21(±0.2)	53(±0.5)
8	VX	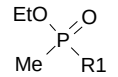	3.5(±0.1) x10^5	7.8(±0.3) x10^3	6.9(±0.1) x10^4	3.7(±0.1) x10^3	3.6(±0.1) x10^4
9	Sarin	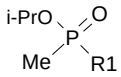	2.6(±0.1) x10^5	9.6(±1.6) x10^3	7.7(±0.2) x10^3	1.7(±0.1) x10^3	5.6(±0.1) x10^3
10	Russian-VX	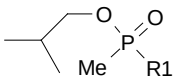	3.4(±0.2) x10^5	1.5(±0.1) x10^4	5.6(±0.1) x10^4	2.2(±0.1) x10^3	3.5(±0.1) x10^4
11	Soman	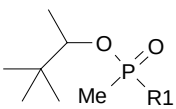	7.8(±0.5) x10^3	1.6(±0.1) x10^2	63(±0.3)	53(±0.1)	16(±0.5)
12	Cyclosarin	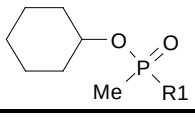	5.7(±0.1) x10^5	2.0(±0.1) x10^4	9.0(±0.1) x10^2	1.83(±0.1) x10^2	4.5(±0.1) x10^2

†, no activity detected. R1,3-chloro-7-hydroxy-4-methylcoumaryl .

The replacement of a *P*-alkoxy group with a *P*-methyl group resulted in substrates with lower reactivity towards the PTEs; diethyl phosphate bearing analogue, **4**/Paraoxon, was hydrolysed approximately 8 times faster by PTE-wt than the ethyl methylphosphono bearing analogue **8**/VX. Efficiencies of hydrolysis for analogues **8**/VX, **9**/Sarin, **10**/Russian-VX, and **12**/Cyclosarin were comparable. In contrast, the PTEs were much less efficient at hydrolysing **11**/Soman analogue, presumably because the binding pocket cannot easily accommodate the bulky pinacolyl side-chain.

Regarding PONs, analogues **3**/Methyl-Paraoxon and **4**/Paraoxon revealed the specialisation in which 2.4PC and 3.2PC were selected for, as the latter has a 100-fold higher k_{cat} /K_M (6.24 x 10^4 s^{-1} M^{-1}) than the PON1-wt. No activity was detected towards the **1**/Methyl-Parathion and **2**/Parathion analogues, highlighting these PONs can resolved between the oxon derivates from the thiono counterparts.

Like PTEs, PONs exhibited a low activity with compounds bearing dimethylamino groups (**6** and **7**). No activity was detected with PON-wt for **5**/DFP analogue; however, hydrolysis was detected with 2.4PC and 3.2PC enzymes. *P*-methyl groups were well accepted as substrates for PONs, in fact ethyl methylphosphono bearing, **8**/VX, was hydrolysed around 100 times faster by PON1-wt than diethyl phosphate bearing analogue, **4**/Paraoxon.

Overall, the replacement for a bulky side chains hinders PONs activity. Bearing the isobutyl group of **10**/Russian-VX analogue, the activity is comparable to ethyl bearing **8**/VX analogue. However, the activity drops 100-fold with the bulkier cyclohexyl moiety of **12**/Cyclosarin analogue, and 1000-fold less with the pinacolyl group of **11**/Soman analogue.

3.3 Discussion

The fluorogenic analogues proved to be suitable substrates for both types of organophosphatases used, bacterial phosphotriesterases (PTEs) and mammalian serum paraoxonases (PONs). Their catalytic specificities (k_{cat}/K_M) ranged across 10^8 M^{-1} s^{-1}, illustrating the functional and structural diversity of the NA analogues and the

promiscuity of these enzymes for such compounds. All the analogues were hydrolysed by PTE-wt, the most reactive being the **2**/Parathion analogue and the poorest the dimethylamino bearing analogues, **6**/Dimefox and **7**/Tabun. Compared with PTE-wt, the Paraoxon evolved variant PTE-H5, showed an overall diminished activity towards the NA analogues. PON1-wt hydrolysed non-bulky analogues with a good efficiency, and clearly distinguished the more toxic oxo phosphonates from the thio analogues. The PON1 evolved variants, 2.4PC and 3.2PC, acquired activity towards **4**/Paraoxon and **5**/DFP analogues, without compromising any of their "PON-wt" activity.

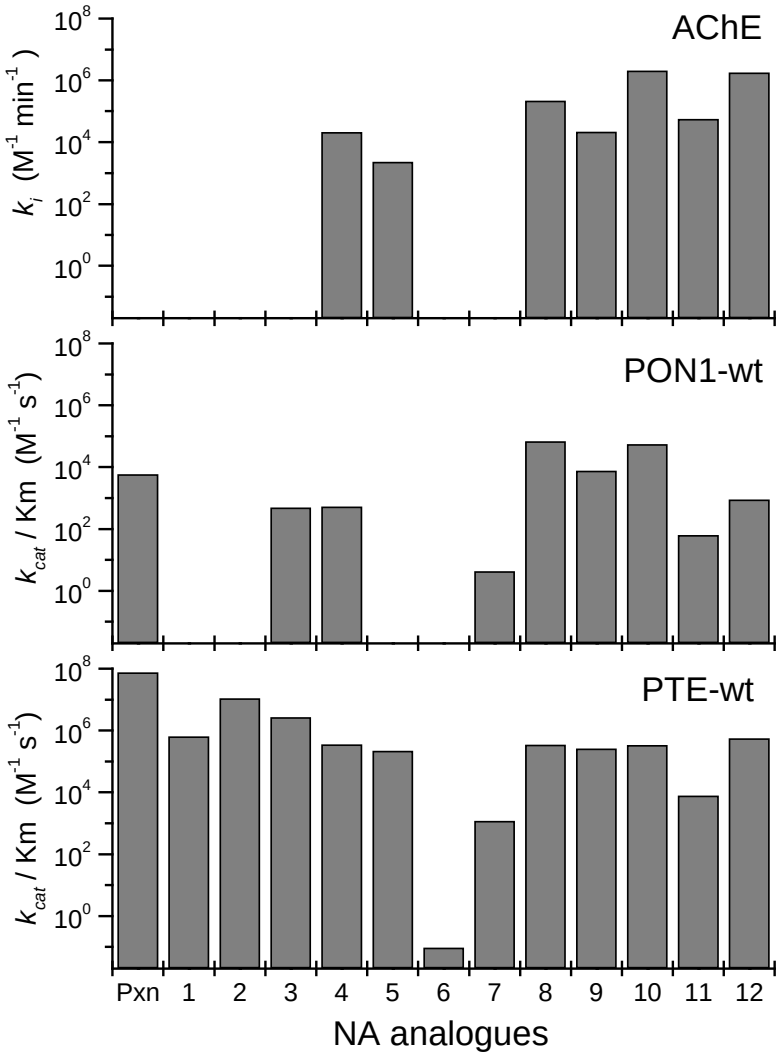

Figure 12. Activity profile of AChE, PTE-wt and PON1-wt with the NA analogues. AChE values were taken from Briseño-Roa (Briseño-Roa, Hill et al. 2004). Pxn, Paraoxon; N.D., not determined.

Collaborators have shown that AChE inhibition assays point to an overall congruency between the functionality of each NA and its analogue (Figure 12). The analogues are between 0.7 and 34-times less potent than the corresponding NA, while retaining the same relative inhibition potency order (Russian VX > Cyclosarin > VX > Sarin > Soman > DFP). The conspicuous exception is **7**/Tabun analogue, for which the lack of detectable inhibition reflects the great leaving facility of the cyanide group of Tabun. The *in vitro* AChE inhibition data is supported by the similar LD_{50} values obtained with Cyclosarin (0.06 mg/kg) and **12**/Cyclosarin analogue (0.4 mg/kg) upon subcutaneous administration in guinea pigs (Briseño-Roa, Hill et al. 2004).

The *in vitro* inhibition and *in vivo* toxicity data for AChE, strongly suggests that the NA fluorogenic analogues do mimic the neurotoxicity of their NA counterparts. In addition, the high sensitivity of the analogues in hydrolysis assays, combined with their low volatility compared to the NAs (data not shown), allows their safe manipulation using standard laboratory precautions for very toxic compounds.

It should be mention that all the compounds were assayed as racemic mixtures. This is relevant, as mention in section 1.3.4, some enantioners of NAs are known to be more toxic than others.

Chapter 4 Screening Platform for Organophosphatases Using Fluorogenic Substrates

4.1 Introduction

As it would be unfeasible to use nerve agents in any kind of high throughput procedure, due to their toxicity and other physicochemical properties such as volatility, analogues of such compounds, especially those with chromogenic or fluorogenic leaving groups, have been extensively used in the past for this purpose.

The screening of large gene libraries is greatly facilitated by having a simple chromogenic assay. In the chromogenic analogues of Sarin and Soman, previously used to study and screen PTE variants, the leaving groups are replaced with a p-nitrophenol moiety (Li, Lum et al. 2001). Fluorogenic substrates, on the other hand, are much more sensitive, allowing screening within a much wider dynamic range. Indeed, the fluorogenic Paraoxon analogue, 7-O-diethylphosphoryl-3-cyano-7-hydroxycoumarin (DEPCyC, has proven very effective in screening *E. coli* colonies containing PON variants that express efficiently and with an increased Paraoxon hydrolysing activity (Aharoni, 2004; Harel, 2004).

This chapter describes a series of model selections on the directed evolution platform based on the screening of *Escherichia coli* colonies using the fluorogenic nerve agents analogues described in Chapter 3 as probes. The methodology can be divided in two consecutive steps: firstly, *E. coli* C41 transformed with PTE variant libraries are plated [25], screened and selected on solid Medium (Colony Fluorescence step, section 4.2.1); subsequently, the selected (positive) clones are grown using microplates [26] filled with liquid medium, and their organophosphatase activity

25 23 x 23cm Plates were used except where otherwise mentioned (sections 2.1.2.5.2.1 and 2.1.2.5.2.2).

26 384-well microplates. See sections 2.1.2.5.2.1 and 2.1.2.5.2.2.

measured *in vivo* (Activity Quantification step, section 4.2.2). A detailed description of the materials and methods can be found in sections 2.1.2.5.2.1 and 2.1.2.5.2.2.

4.2 Results

4.2.1 Colony fluorescence

BugBuster™ Extraction Reagent (Novagen) is a mixture of non-ionic detergents capable of perforating the cell wall without denaturing soluble proteins. In preliminary experiments, it was observed that when *E. coli* C41 / pIVEX-PTE colonies grown on solid medium were put in contact with a Bugbuster™ solution containing Coumaphos [27] (**2**/Parathion analogue), the colonies emitted a pale blue glow (indicating the hydrolysis of the substrate) when illuminated with a UV-lamp. To ensure that this phenomenon was reproducible and that it was possible to resolve between colonies bearing active PTE variants, the following experiment was carried out.

A pIVEX-PTEwt and pIVEX-ΔPTE [28] mixture (1:10) was transformed into *E. coli* C41. The transformed cells were then plated on an Agar Growth Medium plate, covered with a Nitrocellulose membrane, and incubated at 37 °C for 16 hrs. The membrane was carefully detached, inverted onto over an Agar Induction Medium plate, and incubated at room temperature for further 21 hours. Analogue **2**/Parathion was added to Top-Agarose Activity formulation [29], and then poured over the induction plate bearing the colonies to a final concentration of 50 μM. After letting the agarose set for 1 minute at room temperature, the plate was illuminated from above with a 365nm-UV lamp. Colonies with organophosphatase activity were distinct and could be easily resolved (Figure 13).

27 NAs analogues were always handled in the chemical fume hood. For safety measures handling NAs analogues refer to section 2.4.1.

28 ΔPTE is an insoluble and inactive PTE variant in which 82 residues have been removed (T103-A186) (Griffiths and Tawfik, 2003).

29 0.5 (w/v) Agarose, 50 mM HEPES pH 8.0, BugBuster™ (Novagen).

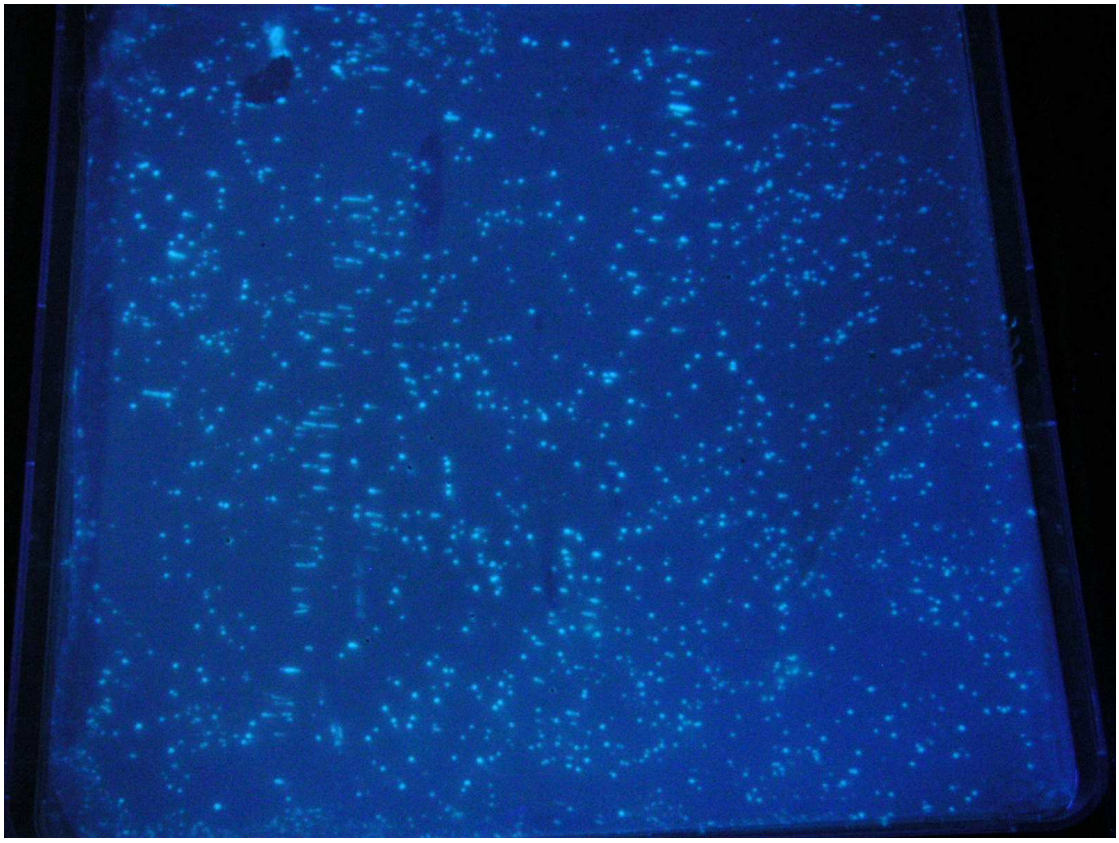

Figure 13 Colony Fluorescence assay. *E. coli* C41 colonies expressing either PTE-wt variant or ΔPTE covered with top agarose containing Bugbuster™ and 50 μM analogue **2**/Parathion, illuminated from above with a 365nm-UV lamp. The blue glow indicates the appearance of the 3-chloro-7-hydroxy-4-methylcoumarin group, thus denoting organophosphatase activity.

4.2.1.1 Cell viability

Once it had been established that active PTE-bearing cells gave a distinctive positive signal, the next step was to ensure that viable cells could be recovered and their DNA retrieved after Bugbuster™ treatment.

E. coli C41 cells were transformed with pIVEX-PTE, plated, and grown at 37 °C until the cfus reached 1 to 2 mm in diameter. Top-Agarose Activity formulation was then added to the plate. A series of batches of five colonies were picked at one minute intervals after exposure to BugBuster™. The colonies picked were transferred and spread onto Agar Growth Petri plates, and incubated further 21 hours at 37 °C. The number of colonies obtained per plate were manually counted, or extrapolated (to 56.7 cm^2) from the number in an area of 1 cm^2. The time of exposure plotted against

the average number of cfus recovered (Figure 14), showed that although cell viability drops as time of exposure increases, cells can indeed be recovered (for up to 10 minutes after exposure) in a reproducible manner.

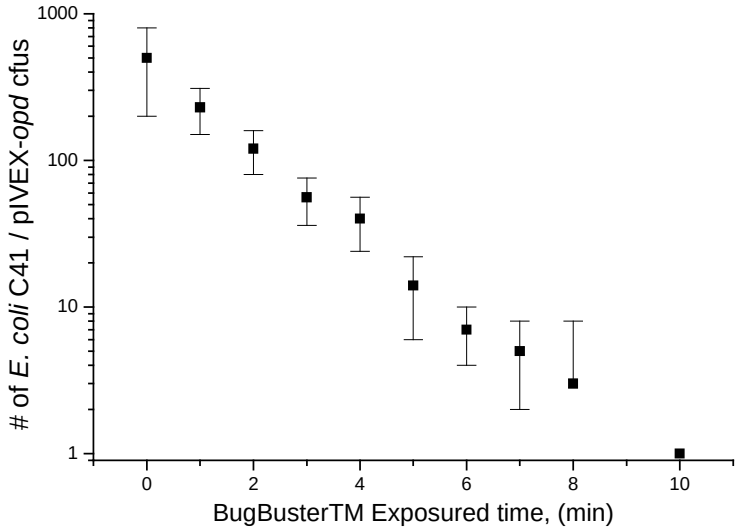

Figure 14. *E. coli* C41/pIVEX-PTE survival after incubation with BugBuster™

Five of the positive colonies were further selected, their plasmid DNA extracted (section 2.1.2.3) and their sequence determined by DNA sequencing using T7For and T7Rev primers (section 2.2.2.11). From the 25 clones sequenced, 14 (56%) proved to be the *opd* (PTE enconding gene), 9 the *Δopd* gene (36%), and 2 gave an ambiguous result (8%) (Table 15). At least two *opd* genes were isolated from each original positive clone picked and the sequence integrity was retained, almost intact.

Table 15. Gene recovery from model selection

	Gene products		
+ve clones	***opd***	***Δopd***	**Mutations per gene**
#1	2	2	1 / 4
#2	5	0	0
#3	2	3	0
#4	2	3	0
#5	3	1	2 / 4

4.2.1.2 Dynamic range

In order to determine the dynamic range of the fluorescent colony detection method, substrates with different reactivity towards PTE-wt were used in the following fashion.

pIVEX-PTEwt was transformed into *E. coli* C41. The cells were plated on a Agar Growth Medium plate, covered with a Nitrocellulose membrane, and incubated at 37 °C for 14 hrs. The membrane was carefully detached and inverted onto an Agar Induction Medium plate. After incubation at room temperature for 20 hrs, the membrane was detached and cut into pieces of approximately 4 x 5 cm. The pieces were laid (colonies up) on separated Growth Medium Agar Petri plates. The same procedure was followed with pIVEX-ΔPTE, as a negative control.

Top-Agarose Activity formulation containing 50 μM substrate (either analogue **2**/ Parathion, **10**/Russian-XV, or **7**/Tabun) was poured over the different plates. After letting the Agarose set of one minute, the plates were illuminated from above with a 365nm-UV lamp and pictures were taken at different time intervals (Figure 15).

The accumulation of diffused product seemed to be proportional to the substrate reactivity towards PTE-wt. Although this was most evident in the case of substrates **2**/Parathion and **10**/Russian-VX, positive signal was also detected in the case of **7**/Tabun. The negative control (pIVEX-ΔPTE) showed no presence of product even after 1 hour after the addition of the Top-Agarose formulation was added (not shown).

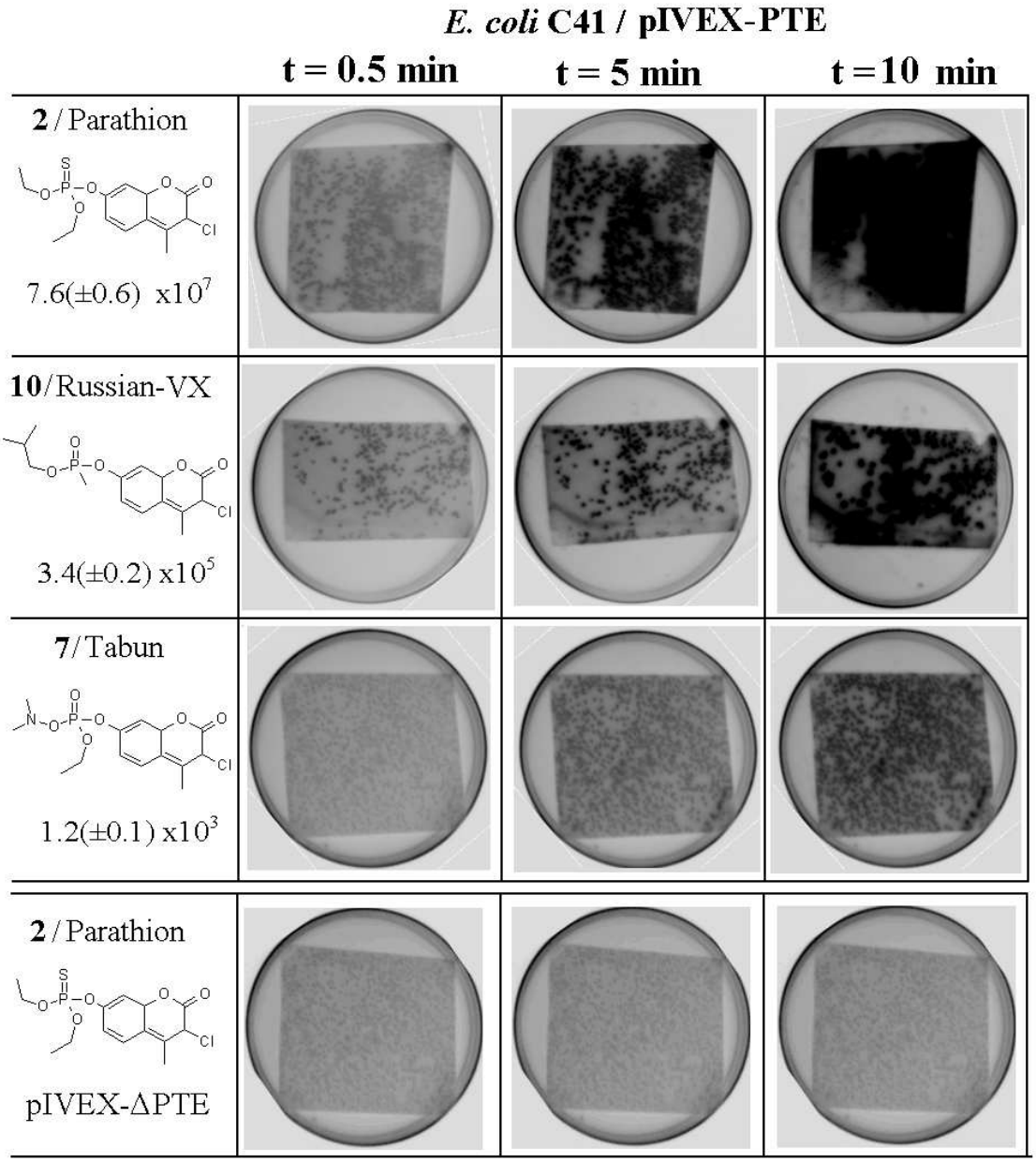

Figure 15. Monochromic images were taken 0.5, 5 and 10 minutes after *E. coli* C41 colonies expressing PTE-wt had been covered with Top-Agarose Activity formulation (see text), containing **2**/ Parathion, **10**/Russian-VX, **7**/Tabun. The name and structure of the substrate used in every case, along with the k_{cat} / K_M for PTE-wt, are given in the left hand column. Cells expressing ΔPTE (negative control) are shown in the bottom row. 365nm-UV illumination with a 418nm cut-off were used.

4.2.1.3 Induction time and pre-transformation

It is important to mention two other features of the screening system presented here. To maintain the DNA (sequence) integrity, the induction time should be kept below 24 hours. It was noticed that when the induction exceeded this period of time, the DNA recovered tended to accumulate point mutations, as high as 12 per 1000 base pairs (data not shown). Secondly, several screening attempts were made using pre-transformed *E. coli* C41 cells stored at –80 °C; the signal both in the first and second rounds steps in these cases was at least 50-times lower than if the bacteria were freshly transformed (data not shown).

4.2.2 Quantification of Activity

Although it is, to some extent, possible to quantify the activity according to the amount of fluorescence emitted by the colonies, this relies in an empirical comparison between colonies with different activity rates. To quantify the clones' activity in a more accurate way, positive colonies were subsequently grown, induced and their activities determined in microplates.

Five colonies from the plate covered with **2**/Parathion were picked and spread on Growth Medium Agar Petri plates. The plates were incubated at 37 °C for 16 hrs. 40 colonies were transfer to a microplate pre-filled with Growth Medium and subsequently incubated at 37 °C for 16 hrs. The Growth Medium plate (Stock Plate) was replicated into 8 microplates pre-filled with Induction Medium (Assay Plate). The Assay Plate was incubated at 37 °C for 16 hrs, while the Stock Plate was stored at 4 °C.

Before acquiring the activity data, the cell density of the Assay Plate wells were determined by measuring the AU_{600nm}. The (*in vivo*) activity was determined in 50mM HEPES pH 8.5, BugBuster, and 1% (v/v) DMF, supplemented with either **2**/Parathion, **4**/Paraoxon, **10**/Russian-XV, **5**/DFP, **12**/Cyclosarin, **11**/Soman or **7**/Tabun analogues, to a final concentration of 10 μM. The change in fluorescence (excitation = 355nm; emission = 460nm; cut-off = 455nm) was followed for 10 minutes immediately after the substrate addition.

The activity values are compiled in Table 16 . The initial averaged velocities obtained for eight repetitions were normalised using the cell density values; these

numbers were subsequently normalised against those obtained with the analogue **2**/Parathion. The resulting figures were plotted against the k_{cat} / K_M (M^{-1} s^{-1}) obtained with pure PTE-wt enzyme (see section 3.2.3).

Table 16. *In vivo* and *in vitro* activity of PTE-wt

	In vivo				*In vitro*
	Activity (RFU s^{-1})	**AU_{600nm}**	**Activity per AU (RFU s^{-1} AU^{-1})**	**Activity relative to 2/P**	**k_{cat} / K_M (M^{-1} s^{-1})**
2/Parathion	57.14 ±8.15	0.22±0.01	256.82±2.37	1.0	1.1(±0.1) x10^7
4/Paraoxon	20.12±6.02	0.24±0.02	84.06±2.83	3.2 x10^{-1}	2.7(±0.3) x10^6
12/Cyclosarin	6.57±1.12	0.25±0.03	26.67±1.06	10.4 x10^{-2}	5.7(±0.1) x10^5
10/Russian-XV	5.15±2.16	0.21±0.01	24.34±2.09	9.5 x10^{-2}	3.4(±0.2) x10^5
5/DFP	5.13±1.48	0.24±0.04	21.21±1.53	8.3 x10^{-2}	2.2(±0.2) x10^5
11/Soman	2.39±0.98	0.22±0.30	10.85±1.37	4.2 x10^{-2}	7.8(±0.5) x10^3
7/Tabun	1.45±0.55	0.23±0.02	6.25±0.97	2.4 x10^{-2}	1.2(±0.1) x10^3
6/Dimefox	N.D	- - -	- - -	- - -	0.094 (±0.01)

N.D. = Not detected

A positive correlation was obtained between the *in vivo* and the *in vitro* activities (Figure 16). More over, this correlation was linear below k_{cat}/K_M values of ~ 10^5. Under the conditions tested, no activity was detected for the **6**/Dimefox analogue.

Using a sterile inoculation loops, five cultures of Growth Medium were inoculated with bacteria from the Stock Plates. These cultures were grown at 37 °C for 16 hrs, the plasmid DNA was extracted (section 2.1.2.3), and its sequence determined by DNA sequencing using the primers T7For and T7Rev (section 2.2.2.11). The five clones exhibited intact *opd* gene sequence.

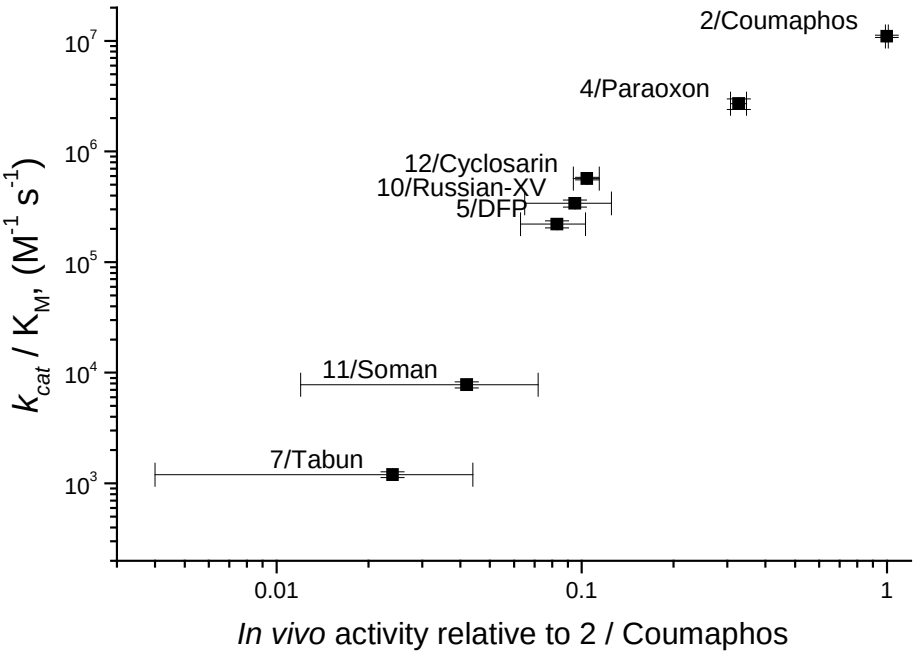

Figure 16. Correlation between *in vivo* PTE-wt activities and selectivity constants obtained *in vitro* with pure PTE-wt (section 3.2.3). *In vivo* activities were normalised against the activity of PTE-wt with **2**/Parthion analogue.

4.3 Discussion

To be suitable for directed evolution experiments, a screening system should link the phenotype and the genotype (section 1.1.3.1.1). The combination of Bugbuster™ and fluorogenic substrates achieves this precisely by releasing the cytoplasm of the cells onto the outer layers of the colony, thus exposing the cloned enzymes to the substrates (Phenotype), while leaving viable cells within the colony's core (see below) unaffected, with their DNA intact. As the cells in a colony arise from a unique clone, there is a biunivocal correlation between the enzymes activity and the DNA (subsequently) recovered.

It was clear from the bacterial survival trials, that the colonies should be transferred to fresh medium no later than 10 minutes after the addition of the Top-

Agarose formulation, to ensure the viability of the cells (Figure 14). This allowed enough time to detect the accumulation of fluorescent products (see below).

The dynamic range of detection in the Colony Fluorescence step was determined by using substrates with different reactivities towards PTE-wt. It was firstly shown that the k_{cat}/K_M values obtained with pure PTE-wt, correlated qualitatively with the accumulation of product in plates bearing *E. coli* C41 / pIVEX-PTE-wt colonies (Figure 15). Additionally, within the window of cell viability (< 10 min), it was possible to detect *in vivo* activities corresponding to k_{cat}/K_M as low as ~10^3 (M^{-1} s^{-1}). Given that the fluorescent probes diffuse throughout the plate, the signal does not reach saturation easily, allowing a clear resolution of activities corresponding to k_{cat}/K_M as high as ~10^7. The dynamic range of k_{cat}/K_M of 10^3 – 10^7 (M^{-1} s^{-1}) obtained from the plate step, is maintained and its resolution increased during the Activity step (see below).

A relatively high number of false positives (36%) were detected in the DNA recovery tests (Table 15). The most probable explanation is that neighbouring colonies hitch a ride when a positive colony was picked [30]. An empirical estimation of colony density was set at around ~10 to 15 x 10^3 colonies per plate [31]. This number makes a good compromise between maximising the number of colonies screened and minimising the number of false positives; however it is possible to resolve false positives in the Activity Quantification step, as *in vivo* activities of several clones (coming from the same selected colony) are measured and compared.

When the activity data is acquired using microplates, normalising by the cell density permits quantification of the activity per cell number, avoiding differential colony growths. Further, when the activity/cells values are normalised against the activity with **2**/Parathion, effects of expression levels or sensitivity to Bugbuster™ can be easily detected. This double normalisation also permits the comparison across *in vivo* measurements made under slightly different conditions.

The clear correlation obtained between the relative *in vivo* activities and k_{cat}/K_M values obtained with pure enzymes has two important implications. Firstly, it indicates that the screen provides a means of acquiring a good estimate of the enzymatic

30 The number of false positives was brought to almost zero in later rounds of screening.

31 Approximately 25 cfus per cm^2. Assuming 22 x 22 cm (484 cm^2), hence 1 – 1.5 x 10^3 cfus per plate.

activities thereby obviating the necessity of obtaining pure enzyme preparations. Secondly, it reflects the fact that actual selection for the improvement of k_{cat} / K_M can be performed.

Chapter 5 Selection using Nerve Agent Analogues as Probes

Our whole problem is to make the mistakes as fast as possible.
John Archibald Wheeler, 1956.

5.1 Introduction

5.1.1 Neutralisation of NAs

The Chemical Weapon Convention treaty, signed in 1992, requires the total destruction of any CW stockpiles held by those countries that ratified it (section 1.2.3). By the late 1990's, however, still thousands of tons of VX and Russian-VX were still held by the United States and Russia, respectively. In addition to V-type agents, both parties also stockpiled thousands of tons of Sarin, Soman and other NAs (Yang 1999). Generally, these stockpiles are destroyed by incineration, although alternative technologies, including catalytic degradation, are needed to neutralise NAs in situations were incineration is not feasible (Yang, Baker et al. 1992).

G-type agents (Sarin and Soman) can be neutralised by enzyme-based catalysis or by hydrolysis with relatively dilute alkali solutions. No enzyme is known, however, that can efficiently degrade V-type agents. Moreover, neither VX nor Russian-VX can be detoxified using base-catalysed hydrolysis, as the phosphonothioates produced from the P–O cleavage are as toxic and persistent as VX and Russian-VX themselves (Yang, Berg et al. 1997).

V-type agents are typically neutralised with copious quantities of aqueous bleach, containing NaOCl or $Ca(OCl)_2$, although this approach has several downsides: solutions must be freshly prepared and are highly corrosive; under basic conditions almost 20moles of OCl^- are needed to degrade 1 mole of VX; and, if the reaction is uncompleted, toxic phosphonothioate by-products remain.

In order to be safely neutralised by catalysis, V-type agents must be exclusively cleaved at the P–S bond. Precisely, it has been reported that PTE-wt catalyses such a reaction albeit with low efficiency (see section 1.3.4) (Rastogi, DeFrank et al. 1997). PTE variants with an increased activity towards V-type agents would provide an invaluable tool with which to neutralise VX and Russian-VX.

5.1.2 Enzyme promiscuity

Enzyme promiscuity is defined as the ability of a single active site to catalyse more than one chemical transformation (Kazlauskas 2005). Promiscuity is biologically relevant because secondary activity may become useful to the organism, if the enzyme is recruited to provide that activity in a new biochemical milieu (Jensen 1976; O'Brien and Herschlag 1999). For technology development, promiscuity has attracted attention for at least two reasons: it could play a role for drug design, as natural targets for drugs that have not evolved to intrinsically bind them (Fernandez, Tawfik et al. 2005), and because promiscuous activities have been used as starting points to obtained efficient catalysts for other non-natural reactions (James and Tawfik 2001; Matsumura and Ellington 2001; Aharoni, Gaidukov et al. 2004).

Several types of promiscuity can be identified according to the similitude between the primary and the promiscuous activities, although a unique classification has not been universally adopted. The most common and relevant to the present work, is cross-reactivity. Cross-reactivity refers to the catalysis of a comparable chemical reaction using a substrate analogue (Copley 2003; James and Tawfik 2003). More precisely, the potential of improving PTE activity towards the NA fluorogenic analogues rests on the notion that its cross-reactivity can be further improved.

5.1.3 Classification of NA Analogues

The NA analogues can be classified as phosphates and phosphonates (section 1.2.1). Phosphates have all their groups attached to the phosphorus via an oxygen, phosphonates have a group, methyl in this case, directly bound to it. Compounds **1** to **7**, and their original NA counterparts, are phosphates; compounds **8** to **12**, and their original NA counterparts, are phosphonates. Depending on the atom double-bonded to the phosphorus centre, the analogues can be classified either as thions, if bearing a

sulphur (S) (compounds **1** and **2**), or oxons if an oxygen (O) atom is bound (compounds **3** to **12**) (section 1.2.1).

This chapter describes the selection and characterisation of *Pseudomonas diminuta* Phosphotriesterase (PTE) variants with improved activities towards some of the Nerve Agent (NA) analogues.

Several gene libraries were synthesised, in each of which four codons of the residues forming PTE's substrate binding site were selectively randomised (Pro-*R*, Pro-*S*, and *Entrance* in section 1.3.4). These libraries were screened as described in Chapter 4 using analogues of Russian-VX and Parathion as probes; approximately a million clones were screened in total. The twenty more active variants, as determined from *in vivo* detection, were expressed and purified. The kinetic parameters of the selected variants towards Paraoxon and the NA analogues were determined.

5.2 Results

5.2.1 Library design

Owing to their role in substrate recognition, the residues comprising PTE binding pockets, Gly-60, Ile-106, Leu-303 and Ser-308 (Pro-*R*); His-254, His-257, Leu-271, and Met-317 (Pro-*S*); and Trp-131, Phe-132, Phe-306, and Tyr-309 (*Entrance*) were chosen for randomisation (section 1.3.4). Given library size constraints (sections 1.1.3.1.1.1 and 4.3), the binding pocket residues were randomised in three separate libraries (namely Lib-Pro*R*, Lib-Pro*S* and Lib-*Ent*). A fourth library (Lib-*ER*) was designed combining some residues of the Pro-*R* and *Entrance* pockets. The residues randomised in each library are compiled in Table 17.

The degenerate NNS codon was utilised to randomise the targeted residues, where 'N' codes for any of the four bases and 'S' only for guanine and cytosine [32] (1970). This represents a good compromise between the aim of introducing all twenty residues, and the number of stop codons (to one). Nevertheless, residues are represented in different proportions: Arg, Ser, and Leu each have a frequency of

32 N stands for aNy, and S for Strong (refering the three hydrogen bonds formed by the pair cytosine – guanine).

0.097; Gly, Ala, Val, Thr, and Pro are codified at a frequency of 0.062. The rest, including *Stop*, are represented at a frequency of 0.031. The residue distribution profile can be seen in Figure 18.

Table 17. Distribution of PTE substrate recognition residues throughout the designed libraries.

Substrate binding Residues	Library			
	ER	**Pro-*R***	**Pro-*S***	***Ent***
G60		NNS		
I106	NNS	NNS		
W131				NNS
F132	NNS			NNS
H254			NNS	
H257			NNS	
L271			NNS	
L303		NNS		
F306				NNS
S308	NNS	NNS		
Y309	NNS			NNS
M317			NNS	
[a] **Size$_{DNA}$**	~1 x10^6	~1 x10^6	~1 x10^6	~1 x10^6
[b] **Size$_{PROT}$**	~1.6 x10^5	~1.6 x10^5	~1.6 x10^5	~1.6 x10^5
Effective Size$_{DNA}$	~3 x10^6	~3 x10^6	~3 x10^6	~3 x10^6

a. The library size refers to the degrees of freedom (namely bases or residues) that are coded for.

b. The effective size refers to the number of clones needed in a library to ensure (95%) that all members are represented (see text).

Each library contains four NNS codons, corresponding to approximately 10^6 DNA alleles that encoded for 1.6 x 10^5 protein variants. The effective size of a library can be approximated by the following calculation: in a library containing L clones, the mean number of occurrences of one variant v_i is given by $\lambda = L / V$, were V is the expected total number of sequence variants. Assuming $\lambda << L$, the number of incidences of v_i approximate to a Poisson distribution, since occurrence of v_i and v_j are independent of one another. Hence the probability that v_i occurs at least once is $1 - P(0) = 1 - e^{-L/V}$. As the expected number of distinct variants is $C = V (1 - e^{-L/V})$, the

completeness of the library (F) is given by the ratio C/V (Patrick, Firth et al. 2003). In the particular case where $V = (4 \times 4 \times 2)^4 \approx 1 \times 10^6$), a library containing ~3×10^6 members (a 3-fold degeneracy) ensures a 95% chance of including at least one copy of each. This figure (3×10^6) also represents the number of clones needed to be screened to ensure that 95% of the library has been sampled at least once (section 5.2.3).

5.2.2 Library Construction

5.2.2.1 The template

To avoid selecting clones that enhance heterologous expression instead of enzyme activity *per se* (Roodveldt and Tawfik 2005), the highly expressible PTE-S5a variant was used as template for the binding pocket libraries. PTE-S5a contains three non-synonymous (K185R/D208G/R319S) and two neutral (D109/T352) mutations that confer a 20-fold increase in heterologous expression in *E. coli* . PTE-S5a has virtually the same catalytic properties against 2-naphthyl acetate and Paraoxon, and has higher stability than the wild type, in its metal-free apoenzyme (Roodveldt and Tawfik 2005).

5.2.2.2 Library construction

Libraries were constructed using cassette mutagenesis, in which a population of oligonucleotides bearing the diversified codons replaced targeted regions on the template DNA (Hermes, Parekh et al. 1989; Kegler-Ebo, Docktor et al. 1994).

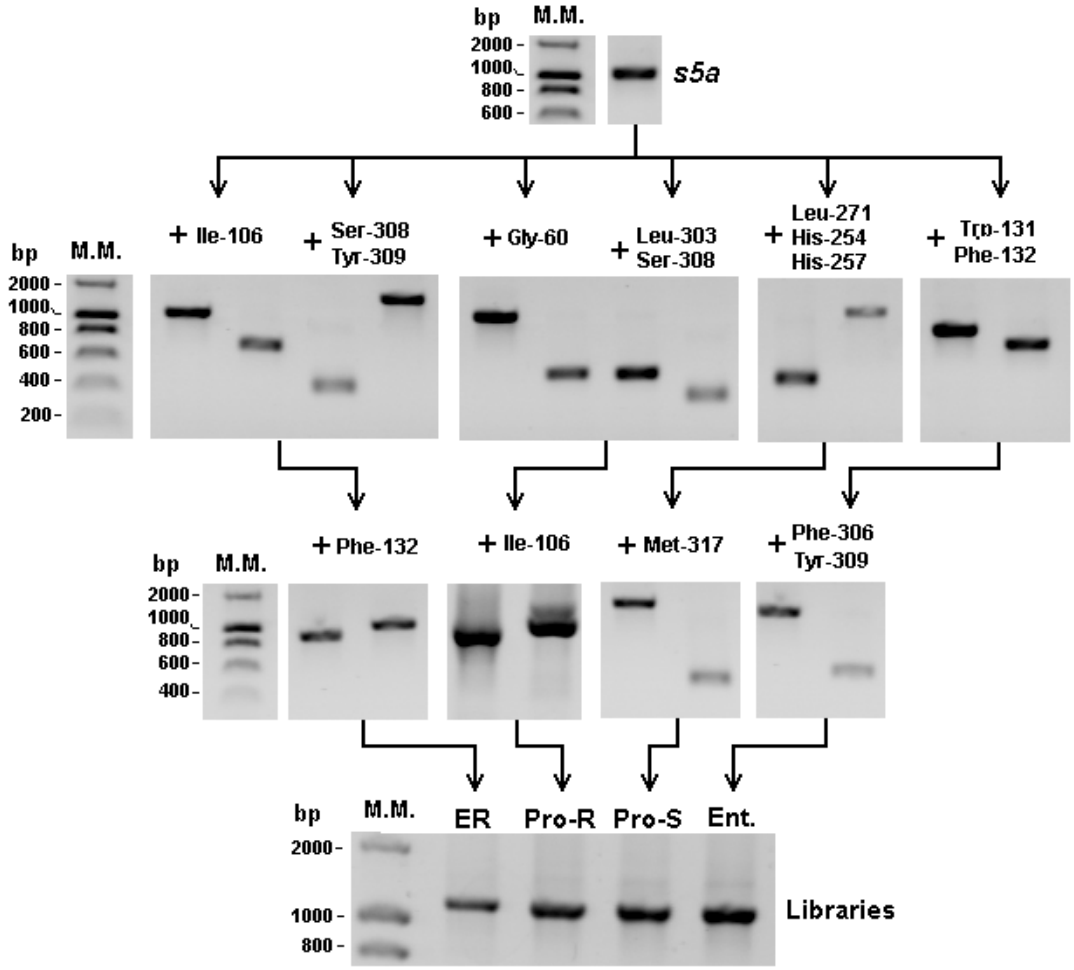

Figure 17. Construction of substrate-binding libraries. Starting from the *s5a* gene, four libraries were constructed by consecutive rounds of PCR/Digestion/Ligation (section 2.2.1.1.1.4). At every step two fragments were synthesised, typically, one bearing the diversity, the other a triple-biotin tag. The fragments were ligated via a BbsI site and purified using streptavidin-coated beads. The residues randomised in each step are indicated. The DNA was analysed by electrophoresis in (1% w/v) agarose gels stained with ethidium bromide (section 2.2.2.4); the primers used in every reaction are shown in Table 1.

Several oligonucleotides were synthesised (section 2.2.1.1) bearing, besides the diversified codons and their neighbouring regions, recognition sites for the restriction endonuclease BbsI (Figure 6 in section 2.2.2.10). These oligonucleotides were used as primers, paired with nested primers bearing a triple-biotin tag (at the 5' end), to generate fragments that were subsequently treated with BbsI (or its isochizomer BpiI), ligated together and purified using streptavidin-coated beads (section 2.2.2.8). For the synthesis of a library to be completed, several rounds of

PCR/Digestion/Ligation were needed (sections 2.2.2.10.1 and 2.2.2.10.2). The final products were re-cloned into pIVEX using NcoI/SacI restriction sites (2.2.2.10.3).
After every step during the construction, the DNA was visualised and analysed by electrophoresis in agarose gels stained with ethidium bromide (section 2.2.2.4). The process of the libraries construction can be followed in Figure 17.

Table 18. Residues obtained from single clones randomly sampled from libraries *ER*, Pro-*R*, Pro-*S*, and *Ent.*

Library	Randomised Residues			
wt	**I106^{atc}**	**F132^{ttc}**	**S308^{agc}**	**Y309^{tat}**
ER	P^{ccc}	A^{gcc}	H^{cac}	G^{ggg}
ER	Y^{tac}	R^{cgc}	R^{agg}	S^{tcg}
ER	S^{agc}	G^{ggg}	G^{ggg}	V^{gtg}
ER	K^{aag}	A^{gcg}	L^{tta}	G^{ggg}
wt	**G60^{ggc}**	**I106^{atc}**	**L303^{ctg}**	**S308^{agc}**
Pro-R	T^{acg}	S^{agc}	G^{ggg}	C^{tgc}
Pro-R	K^{aag}	R^{agg}	V^{gta}	G^{ggg}
Pro-R	C^{tgc}	E^{gag}	H^{cac}	E^{gag}
Pro-R	R^{cgc}	N^{aac}	W^{tgg}	C^{tgc}
wt	**H254**	**H257**	**L271**	**M317**
Pro-S	T^{acg}	G^{ggc}	M^{atg}	R^{cgg}
Pro-S	H^{wt}	P^{ccg}	G^{ggg}	G^{ggc}
Pro-S	P^{ccg}	A^{gcc}	A^{gcg}	M^{wt}
wt	**W131**	**F132**	**F306**	**Y309**
Ent.	G^{ggg}	G^{ggg}	I^{atc}	L^{ttg}
Ent.	A^{gcg}	L^{ttg}	G^{ggt}	C^{tgc}
Ent.	G^{ggg}	G^{ggg}	R^{agg}	G^{ggg}

The libraries were cloned into freshly prepared *E. coli* MC1061 electrocompetent cells (section 2.1.2.1). The cells were plated onto 23 x 23 cm Growth Medium Agar plates, while diluted aliquots were plated on Growth Medium Petri plates. After incubation at 37 °C for 21 hrs, a cell lawn and single colonies were obtained on the 23 x 23cm and Petri plates respectively. The lawn was scraped off the plate and thoroughly mixed. Plasmid DNA was then extracted from the homogenised cells, and from 4 single colonies of each library. The sequences were determined using T7For and T7Rev primers (sections 2.2.1.1.1.1 and 2.2.2.11).

All the clones obtained proved to be adequately cloned into pIVEX. The identity of the residues obtained from the 56 randomly selected library members is compiled in Table 18.

No significant difference was found (X^2 = 17.3, p < 0.001, n=20) between the expected and the obtained frequencies of residue distribution in the randomised codons [33] (Figure 18). Nevertheless, a bias towards guanine was found at DNA-level in the 'N' randomised positions (X^2 = 12.6, p < 0.01, n=3), but again not significant difference was found at the 'S' position (X^2 = 5.4, p < 0.2, n=3) (Figure 19).

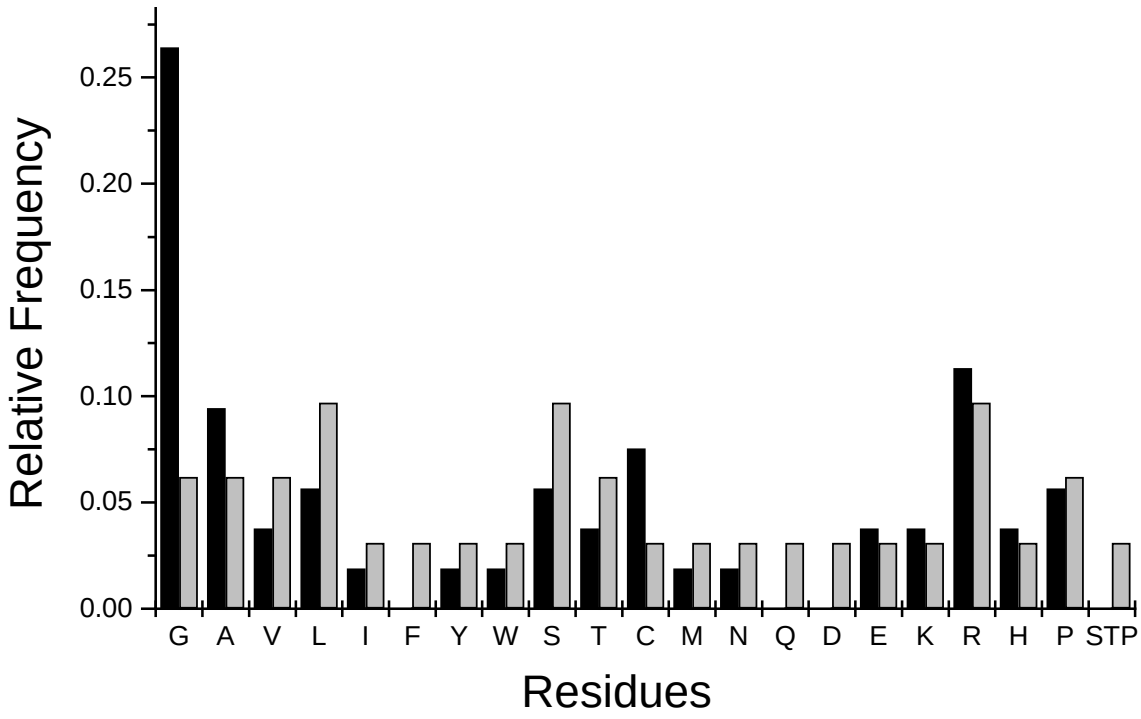

Figure 18. Frequency distribution profile of residues encoded by the NNS codon. The relative frequencies of residues obtained for 54 samples are shown as dark grey columns. The expected frequencies were generated using Codon Controller v1.0 (Dear 1999) and are shown as light grey columns.

33 The two residues with wild-type codons were not included. X^2 values test were done using the service provided at http://www.georgetown.edu/faculty/ballc/webtools/web_chi.html.

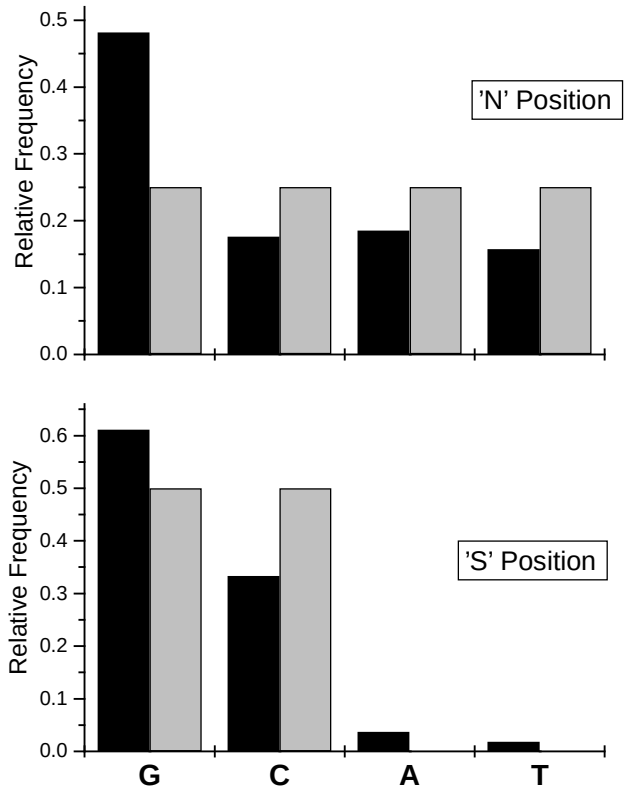

Figure 19. Frequency distribution profile of bases in the 'N' and 'S' positions.

Visual inspection of the chromatograms of the sequencing results generated from the library DNA revealed an excess of guanine in the reaction. Although chromatograms by themselves could not be used to evaluate a library, along with the data obtained from the single colonies, the notion that the libraries were biased towards to presence of guanine was confirmed.

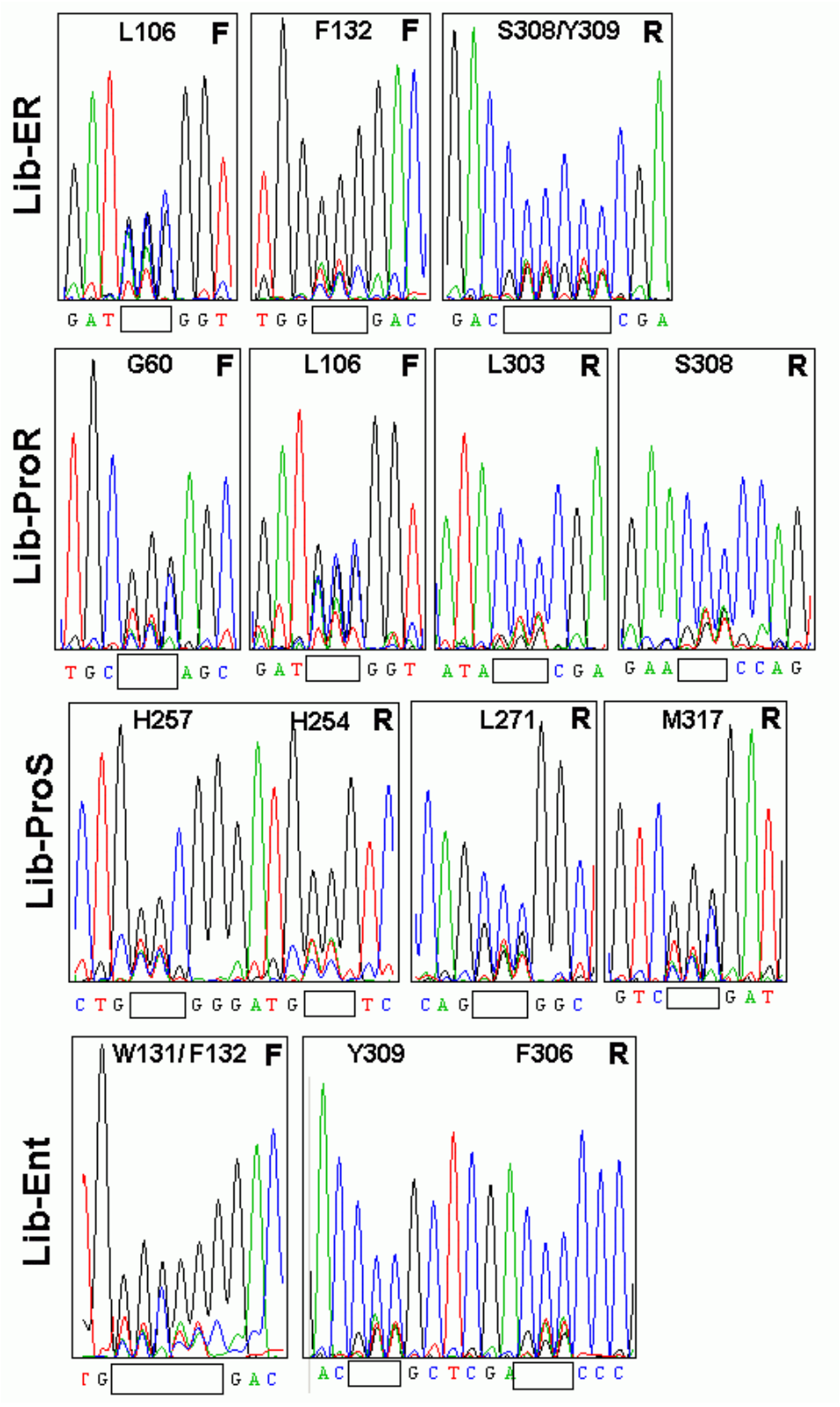

Figure 20. Chromatograms of sequencing reactions using DNA libraries as template. Sections of the sequencing reaction, in which the randomised codons appear, are shown in each panel. Whether T7For (F) or T7Rev (R) primers were used, is denoted in the upper right corner in each panel. Sequencing reactions were done by the MRC Geneservice (Hinxton, UK).

5.2.3 Screening using 10/Russian-VX and 2/Parathion analogues

5.2.3.1 Screening by colony fluorescence

Libraries *ER*, Pro-*R*, Pro-*S* and *Ent* were cloned into *E. coli* C41 cells and screened using **10**/Russian-VX and **2**/Parathion analogues as described in sections 2.1.2.5.2 and 4.2.1. The former was used with the aim of selecting PTE variants with improved activities towards V-type NAs, the latter better variants towards **2**/Parathion itself.

From the screening procedure, it can be seen that colonies exhibited different phosphotriesterase activities (Figure 21): remarkably, when the **2**/Parathion analogue was used as a probe, a substantial reduction in both the number and activity levels of clones was observed compared to the **10**/Russian-XV analogue. *E. coli* C41 cells transformed with pIVEX-PTE-S5a were included as positive control at all times.

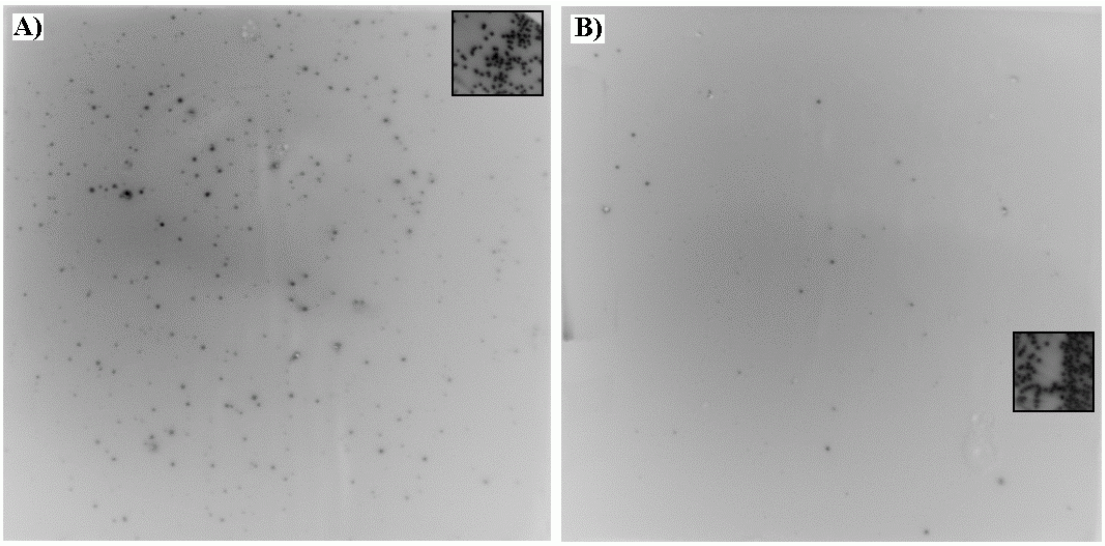

Figure 21. Colony screening of library Pro-*R* using (A) 10/Russian and (B) 2/Parathion analogues as probes. *E. coli* C41 / Lib Pro-*R* after 5 minutes of exposure with Top-Agarose Activity formulation (section 4.2.1). Insets shows *E. coli* C41 colonies expressing PTE-S5a under the same screening conditions. Plates were illuminated from above with 365nm-UV light, using a 418nm cut-off filter, and an aperture and integration time of f/1.2 and 0.4 s respectively.

Between 40 and 280 thousand colonies from each library were screened (Table 19). In spite of this seemingly large number, this represents only between 0.025% and 0.1% of the effectiveness of the libraries. From the approximately one million colonies screened in total, 155 were selected for *in vivo* determination of their activity.

Table 19. Number of clones screened in plate.

Library	# clones (x 10^3) **2**/Parathion	# clones (x 10^3) **10**/Russian-VX	Effective size of library sampled
ER	160 – 280	120 – 160	<0.05 – 0.1 %
Pro-*R*	80 – 160	40 – 60	<0.01 – 0.02 %
Pro-*S*	- - -	80 – 160	<0.025 – 0.05 %
Ent	40 – 60	80 – 160	<0.01 – 0.05 %

5.2.3.2 *In vivo* quantification of activity

The *in vivo* activity of the 155 selected clones towards **10**/Russian and **2**/Parathion analogues was measured in 384-well microplates as describe in sections 2.1.2.5.3 and 4.2.2. The activities were normalised, first according to cell density (OD_{600nm}) and then against the activity obtained for the positive control. The ratio between the two substrates was used to rule out changes in the activity levels due to variations in the expression of the enzymes.

Of the 155 clones originally selected, significant activity for both **10**/Russian-VX and **2**/Parathion analogues was detected in 70. Most of these clones were less active than the control for both **10**/Russian-VX (65% of counts $\leq$ 1) and **2**/Parathion (95% of counts $\leq$ 1) analogues; 25 mutants, however, showed an activity higher than the control for the **10**/Russian-VX analogue (Figure 22).

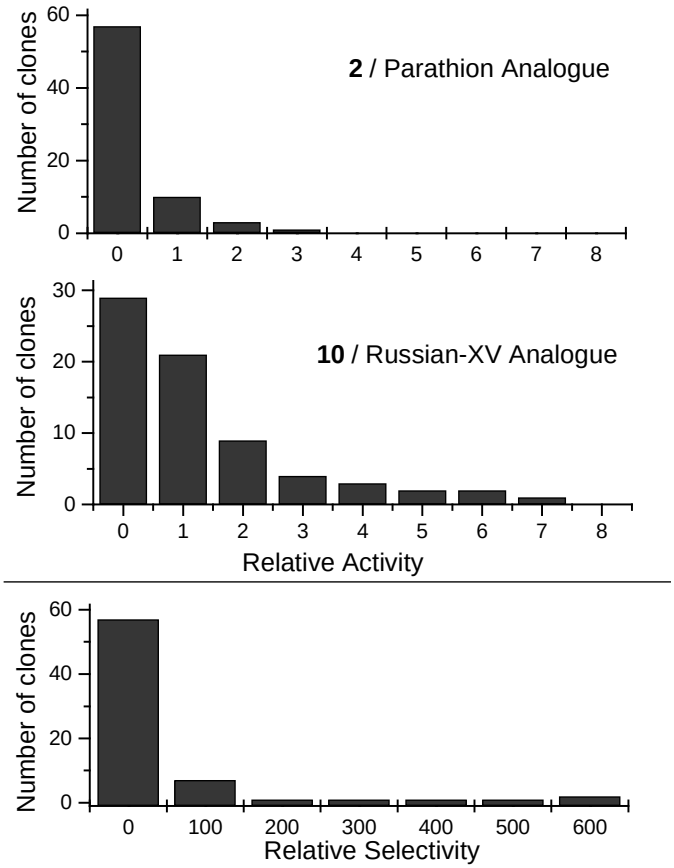

Figure 22. Histograms of the activities and selectivities against the **10**/Russian-VX analogue and the **2**/Parathion analogue. The activity was normalised with the values obtained for the positive control (wild-type). The relative selectivity is the ratio of the activity towards **10**/Russian-VX relative to **2**/Parathion (selectivity), normalised by the selectivity by the that of the wild-type.

Most of the mutants exhibited no selectivity change (60% of counts $\leq$ 3), although, in some cases, the selectivity shifted as much as 600-fold (Figure 22). These high values are due to an acute drop of activity towards **2**/Parathion. There is no clear correlation between the activities of the selected mutants against **2**/Parathion or **10**/Russian-VX activities.

The sequence of the 20 most active mutants was determined, and is compilied in Table 20. Of the 16 and 41 mutants selected from the Pro-*S* and *Ent* library plates respectively, none showed activity nor selectivity changes high enough, to be amongst the top 20.

Table 20. Mutants which exhibited the highest *in vivo* activity and relative selectivity. The mutants are sorted according to the library from which they were isolated and their sequence similarities.

Clone	Activity [a]		Selectivity [b]	Probe	Library-*ER*			
#	**2**/Pthion	**10**/R-VX			**I106**	**F132**	**S308**	**Y309**
A	2.68	2.33	0.87	10/RXV	T	-	-	-
B	0.09	5.98	63.31	10/RXV	L	-	-	-
C	0.53	1.44	3	10/RXV	V	C	-	-
D	0.91	2.65	2.9	2/Pthn	A	G	-	-
E	1.51	2.24	1.49	2/Pthn	V	L	-	-
F	0.24	3.95	16.6	2/Pthn	L	G	-	-
G	0.02	4.59	189	10/RXV	L	G	G	-
H	0.21	7.44	35.94	10/RXV	T	V	A	W
I	0.04	3.9	108.24	10/RXV	L	G	V	W
J	0.04	4.26	120	10/RXV	L	L	S	L
K	0.01	4.06	363.24	10/RXV	L	G	V	V
L	0.06	3.23	52.64	10/RXV	L	G	G	W
M	0.14	6.14	43.6	10/RXV	L	G	T	V
					Library-Pro*R*			
					G60	**I106**	**L303**	**S308**
N	0.33	3.21	9.58	2/Pthn	A	-	-	-
O	0.15	3.29	22.21	2/Pthn	V	V	V	-
P	0.29	2.88	10	10/RXV	A	A	-	T
Q	0.005	3.02	633.11	10/RXV	V	L	-	G
R	0.046	3.71	80.41	2/Pthn	V	T	I	W
S	0.1	5.41	52	10/RXV	V	M	E	D
T	0.01	3.25	600	10/RXV	V	S	P	G

a. Normalised to PTE-S5a (positive control). **b.** Selectivity towards **10**/Russian-VX relative to **2**/Parathion, was normalised to that obtained with the positive control.

5.2.4 Determination of kinetic parameters

Genes from selected clones were extracted by PCR and re-cloned into the vector pHLT. pHLT contains a upstream 6xHis Tag followed by the hypersoluble lipoyl domain, both of which can be removed from the polypeptide product using Tobacco

Etch Virus (TEV) protease by cleavage at the TEV site encoded downstream of the lipoyl domain (section 2.2.1.3.3). The selected PTE variants were produced *E. coli* C41, grown in autoinduced media (section 2.1.2.6.2), and affinity purified using a Nickel-NTA (Qiagen) column. Both the lipoyl domain and the 6xHis Tag were indeed removed (section 2.3.2.3). The purity of the protein preparations was ensured to be above 90% by PAGE (section 2.3.2.5.1)(Figure 23). The extinction coefficients (at 280nm) were calculated by sequence, and the protein concentration was measured by absorbance at 280nm (section 2.3.2.5.2.1).

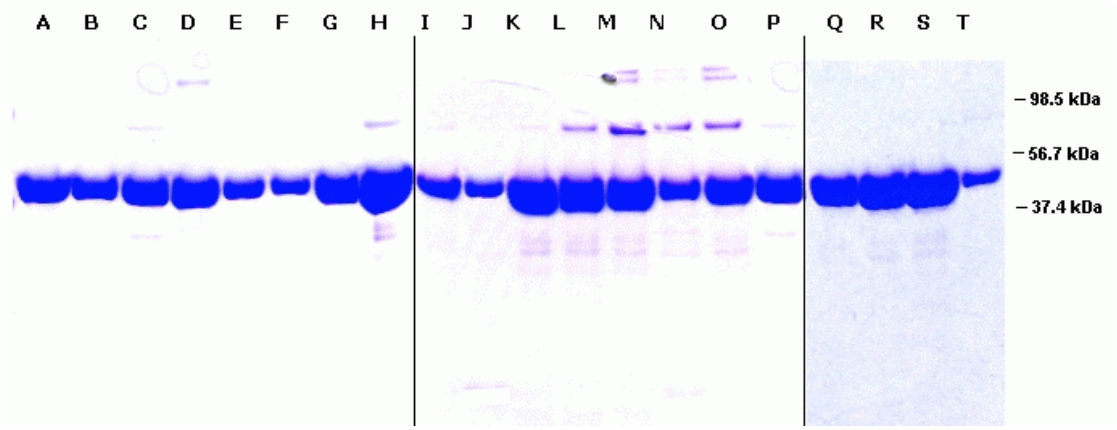

Figure 23. PTE selected variants (**A** to **T**) obtained after purification process, and run on a 12% Bis-Tris SDS-PAGE gel with MES Buffer.

The kinetics parameters k_{cat} and K_M of the variant towards Paraoxon were obtained as described in sections 2.3.2.5.3 and 3.2.2; the k_{cat}/K_M was measured for all fluorogenic analogues, with the exception of **6**/Dimefox analogue, as described in sections 2.3.2.5.4 and 3.2.3. The activity on this occasion was measured in the presence of BSA as carrier (0.1 mg/ml), $ZnCl_2$ (10 μM), and freshly prepared $KHCO_3$ pH = 8.5 (100 μM), to ensure that most of the enzyme was present in its holo form.

5.2.4.1 Activity of PTE-S5a

PTE-S5a showed similar kinetic properties towards Paraoxon to PTE-wt, although when it was tested with NA analogues some important differences appeared. PTE-S5a was more active towards most of the NA analogues with the exception of **4**/Paraoxon,

11/Soman and **12**/Cyclosarin. The main difference was found for the **5**/DFP analogue, as PTE-S5a hydrolyses it almost five times better than PTE-wt (Table 21).

Table 21. Kinetics properties of PTE-wt and PTE-S5a

	PTE		
	wt	**S5a**	**Ratio**
Paraoxon			
k_{cat} (s^{-1})	5954 ± 188	6441 ±322	1.01
K_M (mM)	0.029 ± 0.012	0.037 ± 0.007	1.27
	k_{cat}/K_M (M^{-1} s^{-1})		
Paraoxon	2.1 x10^8	1.8 x10^8	0.85
1/Methyl-parathion	1.3 (±0.02) x10^6	2.5 (±0.06) x10^6	1.45
2/Parathion	2.2 (±0.09) x10^7	2.3 (±0.36) x10^7	1.07
3/Methyl-paraoxon	7.2 (±0.05) x10^5	1.8 (±0.01)x10^6	2.52
4/Paraoxon	5.3 (±0.41) x10^6	1.8 (±0.26)x10^6	0.31
5/DFP	4.5 (±0.16) x10^5	2.1 (±0.24)x10^6	4.65
7/Tabun	2.3 (±0.79) x10^3	4.6 (±0.43)x10^3	1.98
8/VX	6.9 (±0.38) x10^5	2.2 (±0.18)x10^6	3.25
9/Sarin	5.2 (±0.01) x10^5	1.3 (±0.13)x10^6	2.46
10/Russian-VX	6.7 (±0.17) x10^5	2.1 (±0.8)x10^6	3.40
11/Soman	1.6 (±0.06) x10^4	5.7 (±0.8)x10^3	0.29
12/Cyclosarin	1.1 (±0.15) x10^4	4.7 (±0.5)x10^5	0.31

5.2.4.2 Activity of the selected variants

In the following sections, the changes in activity and selectivity will be presented and described relative to the values obtained for PTE-S5a in order to facilitate the data analysis. The raw data obtained can be found compiled in the Supplementary Information section. No correlation was found between the k_{cat}/K_M obtained with pure enzymes and the *in vivo* activities measured during the screening process (not shown).

5.2.4.2.1 k_{cat} and K_M towards Paraoxon

All the mutants selected exhibited a higher K_M and lower k_{cat}/K_M than PTE-S5a (Table 23), three variants, however, showed higher turnover rates. PTE-**A** and **D** had only marginal increases in their k_{cat}; PTE-**H** proved to have a turnover rate (31,016 s^{-1}) almost 5-fold higher than PTE-S5a, and even slightly higher than the *in vitro* selected mutant PTE-H5 (Griffiths and Tawfik 2003).

5.2.4.2.2 k_{cat}/K_M towards NA analogues

The variants selected showed significant reductions – up to 10^5 fold – in their activities towards most of the NA analogues (Table 24). Nonetheless, improvements towards one or more were found in 11 mutants.

PTE-**A**, **C**, **D** and **F** doubled their activity towards the **4**/Paraoxon analogue, PTE-**E** quadrupled it. PTE-**F** almost recovered its wild-type activity levels towards phosphonate substrates (analogues **8** to **12**, see section 5.1.3). PTE variants **-H**, **I** and **L** presented a slight increase in their activity towards **11**/Soman analogue; PTE-**I** also doubled its activity towards the **12**/Cyclosarin analogue. PTE-**Q** exhibited a 2-fold improvement towards analogue **10**/Russian-VX; it also showed a small increase towards the **12**/Cyclosarin analogue and more than 10-fold towards analogue **11**/Soman. Variants PTE-**S** and **T** doubled their original activity towards **11**/Soman, along with 5 and 6-fold increases respectively against **12**/Cyclosarin.

The increases for PTE variants **Q**, **S** and **T**, relative to PTE-wt, are compiled in Table 22. The profile of activity changes of PTE-**Q** relative to PTE-wt are represented as bars in Figure 24.

Table 22. Net activity improvements of PTE-Q, S and T variants.

Substrate	PTE variant						
	wt	Q	S	T	Q	S	T
	k_{cat}/K_M (M^{-1} s^{-1})				Ratio		
Paraoxon	2.1×10^{8}	4.66×10^{5}	1.62×10^{5}	5.27×10^{4}	2×10^{-3}	8×10^{-4}	3×10^{-4}
1/Methyl-parathion	1.3×10^{6}	1.2×10^{5}	3.0×10^{4}	2.2×10^{4}	0.09	0.02	0.02
2/Parathion	2.2×10^{7}	2.4×10^{4}	7.4×10^{4}	4.6×10^{4}	1×10^{-3}	3×10^{-3}	2×10^{-3}
3/Methyl-paraoxon	7.2×10^{5}	6.3×10^{4}	1.1×10^{4}	1.2×10^{4}	0.09	0.02	0.02
4/Paraoxon	5.3×10^{6}	9.0×10^{4}	8.1×10^{4}	3.7×10^{4}	0.02	0.02	0.01
5/DFP	4.5×10^{5}	1.0×10^{3}	1.4×10^{4}	7.4×10^{3}	2×10^{-3}	0.03	0.02
7/Tabun	2.3×10^{3}	5.4×10^{1}	3.1×10^{1}	†	0.02	0.01	†
8/VX	6.9×10^{5}	4.5×10^{5}	1.4×10^{5}	1.3×10^{5}	0.65	0.20	0.19
9/Sarin	5.2×10^{5}	1.1×10^{6}	4.3×10^{5}	4.9×10^{5}	2.12	0.83	0.94
10/Russian-VX	6.7×10^{5}	5.1×10^{6}	2.1×10^{6}	1.9×10^{6}	7.61	3.13	2.84
11/Soman	1.6×10^{4}	7.8×10^{4}	1.3×10^{4}	1.3×10^{4}	4.88	0.81	0.81
12/Cyclosarin	1.1×10^{4}	6.9×10^{5}	2.3×10^{6}	2.8×10^{6}	6.27	20.91	25.45

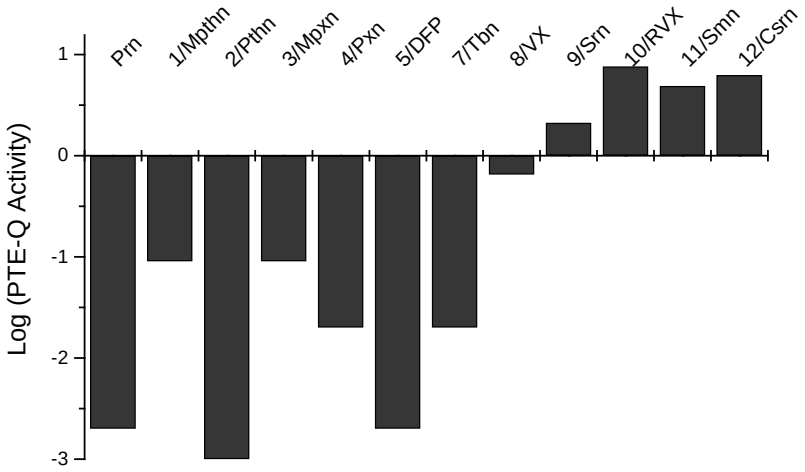

Figure 24. Net activity profile of PTE-Q relative to wild type.

Table 23. Kinetic values, relative PTE-S5a, for the hydrolysis of Paraoxon.

	Selected PTE variants																			
	H5	**A**	**B**	**C**	**D**	**E**	**F**	**G**	**H**	**I**	**J**	**K**	**L**	**M**	**N**	**O**	**P**	**Q**	**R**	**S**	**T**
k_{cat}	4.3	1.12	4×10^{-3}	0.15	1.38	0.32	0.53	2×10^{-4}	4.82	0.19	0.02	0.4	0.35	0.36	0.12	0.25	0.49	0.01	8×10^{-4}	4×10^{-3}	4×10^{-3}
$\boldsymbol{K_M}$	23.2	9.53	47.21	2.14	7.65	1.68	5.11	7.67	22.89	8.47	19.71	116.67	19.01	113.82	4.38	15.41	11.06	4.23	18.87	4.26	14.48
$k_{cat}/\boldsymbol{K_M}$	0.018	0.12	9×10^{-5}	0.07	0.18	0.19	0.1	2×10^{-4}	0.21	0.02	9×10^{-4}	3×10^{-3}	0.02	3×10^{-3}	0.03	0.02	0.04	3×10^{-3}	4×10^{-5}	9×10^{-4}	3×10^{-4}

Grey boxes highlight k_{cat} values >1. (For raw data see Supplementary Information section).

Table 24. k_{cat}/K_M, relative PTE-S5a, for the hydrolysis of NAs analogues.

	Selected PTE variants																			
Analogue of	**A**	**B**	**C**	**D**	**E**	**F**	**G**	**H**	**I**	**J**	**K**	**L**	**M**	**N**	**O**	**P**	**Q**	**R**	**S**	**T**
1/Methyl-parathion	0.04	6.3 x 10^{-5}	0.03	0.05	0.03	0.02	0.002	7.5 x 10^{-4}	0.003	0.002	0.002	0.002	4.8 x 10^{-4}	0.65	0.06	0.12	0.05	0.04	0.01	0.009
2/Parathion	0.07	1.4 x 10^{-4}	0.16	0.24	0.31	0.02	0.006	0.019	0.004	5.2 x 10^{-4}	0.002	0.002	7.5 x 10^{-4}	0.12	0.05	0.13	0.001	2.0 x 10^{-4}	0.003	0.002
3/Methyl-paraoxon	0.03	1.8 x 10^{-4}	0.08	0.04	0.02	0.18	5.4 x 10^{-4}	0.01	0.08	0.003	0.004	0.03	0.02	0.17	0.06	0.07	0.03	0.01	0.006	0.006
4/Paraoxon	1.8	0.003	2.2	2.8	4.2	1.9	0.02	0.5	0.69	0.01	0.39	0.2	0.09	0.33	0.15	0.53	0.05	8.4 x 10^{-4}	0.05	0.02
5/DFP	0.2	3.1 x 10^{-5}	0.42	0.31	0.04	0.004	0.001	0.04	0.002	6.7 x 10^{-5}	0.001	0.002	4.1 x 10^{-4}	0.01	0.008	0.03	5.0 x 10^{-4}	†	0.007	0.004
7/Tabun	0.02	†	0.12	0.06	0.03	0.11	†	0.03	0.08	†	†	0.03	†	0.28	0.03	0.06	0.01	0.006	0.007	†
8/VX	0.06	0.001	0.07	0.07	0.04	0.62	0.001	0.08	0.16	0.005	0.04	0.05	0.05	0.11	0.1	0.06	0.2	0.05	0.06	0.06
9/Sarin	0.07	0.003	0.08	0.06	0.04	0.89	0.004	0.13	0.5	0.02	0.11	0.16	0.12	0.5	0.4	0.23	0.81	0.14	0.3	0.37
10/Russian-VX	0.08	0.004	0.06	0.02	0.04	0.88	0.008	0.16	0.82	0.04	0.16	0.3	0.21	0.7	0.42	0.34	2.4	0.07	1.0	0.92
11/Soman	0.15	†	0.17	0.05	0.03	0.59	†	1.4	1.1	0.13	0.32	1.3	0.21	0.9	0.4	0.26	13.7	0.33	2.3	2.4
12/Cyclosarin	0.09	0.004	0.01	0.05	0.02	0.93	0.007	0.32	2.1	0.11	0.42	0.8	0.28	0.4	0.4	0.44	1.4	0.06	4.8	6.0

† No detection. Grey boxes highlight k_{cat} values >1. ND, not determined. (For raw data see Supplementary Information section).

Table 25. Selectivity values towards NA analogues relative to Paraoxon

			Selected PTE variants																		
Analogue of	**wt**	**S5a**	**A**	**B**	**C**	**D**	**E**	**F**	**G**	**H**	**I**	**J**	**K**	**L**	**M**	**N**	**O**	**P**	**Q**	**R**	**S**	**T**
1/Methyl-parathion	0.006	0.01	0.68	1.5	2.3	1.3	1.6	0.19	252.9	0.09	0.16	0.58	0.45	0.12	0.23	4.1	3.0	2.9	0.4	4.8	3.5	6.7
2/Parathion	0.10	0.13	0.36	0.7	0.45	0.27	0.17	0.18	79.2	0.004	0.12	2.1	0.35	0.075	0.15	22.8	4.0	2.8	17.9	1031.2	13.1	29.0
3/Methyl-paraoxon	0.003	0.014	0.22	2.0	1.1	0.21	0.12	1.7	21.5	0.05	3.5	3.0	1.0	1.5	4.9	6.1	3.5	1.7	12.9	294.2	6.8	21.1
4/Paraoxon	0.025	0.01	15.1	29.9	31.12	15.6	21.9	18.6	732.7	2.5	31.1	11.7	115.0	12.0	27.4	11.5	9.5	11.9	19.1	19.7	49.1	69.6
5/DFP	0.002	0.012	2.0	0.34	6.0	1.7	0.18	0.03	44.1	0.17	0.11	0.075	0.33	0.097	0.13	0.5	0.5	0.8	0.2	†	7.2	11.9
7/Tabun	1×10^{-5}	2×10^{-5}	0.19	†	1.6	0.33	0.14	1.0	†	0.13	3.6	†	†	1.8	†	9.7	2.0	1.4	4.4	129.3	7.2	†
8/VX	0.003	0.01	0.52	12.8	0.91	0.38	0.18	5.9	48.0	0.42	7.2	5.8	11.0	2.9	14.5	4.1	6.4	1.4	74.5	1090.6	65.8	187.8
9/Sarin	0.002	0.008	0.60	35.8	1.16	0.31	0.18	8.5	133.4	0.61	21.2	21.6	31.3	8.7	37.4	17.6	22.1	5.1	303.4	3271.3	350.0	1219.8
10/Russian-VX	0.003	0.01	0.71	41.5	0.86	0.09	0.22	8.4	310.0	0.78	36.8	40.2	47.8	15.4	67.1	24.3	25.9	7.6	903.2	1527.2	1070.3	3067.3
11/Soman	8×10^{-5}	3×10^{-5}	1.3	†	2.4	0.29	0.15	5.6	†	6.8	49.5	139.2	93.0	68.1	66.2	30.3	25.5	5.8	5167.2	7783.0	2384.8	7891.5
12/Cyclosarin	0.001	0.003	0.79	39.1	1.4	0.25	0.12	8.9	256.3	1.5	91.8	126.1	122.1	43.0	90.5	15.3	25.0	10.0	546.7	1421.3	5254.4	20001.3

† No detection. The changes in grey tone from light to dark, indicate 10-fold increases in the selectivity values. The horizontal dashed box indicates values for the **4**/Paraoxon analogue.

Table 26. Selectivity values towards NA analogues relative to 4/Paraoxon analogue

	Selected PTE variants																				
Analogue of	**wt**	**S5a**	**A**	**B**	**C**	**D**	**E**	**F**	**G**	**H**	**I**	**J**	**K**	**L**	**M**	**N**	**O**	**P**	**Q**	**R**	**S**	**T**
Paraoxon	39.6	98.5	0.07	0.03	0.03	0.06	0.05	0.05	$1x\ 10^{-3}$	0.41	0.03	0.09	0.01	0.08	0.04	0.09	0.11	0.08	0.05	0.05	0.02	0.01
1/Methyl-parathion	0.24	1.4	0.02	0.02	0.01	0.02	0.01	0.01	0.11	$1x\ 10^{-3}$	$4x\ 10^{-3}$	0.18	$3x\ 10^{-3}$	0.01	0.01	1.98	0.42	0.23	0.94	52.43	0.27	0.42
2/Parathion	4.1	12.7	0.04	0.05	0.07	0.08	0.07	0.01	0.35	0.04	0.01	0.05	$4x\ 10^{-3}$	0.01	0.01	0.36	0.32	0.25	0.02	0.24	0.07	0.10
3/Methyl-paraoxon	0.14	1.1	0.01	0.07	0.03	0.01	0.01	0.09	0.03	0.02	0.11	0.25	0.01	0.12	0.18	0.53	0.37	0.14	0.68	14.9	0.14	0.30
5/DFP	0.08	1.17	0.13	0.01	0.19	0.11	0.01	$2x\ 10^{-3}$	0.06	0.07	0.00	0.01	$2x\ 10^{-3}$	0.01	0.00	0.04	0.05	0.07	0.01	†	0.15	0.17
7/Tabun	$4x10^{-4}$	0.003	0.01	†	0.05	0.02	0.01	0.06	†	0.05	0.12	†	†	0.15	†	0.84	0.21	0.12	0.23	6.5	0.15	†
8/VX	0.13	1.26	0.03	0.43	0.03	0.02	0.01	0.32	0.07	0.17	0.23	0.50	0.10	0.24	0.53	0.4	0.68	0.12	3.9	55.4	1.3	2.70
9/Sarin	0.098	0.75	0.04	1.19	0.04	0.02	0.01	0.46	0.18	0.25	0.68	1.8	0.27	0.72	1.3	1.5	2.3	0.43	15.8	166.3	7.1	17.5
10/Russian-VX	0.13	1.19	0.05	1.38	0.03	0.01	0.01	0.45	0.42	0.32	1.1	3.4	0.42	1.2	2.4	2.1	2.7	0.64	47.3	77.6	21.7	44.0
11/Soman	0.003	0.003	0.09	†	0.08	0.02	0.01	0.31	†	2.8	1.5	11.8	0.81	5.6	2.4	2.6	2.6	0.48	270.6	395.7	48.5	113.4
12/Cyclosarin	0.021	0.27	0.05	1.31	0.04	0.02	0.01	0.48	0.35	0.62	2.9	10.7	1.6	3.5	3.2	1.3	2.6	0.84	28.6	72.2	106.9	287.4

† No detection. The changes in grey tone from light to dark, indicate 10-fold increases in the selectivity values. The horizontal dashed box indicates phosphonate substrates

5.3 Discussion

5.3.1 Library construction bias

When the libraries were synthesised, a bias in the presence of guanine was observed, both in the sequence of randomly selected clones and in the reaction chromatograms resulting from the direct sequencing for the libraries. In principle, any bias represent a liability to the quality of a library. It was, however, decided to utilise these G-biased libraries for the following reasons: no significant bias was detected at residue level; it seems that the PTE binding pocket needed to be enlarged in order to more readily accept NAs, and therefore an enrichment towards Gly, Ala, or Val – whose codons are predominantly composed of guanine – could be advantageous.

5.3.2 Screening

Between 80,000 and 500,000 bacterial colonies were screened per library using both probes; this represented less than 1% of the libraries' effective size. Approximately, one million bacterial colonies were screened in total, 155 of which were selected for their activity to be quantified *in vivo*.

When the **2**/Parathion analogue was used as a probe, a decrease in the number of positive clones was observed and in the intensity of their signals, relative to **10**/Russian-VX. This could suggest that, overall, PTE activity towards the **2**/Parathion analogue was less robust to mutations than towards **10**/Russian-VX (Figure 21). It cannot be ruled out, however, that the **10**/Russian-VX analogue is in fact more reactive than **2**/Parathion under the screening conditions used. Clones probed by both **10**/Russian-VX and **2**/Parathion were in the selected group.

Two values were obtained *in vivo*, the activity relative to the PTE-S5a (positive control) and the activity towards the **10**/Russian-VX analogue relative to **2**/Parathion. Most of the clones were less active than the control for both the **10**/Russian-VX (65%) and **2**/Parathion (95%) analogues (Figure 22). Once again, the activity towards **2**/Parathion seemed to be more impaired than towards **10**/Russian-VX. Following a similar trend, most of the mutants (60%) showed no change in their preference for **10**/Russian-VX. The number of clones isolated exhibiting higher

activity than the control towards **10**/Russian-VX, were 13 and 7 for the *ER* and Pro-*R* libraries, respectively. No clones from either of the Pro-*S* or *Ent* libraries were selected. The sequences of the 20 clones were determined, and each tagged with a letter of the alphabet (Table 20).

No correlation was found between the relative *in vivo* activity and selectivity (not shown), however the clones with higher activities, also exhibited the highest selectivity towards **10**/Russian-VX. Moreover, when the kinetic values were obtained with pure enzymes (see below), it was found that these values did not correspond to those measured *in vivo*. Most likely, differential expression, coupled with changes in the clone's substrate selectivity, accounted for this mismatch.

5.3.3 Kinetic properties of PTE-S5a

PTE-S5 is a of itself a product of directed evolution experiments. It was created by shuffling seven mutants that resulted from the random mutagenesis of PTE-wt, and the libraries being screened by the coupling of the hydrolysis of 2-naphthyl acetate (2NA) with Fast Red dye (Roodveldt and Tawfik 2005). PTE-S5a contains three non-synonymous (K185R/D208G/R319S) and two synonymous (D109/T352) mutations. Lys-185 maps to the α-helix 4 and its solvent exposed; Asp-208 is located at the β/α loop 5, with its side chain buried between β/α loops 4 and 5; and Arg-319 locates in β/α loop 8. None of these mutations is directly involved in the binding of substrate. Nevertheless PTE-S5a exhibited a different kinetic profile towards the NA analogues (Table 21).

Amongst the phosphonate analogues, PTE-S5a hydrolysed **8**/VX, **9**/Sarin, **10**/Russian-VX analogues between 2.5 and 3.5 times more readily than PTE-wt. Conversely, towards **11**/Soman and **12**/Cyclosarin analogues, its activity is only 70% of that of the wild type.

5.3.4 Kinetic parameters of the selected PTE variants

5.3.4.1 PTE variants with increased turnover rates towards Paraoxon

All the variants selected showed a higher K_M than that of the PTE-S5a, irrespective either of the library from which the variant was selected or of the probe used to select

it; three clones, however, exhibited higher k_{cat} than PTE-S5a: PTE -**A** (I106T), **C** (I106L), and **H** (I106T/F132V/S308A/Y309W). The turnover rates for these variants were 7184, 8884 and 31016 s^{-1}, respectively. PTE-**A**, **C** and **H** were isolated from library *ER*, PTE-**A** and **C** was probed by **2**/Parathion, and PTH-**H** by **10**/Russian-VX.

Coincidently named, it was the variant PTE-**H** that showed kinetic properties similar to the *in vitro* evolved PTE-H5 (I106T/F132L). The two main differences between these variants were the higher turnover rate of PTE-**H** for Paraoxon and its preference [34] for phosphonates, in particular **11**/Soman analogue (Table 35 and Table 40 in the Supplementary Information section). This latter property reflected the fact that PTE-**H** was selected using a **10**/Russian-VX probe.

Enzymes which have their k_{cat}/K_M maximised – in this case close to the diffusion limit – can still increase their rates by weakly binding the substrate (section 1.1.2.5). Precisely, the evolved PTE-**H** variant showed a 5 and 25-fold increases in its k_{cat} and K_M, respectively.

5.3.4.2 Affinity of the selected variants for the fluorogenic leaving group

One of the main concerns of using substrate analogues is that "you can get what you select for"; in this particular case, variants with improved activities towards compounds bearing the 3-chloro-7-hydroxy-4-methylcoumarin moiety. This is relevant because changes in the affinity for the fluorogenic leaving groups should be avoided, if the increases in activity towards the analogues are to be translated to the original NAs.

In order to investigate to what extent the selected variants' improved activity came solely from a better fit to the fluorogenic leaving groups, the change in activity towards **4**/Paraoxon relative to Paraoxon, was used as a measure of preference for the 3-chloro-7-hydroxy-4-methylcoumarin leaving group over the p-nitrophenol (Table 25). All the selected variants did indeed have an increased preference for the fluorogenic leaving group. For PTE-S5a, the p-nitrophenol is preferred to the coumarin moiety by approximately 100:1; this ratio was reversed for the selected variants, ranging from 1:4 for PTE-**H**, to 1:700 for PTE-**G.**

34 Quantifying changes in the preferences of substrates can be done using equation 13 (section 1.1.2.4), in which the selectivity of an enzyme towards one substrate relative to another can be calculated by taking the ratio of their respective k_{cat}/K_M values.

Five clones were selected from the *ER* library, which showed an improved k_{cat}/K_M towards the **4**/Paraoxon analogue (Table 24 and Table 41 in the Supplementary Information section): PTE-**A** (I106T), **C**(I106V/F132C), **D** (I106A/F132G), **E** (I106V/F132lL), and **F** (I106L/F132G). No relationship was found between the probes by which these mutants were selected nor between their activities or selectivities. For this set, it is indeed possible that the improvement came solely from a change in selectivity towards the coumarin moiety relative to the p-nitrophenol (Table 25). Nonetheless, most of the variants showed a selectivity towards phosphonate substrates, meaning that, at least in this particular context, these mutants have selectivity (and activity) changes for regions other than the leaving groups of the substrates. This is particularly clear in the case of PTE variants **Q** (G60V/I106L/ S308G), **R** (G60V/I106T/L303I/S308W), **S** (G60V/I106M/L303E/S308E), and **T** (G60V/I106S/ L303P/S308G).

5.3.4.3 PTE variants with increased activities for phosphonate substrates

In the most toxic NAs, both G and V-type, one of the alkoxy groups attached to the phosphorus centre is substituted by a methyl group. Hence, improvement in PTE's catalytical power against phosphonates might translate into an increase in its activity towards NAs.

Relative to the **4**/Paraoxon analogue, PTE-S5a exhibited a preference for sulphur as the atom double-bonded to the phosphorus centre (**2**/Parathion), and a slight preference towards both *O*-ethyl methyl phosphonate and *O*-isopropyl methyl phosphonate groups (**8**/VX and **10**/Russian-VX respectively). Several PTE variants (**A**, **C**, **D**, **E**, **F**, **G** and **P**) preferred the **4**/Paraoxon analogue above every other substrate. However, relative to PTE-S5a, some of them, most clear in the case of PTE-**P**, shifted a tad towards phosphonates. Another set of variants (**B**, **H**, **I**, **J**, **K**, **L**, **M**, and **O**) showed a clear preference for phosphonates, only when the *O*-ethyl group was substituted. PTE-**Q**, **R**, **S** and **T**, showed a much higher preference towards all phosphonates (Table 42 in the Supplementary Information section). This is the only group of variants for which the *O*-ethyl methyl phosphonate (**8**/VX) is preferred over the 2-*O*-diethyl phosphate found in **4**/Paraoxon. PTE-**Q** had a preference for the *O*-cyclohexane group of **12**/Cyclosarin above the *O*-ethyl of **4**/Paraoxon, to the degree of 28:1 (compare this to 1:4: in the case of PTE-S5a). PTE-**R**, also showed an increase

towards the 2-*O*-dimethyl phosphate in **1**/Methyl-parathion and **3**/Methyl paraoxon (Table 38 and Table 39, in Supplementary Information section); it seems that its binding site can accomodate *O*-methyl phosphates more readily than bulkier *O*-ethyl phosphates, but is incapable of stretching this resolution further to methyl phosphonates.

There was some correlation between the increases obtained both in activity and selectivity and the volume of the pro-S group. A bulky group in the pro-S position may somehow compensate for the reduction in size produced by the methyl group on the opposite arm of the substrate.

All the variants with a k_{cat}/K_M higher than the wild-type towards the **10**/Russian-VX, **11**/Soman or **12**/Cyclosarin analogues were selected using the **10**/RussianVX analogue as probe. The relative preference for phosphonates, however, depended, not only on the probe used but also on the library screened. Clones selected from the *ER* library that exhibited such a preference were probed using **10**/Russian-VX, whilst clones selected from library Pro-*R* with the same preferences were probed using either **10**/Russian-VX or **2**/Parathion. Hence, for the latter library, using a "phosphonate-like' substrate (**2**/Parathion) probe is enough to obtain changes in selectivity towards phosphonates, but not enough to generate increased activity. For this a phosphonate is required. For the ER library, selectivity for phosphonatase activity can only be generated by phosphonate probes. These generate increased, although only marginally increased, in activity.

Apart from differences in selectivity, the activity levels selected for in the two libraries differs: phosphonate probes generate higher activity levels in the Pro-*R* library than those obtained from the *ER*.

5.3.5 Activity towards Nerve Agents

Having pulled out mutants that are more selective for phosphonate substrates than for phosphates, increases the chances that their activities can be translated to NAs. Nevertheless, it is not possible to conclude that these variants will retain such preferences in a different structural context. Testing PTE-S5a, **Q**, **S** and **T** against the real NA is currently being carried out in the laboratory of Dr. Christopher M. Timperley in the Chemical and Biological Defence Sector at the Defence Science and Technology Laboratory (Porton Down, UK).

5.3.6 Relationship between selectivity and activity

No relationship has been found between the selectivity and activity for a particular substrate (data not shown), however, there seems to be certain degree of proportionality between them. Relative to Paraoxon, all the variants showed an increased selectivity towards most of NA analogues, particularly towards the **4**/Paraoxon analogue and phosphonates (Table 25). For the variants PTE-**A**, **C**, **D**, **E** and **F**, these changes in selectivity were also accompanied by improved activities towards **4**/Paraoxon. In a similar way, PTE-**Q**, **S** and **T**, had both a higher selectivity and activity towards phosphonates. A similar trend was found with the clones for which activity was quantified solely *in vivo*. As there were cases, like PTE-**R**, in which substantial increases in selectivity were not translated into significant increases in activity, it seems that an increase in the selectivity for a substrate is necessary but not sufficient to ensure increments in activity.

5.3.7 Improvements in activity relative to PTE-wt

Owing that PTE-S5a presented a different activity profile to PTE-wt for the NA analogues, the changes obtained by the selected mutants were different relative to PTE-wt than to PTE-S5a (Table 22). PTE-**Q** exhibited a 7-fold improvement towards the **10**/Russian-VX and **12**/Cyclosarin analogues, whilst showing a 2 and 5-fold increase towards **9**/Sarin and **11**/Soman analogues, respectively. PTE-**S** and PTE-**T** improved on activity for **10**/Russian-VX and **12**/Cyclosarin analogues by 3 and 25-fold respectively.

In general, the major change in the kinetic properties of the selected variants was a conserved loss of function towards the phosphate substrates (compounds **1** to **8**). For the *wild-type* substrate, the k_{cat}/K_M of PTE-**Q**, **S**, and **T** variants towards Paraoxon (and **2**/Parathion analogue) was reduced 1000-fold.

5.3.8 Changes in the activity towards wild-type substrate

Tawfik and colleagues have observed that it is possible to find evolutionary pathways in which promiscuous activities increased while the native ones remained virtually unchanged (Aharoni, Gaidukov et al. 2005). The mutations in these pathways are primarily in flexible regions of the protein scaffold rather than in the catalytic or

substrate binding residues (Fernandez, Tawfik et al. 2005). Along with several other examples (Gould and Tawfik 2005; Khersonsky and Tawfik 2005), the *in vitro* evolution of PTE-S5a followed precisely this kind of pathway.

The semi-rational strategy followed in this work permitted the exploitation of the wealth of structural information known about PTE albeit at the expense of neglecting non-pocket residue changes that might have had the potential to alter substrate selectivity, or, in the context of Tawfik's proposal, to increase promiscuity while maintaining wild-type (paraoxonase) activity.

Chapter 6 Replacement of Lys-169 in PTE Metal Binding Site

This chapter describes experiments done to investigate the possibility of replacing the metal binding carboxylated Lys-169 of PTE by any other residue while retaining enzymatic activity.

6.1 Introduction

6.1.1 Metal binding via carboxylated lysines

When the crystallographic structure of *Pseudomonas diminuta* phosphotriesterase (PTE) was first elucidated (section 1.3.1), it became clear that the transition metal cations, bound within its structure, were bridged through a covalently modified lysine (Lys*-169). This modification consists of a carboxylation resulting from the spontaneous reaction between the N^{ε} of Lys-169 and carbon dioxide (Kuo, Chae et al. 1997).

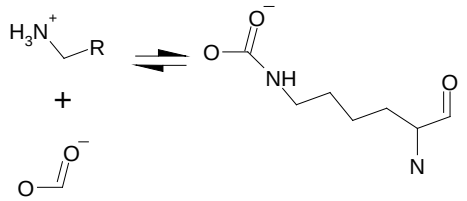

Scheme 6

It has been proposed that the carboxyl group of Lys*-169 serves as a dianionic bridging ligand that holds the metal cations in the right position, without any direct role in the catalysis. It is little understood why PTE uses a modified lysine, instead of using the carboxyl group of a glutamate or aspartate (Kuo, Chae et al. 1997).

Carboxylated lysine residues are known to function as metal centre ligands in other enzymes: dihydroorotase (Thoden, Phillips et al. 2001), urease (Jabri, Carr et al.

1995), and RUBISCO (Lorimer and Miziorko 1980). The dihydroorotase from *Escherichia coli* and the urease from *Klebsiella aerogenes* bind two metal ions at metal centres almost identical to that of PTE: nickel and zinc ions in urease and dihydroorotase, respectively. In the case of RUBISCO from *Rhodospirillum rubrum*, the Lys-carbamate serves as a ligand to the mononuclear magnesium centre (Estelle, Hanks et al. 1985).

6.1.2 Protein Homologue to PTE from *Escherichia coli* (ePHP)

The residues that bind the metal ions in PTE are known to be conserved in around 30 different proteins. From this PTE-like family, only a handful have been characterized, and, excluding PTE itself, only one structure has been determined: the Protein Homologue to PTE from *Escherichia coli* (ePHP) (Buchbinder, Stephenson et al. 1998).

ePHP and PTE share only 28% of identity in their protein sequences, although the structures are very similar. When superimposed (section 2.5.1.3), the RMSD between the C_α from most of the α/β barrel is as low as 1.16 Å (Figure 25.A). In particular, when the metal binding centres are compared, the main difference is the substitution of the carboxylated lysine (Lys*-169) in PTE for a glutamate residue (Glu-125) in ePHP (Figure 25.B). The shorter side-chain of the glutamate is compensated by the presence of an extra residue, an alanine (Ala-124). Both Lys-169 and Ala-124/Glu-125 form part of the fourth β-strand of the α/β barrel in their respective structures.

Although neither activity nor substrate have been described for the ePHP, the high structural similarity between its metal site and that of PTE suggests that ePHP supports a metal-based hydrolase activity.

The replacement of Lys*-169, in PTE, for other residues (methionine, alanine, glutamate) yielded mutants several orders of magnitude less active than the wild type. The activity in these mutants was partially restored by incubation with short carboxylic acids (Hong, Kuo et al. 1995). Mutation of Lys-169 to Glu, preceded by an alanine, was reported to abolish the expression of PTE in *E. coli* (Kuo, Chae et al. 1997).

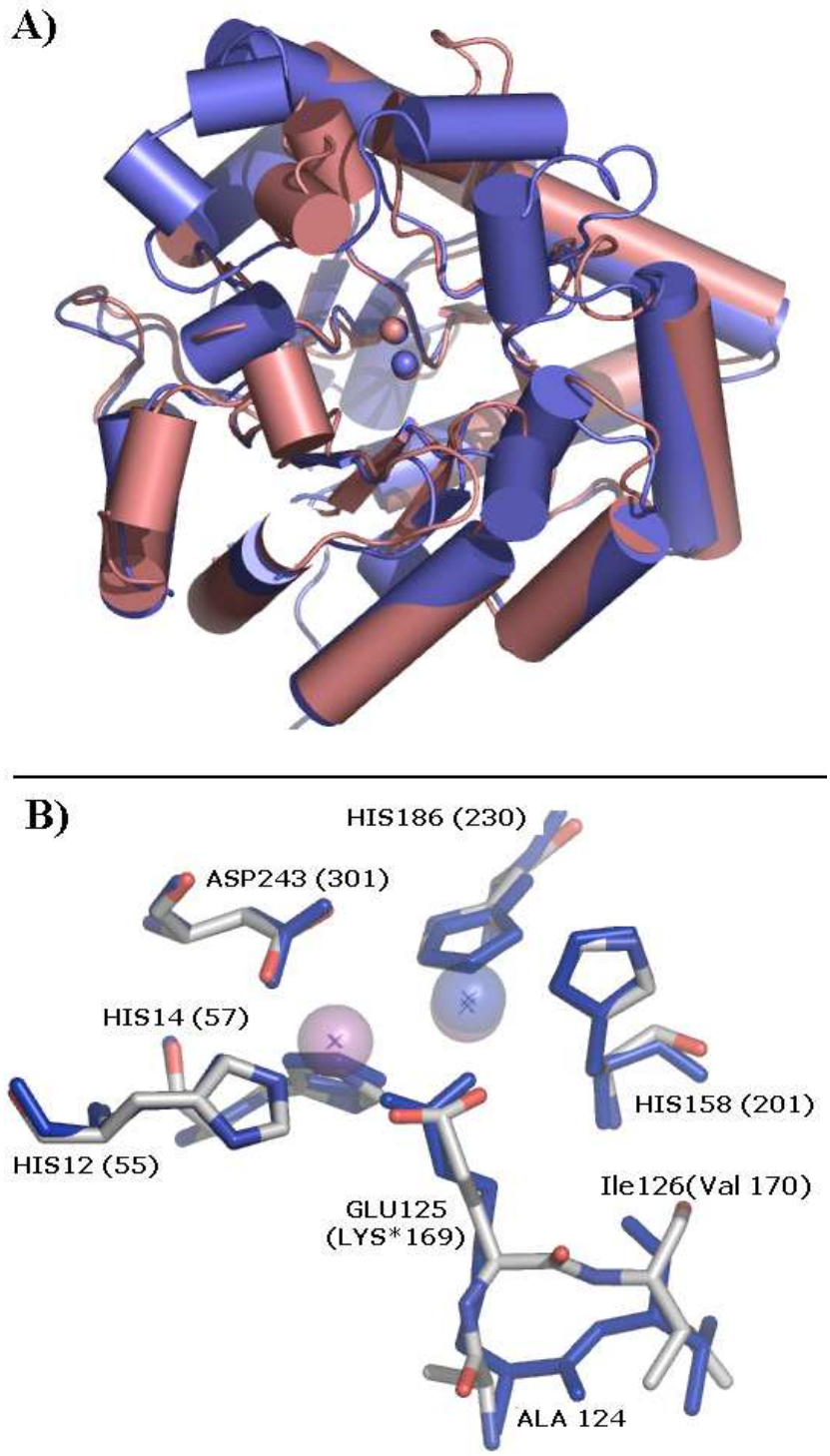

Figure 25. (A) Superposition of the structures of PTE-Zn(II) (blue) and *E. coli e*PHP-Zn(II) (red). **(B)** Superposition of the metal binding residues of PTE (blue and numbers in parenthesis) and *e*PHP-Zn(II) (purple spheres and grey residues). The overlap was done with Deep View / Swiss-Pdb Viewer v3.7 using the His-55, His-57, His-201, His-230 and Asp-301 residues as reference for the alignment (RMSD = 0.30 Å).

6.2 Results

6.2.1 PTE-like family multiple alignment

A multiple alignment of the protein sequences of the PTE-like family members was done as described in section 2.5.1.2. Relative to the residues found in the position homologous to Lys*-169 in PTE, the members of the PTE-like family can be classified in two groups (Figure 26). In the group *K*, which includes *P. diminuta* PTE and *A. tumefaciens* Organophosphate Hydrolase, the only two proteins that are known to posses phosphotriesterase activity, a lysine residue is conserved. In the group *E*, on the other hand, this lysine is replaced by a glutamate preceded by alanine or glycine residue. Other positions also exhibited residue conservation: Gly-166 was conserved, Ile-168 was substituted only by similar residues (Val and Leu), and in the position of Ala-170, only Ala or Gly were found. At the positions of Val-170 and Ile-167, less consensus was found.

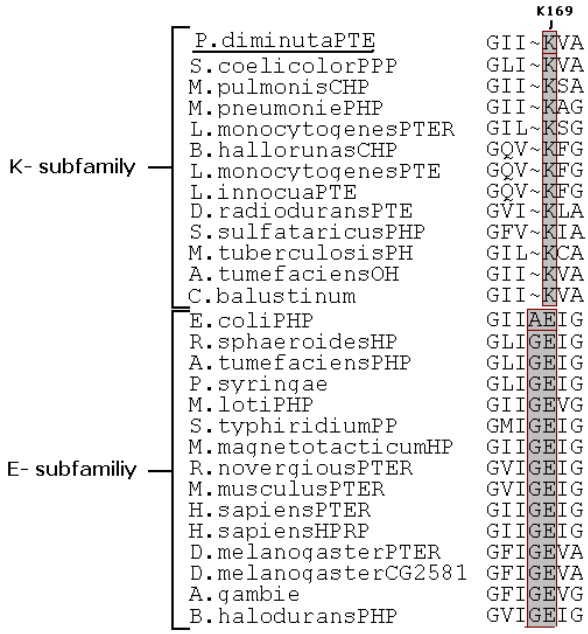

Figure 26. Multiple alignment of the PTE-like family in the region corresponding to the fourth β-strand of the α/β barrel in PTE. Two groups, *K* and *E*, can be distinguished according to the residue that (putatively) bridges the two metal ions.

A phylogeny tree for the PTE-like family was generated from a multiple alignment of the full protein sequences using the urease from *E. coli* as an external group (Figure

27) (see section 2.5.1.2). It revealed that, excepting for *E. coli* ePHP and *B. halodurans* PHP, the groups *K* and *E* mapped into two distinct phylogenetically related subfamilies.

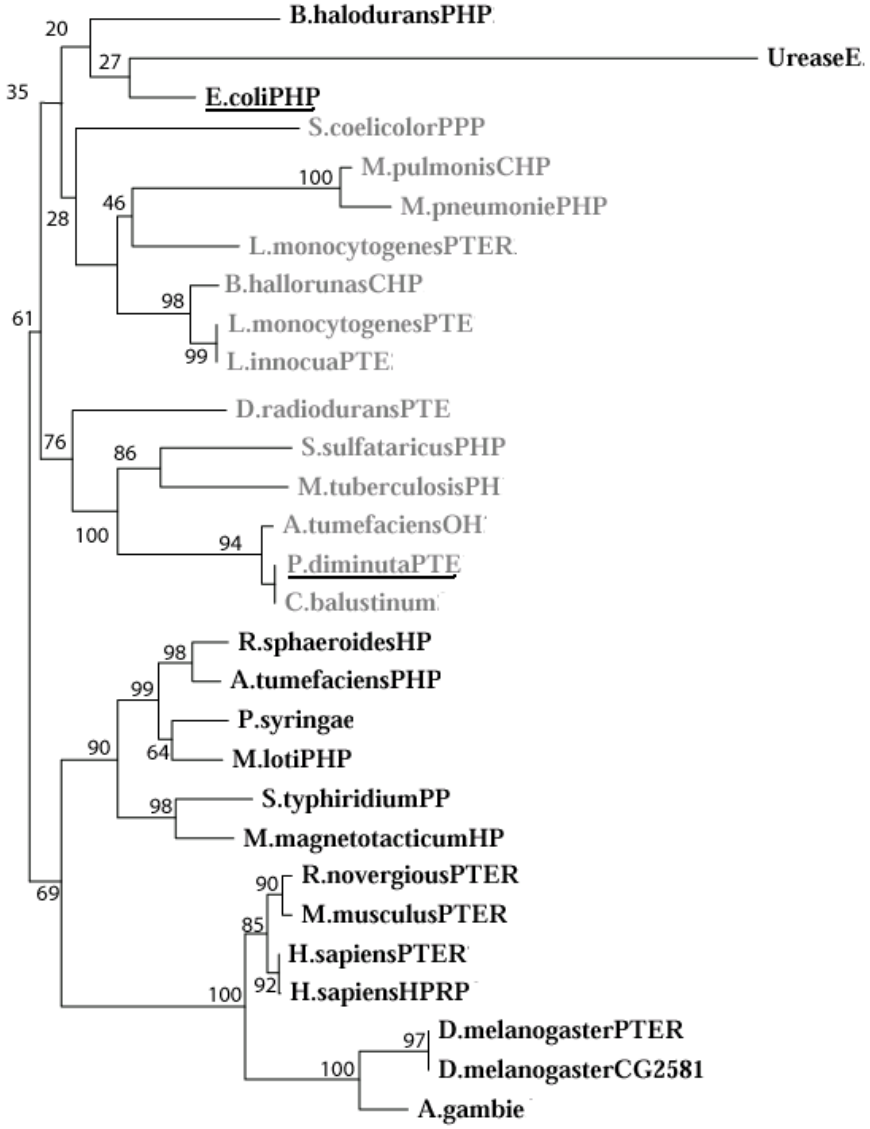

Figure 27. Phylogenetic tree of the PTE-like family. Those proteins with a conserved lysine in the homologue position of Lys*-169 of PTE (subfamily *K*) were coloured light grey. Those that instead have glutamate preceded by alanine or glycine (subfamily *E*) are coloured black. *P. diminuta* PTE and *E. coli* PHP are underlined. The Neighbour Join algorithm was used to generate the tree; the number in each node indicates the bootstrap values after 1000 replicates.

6.2.2 Design of point mutants

The list of the modifications introduced by point mutagenesis in PTE, and the nomenclature used, are compiled in Table 27. The general idea behind these constructs was to substitute Lys-169 by Glu preceded by either Ala or Gly, as in mutants PTE-A1 and PTE-G1, respectively. The mutation K169AE was also introduced in combination with several other mutations. Some constructs (A2 and G2) included the substitution of the residues Val-170 and Ala-171 by those residues present in ePHP: Ile and Gly, respectively (section 2.2.2.9).

It is possible that the internal bulge at the core of ePHP, caused by the presence of Ala-124, is stabilised by the presence of Asn-56 and/or Cys-80 (not shown). At the homologous positions, PTE has Thr-103 and Ala-127; therefore, these residues were mutated to Asn and Cys, respectively. The mutants PTE-TN and PTE-AC were designed to serve as controls.

Table 27. Nomenclature for the designed mutants.

Code	Mutation
A1	K169AE
G1	K169GE
A2	K169AE/V170I/A171G
G2	K169GE/V170I/A171G
A1N	K169AE/T1O3N
A2N	K169AE/V170I/A171G/T1O3N
A1C	K169AE/A127C
A2C	K169AE/V170I/A171G/A127C
A1NC	K169AE/T103N/A127C
A2NC	K169AE/V170I/A171G/T103N/A127C
TN	T103N
AC	A127C

6.2.3 Construction of mutants by directed mutagenesis.

All the mutants described in Table 27 were constructed, as described in section 2.2.2.9, using pIVEX-PTEwt as template (not shown). The mutation K169GE (named G1) was also introduced in the previously constructed vectors pIVEX-S5a, pIVEX-PTE-H5, pMAL-PTE-wt, pMAL-PTE-S5a, and pMAL-PTE-H5a (section 2.2.1.3.4).

The mutations were confirmed by sequencing with the appropriate primer (section 2.2.2.11 and Table 6).

6.2.4 Determination of activity *in vivo*

The constructs were transformed into *E. coli* C41 cells, grown, and induced as described in section 2.1.2.6.1. *E. coli* ePHP cloned into pIVEX was used as negative control. 100 µl of the cultured cells was resuspended and lysed with Bugbuster™ (section 2.1.2.7.2). After mixing 50 µl of the cell lysate and 150 µl of the activity formulation (50 mM Hepes pH 8.5, 1 mM $ZnCl_2$, 0.5 mM Paraoxon), the release of p-nitrophenol was followed for 24 hours (see section 2.3.2.5.3). The results obtained are compiled in Table 28 and Table 29.

Table 28. Activity *in vivo* for constructs based in PTE-wt.

Construction	Activity	
	(mM min^{-1})	Ratio (PTE-wt =1)
PTE	6.0 (±1.2) x 10^3	1
PTE-TN	48.2 (±4.2)	8 x 10^{-3}
PTE-AC	3.5 (±2.7) x 10^3	0.58
PTE-A1	†	---
PTE-A1N	†	---
PTE-A1C	†	---
PTE-A1NC	†	---
PTE-A2	†	---
PTE-A2N	†	---
PTE-A2C	†	---
PTE-AENC	†	---
PTE-G1	†	---
PTE-G2	†	---
G1	†	---
G2	†	---
ePHP	†	---

Table 29. Activity *in vivo* for constructs bearing the K169GE mutation

Construct	Activity [a] mM min^{-1}
pIVEX- PTE-WT	1.89 (±0.13) x 10^4
pIVEX- PTE-S5a	1.82 (±0.27) x 10^6
pIVEX- PTE-H5	2.11 (±0.78) x 10^5
pIVEX- PTE-WT(G1)	†
pIVEX- PTE-S5a(G1)	63.46 (±0.48)
pIVEX- PTE-H5(G1)	48.05 (±0.02)
pMAL- PTE-WT	7.54 (±0.03) x 10^3
pMAL- PTE-S5a	3.48 (±0.14) x 10^5
pMAL- PTE-H5	3.61 (±0.32) x 10^4
pMAL- PTE-WT(G1)	†
pMAL-PTE-S5a(G1)	5.79 (±0.18)
pMAL-PTE-H5(G1)	†

a. Paraoxon (ε_{280nm} = 18.8 mM cm^{-1}). G1 stands for the mutation K169GE. † No activity detected.

None of the constructs in which the Lys-169 was replaced by Glu and PTE-wt was used as template exhibited paraoxonase activity. Moreover, the mutation of Thr-103, a residue not directly involved in the binding of metal to Asn reduced the activity by 125-fold. Activity was found in the variants S5a(G1) and H5a(G1), when pIVEX was used as expression vector. The fusion of Maltose Binding Protein with the PTE variants inhibited the activity by approximately 10-fold. Aliquots of the crude and soluble fractions were analysed by SDS PAGE (Figure 28). Irrespective of the template or vector used, constructs bearing the mutation K169GE were highly insoluble in the bacterial cell.

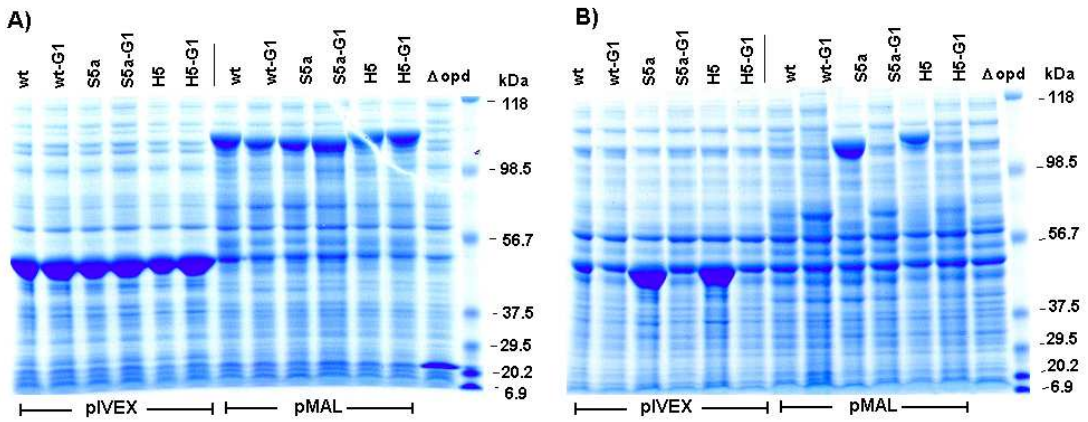

Figure 28. SDS PAGE of the **(A)** crude and **(B)** soluble fractions of several mutants bearing the mutation K169GE run in a 12% Bis-Tris SDS-PAGE gel with MES Buffer.

6.2.5 Refolding

Inclusion bodies of PTE-WT(G1), PTE-S5a(G1) and PTE-H5(G1) were prepared, as described in section 2.3.2.4.1. The purification process can be followed in Figure 29. The proteins obtained in the inclusion bodies were denature by resuspending the inclusion bodies in a buffer containing 6 M GdmHCl (6 M GdmHCl, 50 mM HEPES pH = 8.0, 500 mM NaCl, 1 mM 2-mercaptoethanol, 50 μM $ZnCl_2$). The refolding of the denatured preparations was attempted by dialysis (section 2.3.2.4.2) and *infinite* dilution (section 2.3.2.4.3).

The denatured inclusion bodies were dialysed stepwise against Refolding Buffer (50 mM HEPES pH = 8.0, 5 mM DTT, 50 μM $ZnCl_2$) with decreasing concentrations (5, 4, 3.5, 2 and 1 M) of GdmHCl at 4 °C. Each step was left to equilibrate for 4 to 8 hours. The three constructs were found to aggregate when the GdmHCl concentration reached 4 M (Figure 30).

The denatured inclusion bodies were added dropwise to a stirring Refolding Buffer at 4 °C. The volume ratio between the denatured inclusion bodies added and the buffer was approximately $1:10^5$. The *refolded* material was filtered and concentrated using an anion exchange column; the elution fraction was analysed by SDS PAGE (Figure 22). None of the loaded, flow-through or eluted fractions showed paraoxonase activity even after 24 hours of incubation with 0.5 mM Paraoxon at 25 °C (not shown).

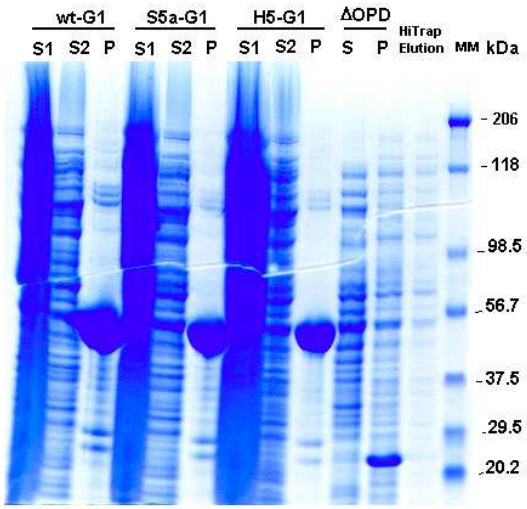

Figure 29. Preparation and purification of inclusion bodies. The constructs were washed with 50 mM HEPES pH 8.0 (**S1**) and 50 mM HEPES pH=8.0, 500 mM NaCl, 1% (v/v) Triton X-100 pH=8.0 (**S2**). The purified pellet (**P**) was obtained by resuspension in 50 mM HEPES pH =8.0, 5 mM DTT, 50 μM $ZnCl_2$. The soluble (S) and insoluble fractions of ΔOPD are shown as reference. The refolded fraction, concentrated in a HiTrap anion exchange column, is shown (Hi Trap Elution).

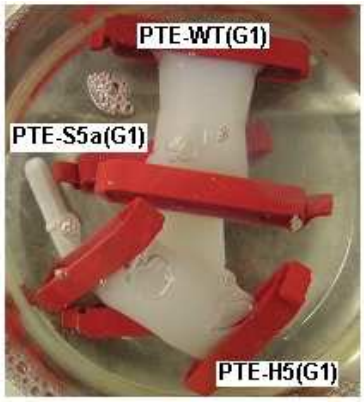

Figure 30. Protein aggregates obtained from the refolding attempt of PTE-WT, PTE-S5a(G1) and PTE-H5(G1) constructs by dialysis. The picture was taken when the mutants were dialysed against 4M GdmHCl.

6.2.6 Library design

Five libraries were designed: *AE*, *BE*, *CE*, *DE* and *EE* (Table 30). In libraries *AE* and *BE*, the residues Lys*-169, V-170, and A171 were randomised; in library *BE*, residue Ala-171 was only randomised to Ala or Gly. The three remaining libraries included an insertion of a codon preceding the position of Lys*-169. In *CE* and *DE* libraries, a Glu

was fixed in position 169, and both Val-170 and Ala-171 were randomised in accordance with the conservation seen in the alignment of several PTE related genes (Figure 26).

Table 30. Libraries designed for the substitution of K169 in PTE.

	Library				
Residues	**AE**	**BE**	**CE**	**DE**	**EE**
K169	NNS	NNS	GSA [c] / E	NNS / E	NNS / NNS
V170	NNS	NNS	VYY [d]	NNS	NNS
A171	GSA [c]	NNS	GSA [c]	GSA [c]	NNS
[a] **$Size_{DNA}$**	~ 2×10^3	~ 3×10^4	~ 32	~ 2×10^3	~ 6×10^6
[b] **$Size_{PROT}$**	~ 8×10^2	~ 8×10^3	~ 24	~ 8×10^2	~ 1×10^4
Effective $Size_{DNA}$	~ 7×10^3	~ 1×10^5	~ 100	~ 6×10^3	~ 2×10^7

a. The library size refers to the degrees of freedom (namely bases or residues) that are encoded for.

b. The effective size refers to the number of clones needed in a library to ensure (95%) that all members are represented (see section 5.2.1).

c. GSA codes for Gly or Ala, each with a frequency of 0.5.

d. VYY [35] codes for Ile, Val, Ala, Thr, Pro or Leu, each with a frequency of 0.17.

6.2.7 Library construction

Libraries were constructed using cassette mutagenesis as described in sections 2.2.2.10 and 5.2.2.2. The oligonucleotides used for the library synthesis can be found in section 2.2.1.1.1.4.2 and Table 10. Two sets of libraries were constructed, using *opd* and *opd-h5* as templates (Figure 32). The final products were re-cloned into pIVEX using NcoI/SacI restriction sites (section 2.2.2.10.3).

Plasmid DNA libraries were obtained by transforming freshly prepared *E. coli* MC1061 cells as described in section 5.2.2.2. Visual inspection of the chromatograms of the sequencing results generated from the library DNA revealed that targeted residues were indeed randomised (Figure 31). No individual clones were sent for sequencing.

35 V stands for not-U (V follows U), and Y for pYrimide.

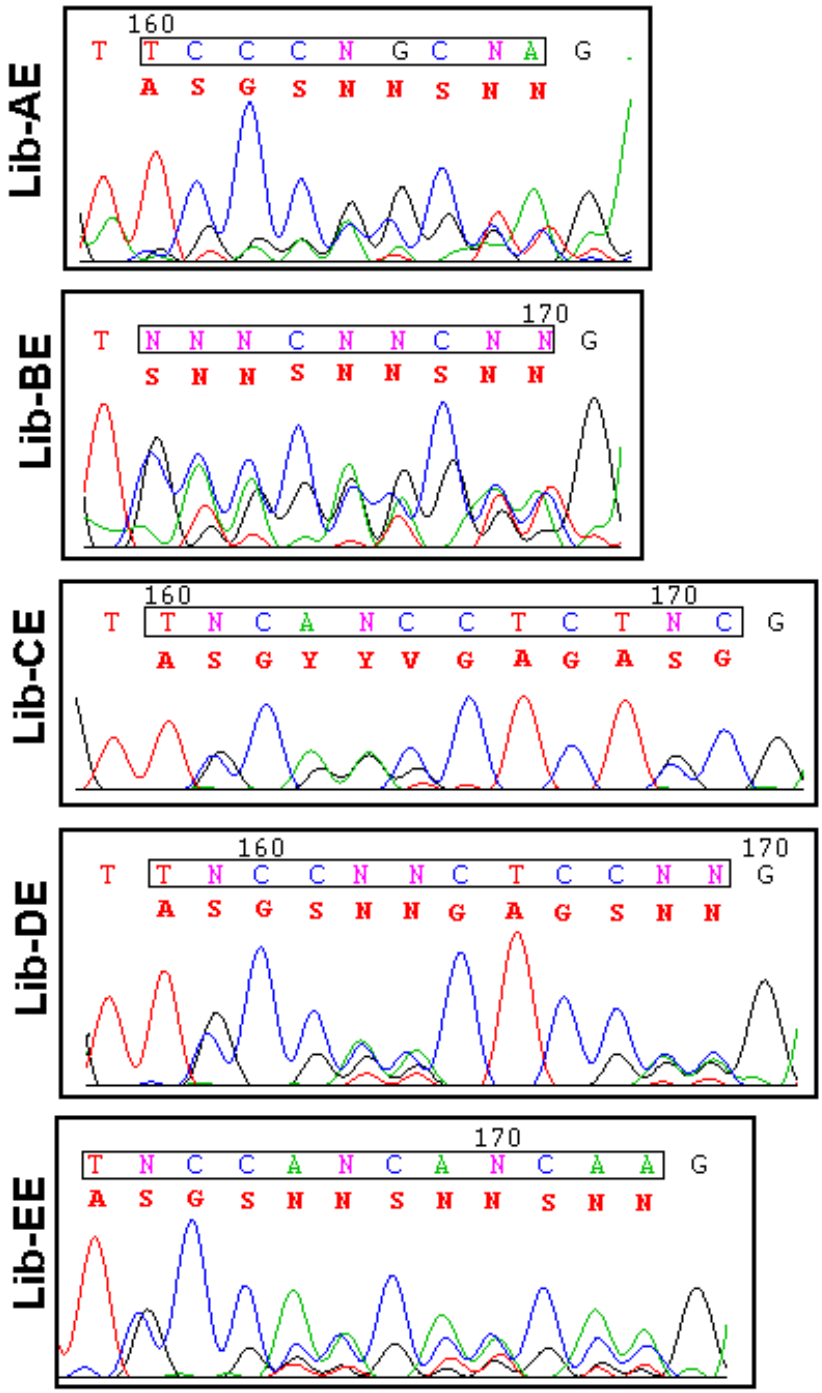

Figure 31. Chromatograms of sequencing reactions using libraries *AE to EE* as templates. Sections of the sequencing reaction, using T7Rev primer, in which the codons are randomised. The sequencing reactions were done by the MRC Geneservice (Hinxton, UK).

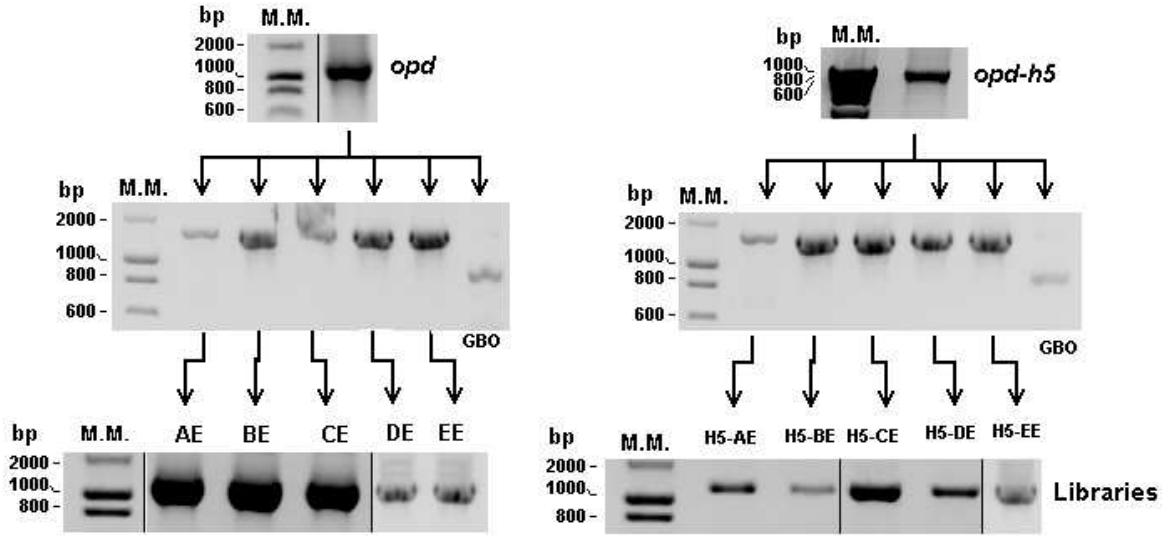

Figure 32. Construction of metal-binding libraries. Starting from the *opd* and *opd-h5* genes, five libraries were constructed by consecutive rounds of PCR, digestion and ligation (section 2.2.1.1.1.4). Two fragments per library were synthesised, one bearing the diversity, the other a triple-biotin tag (GBO). The fragments were ligated via a BbsI site and purified using streptavidin-coated beads. The DNA was analysed by electrophoresis in agarose gels stained with ethidium bromide (section 2.2.2.4).

6.2.8 Library screening

The libraries were transformed into *E. coli* C41 cells and screened using **2**/Parathion analogue as described in sections 2.1.2.5.2 and 4.2.1. For most of the libraries synthesised, approximately 10,000 clonies were screened (Table 31). Libraries *AE* and *H5-AE* were not screened, and 40,000 colonies were screened for libraries *EE* and *H5-EE*.

Table 31. Number of clones screened in plate using 2/Parathion

Library	# clones	Effective size of library sampled
AE	NS	- - -
BE	~1 x 10^4	~10 %
CE	~1 x 10^4	100%
DE	~1 x 10^4	100%
EE	~4 x 10^4	<0.5 %
H5-AE	NS	- - -
H5-BE	~1 x 10^4	~10 %
H5-CE	~1 x 10^4	100%
H5-DE	~1 x 10^4	100%
H5-EE	~4 x 10^4	<0.5 %

NS, not screened.

No positive clones were found in libraries *CE*, *H5-CE*, *DE* or *H5-DE*. For libraries *BE*, *H5-BE*, *EE* and *H5-EE*, several hundred colonies proved to be active (not shown). Only a total of 50 colonies were chosen, sequenced and *in vivo* activities towards **2**/Parathion measured, as described in sections 2.1.2.5.3 and 4.2.2. Both the sequence and *in vivo* activities, relative to wild type, are compiled in Table 32 and Table 33.

Table 32. Mutants selected from libraries *BE* and *H5-BE*. The *in vivo* activity is reported relative to PTE-wt and PTE-H5 for libraries *BE* and *H5-BE*, respectively.

Clone	Library	R. activity	Position		
			K169	V170	A171
ME1	*BE*	0.045	E	S	G
ME2	*BE*	2.5	K	L	G
ME3	*BE*	0.5	K	A	S
ME4	*BE*	2.5	K	C	T
ME5	*BE*	0.5	K	V	S
ME6	*BE*	1	K	L	A
ME7	*BE*	3	K	V	V
ME8	*BE*	3	K	C	M
ME9	*H5-BE*	0.003	R	V	H
ME10	*H5-BE*	0.2	K	L	S
ME11	*H5-BE*	0.06	K	T	I
ME12	*H5-BE*	0.15	K	T	I
ME13	*H5-BE*	0.2	K	L	V
ME14	*H5-BE*	1	K	L	A
ME15	*H5-BE*	0.18	K	V	M
ME16	*H5-BE*	1	K	L	G
ME17	*H5-BE*	1	K	V	A
ME18	*H5-BE*	0.14	K	C	I
ME19	*H5-BE*	0.008	G	V	S
ME20	*H5-BE*	0.076	K	C	P
ME21	*H5-BE*	0.006	V	S	V
ME22	*H5-BE*	0.001	S	S	G
ME23	*H5-BE*	0.12	K	A	T
ME24	*H5-BE*	0.4	K	V	L

Mutants chosen to be expressed and purified are shown in grey boxes.

Most of the selected variants from the library *BE* had a conserved lysine at the position 169, and Val, Ile, Leu, Ala, Ser at positions 170 and 171 (Table 32). The activity *in vivo* of these mutants was similar to that of PTE-wt. One mutant (ME1), however, was recovered in which the mutations K169E, V170S and A171G were found. The activity *in vivo* of PTE-ME1 was 40-fold less than PTE-wt.

In most of the variants sequenced from *H5-BE*, the Lys-169 was conserved, with the exception of ME9, ME19, ME20 and ME21 in which Arg, Gly, Val and Ser were obtained. These mutants were between 100 and 1000-fold lower active *in vivo* than PTE-H5.

Table 33. Mutants selected from libraries *EE* and *H5-EE*. The *in vivo* activity is reported relative to PTE-wt and PTE-H5 for libraries *EE* and *H5-EE*, respectively.

Library	Library	R. activity	Position		
			K169	V170	A171
ME25	*EE*	0.05	KV	Q	G
ME26	*EE*	0.025	KC	G	G
ME27	*EE*	0.25	KV	A	G
ME28	*EE*	0.38	KV	G	G
ME29	*H5-EE*	0.612	KV	V	A
ME30	*H5-EE*	0.018	LC	A	A
ME31	*H5-EE*	0.02	LA	S	G

Mutants chosen to be expressed and purified are shown in grey boxes.

All the variants sequenced from library *EE* presented a conserved Lys as the first residue in position 169, and most contained Val as second residue at position 169. Ala and Gly were predominant at positions 170 and 171. The activities *in vivo* of these selected variants were between 2 to 40-fold lower than PTE-wt.

From the three clones selected and sequenced from the library *H5-EE*, one (ME29) exhibited a Lys/Val combination at position 169, while maintaining Val and Ala residues at positions 170 and 171, respectively (Table 33). The PTE variants ME30 and ME31 contained non-lysine residues at position 169, with Leu/Cys and Leu/Ala, respectively. The activities *in vivo* of these two variants were 50-fold lower than PTE-wt.

6.2.9 Metal binding mutants purification

Eight of the variants obtained were chosen to be purified and their paraoxonase activity measured *in vitro* (Table 32 and Table 33). PTE-H5 was used as template for libraries due to its high expression yield in C41 *E. coli* – compare, for instance, the soluble fractions of PTE-wt and PTE-H5 in Figure 28B. The modifications obtained in variants ME1 and ME28 were introduced to PTE-H5 by iPCR, using as primers the oligonucleotides P270804A, P270804B, P290704E and P290704F (sections 2.2.2.1.2 and 2.2.1.1.1.3) (data not shown).

Genes from selected clones were extracted by PCR and re-cloned into the vector pHLT (data not shown) (section 2.2.1.3.3). The selected PTE variants were produced *E. coli* C41, grown in autoinduced media (section 2.1.2.6.2), and affinity purified using a Nickel-NTA (Qiagen) column. Only PTE-H5 and three of the mutants, PTE-ME9, ME28 and ME30, could be expressed under these conditions. The purity of the protein preparations was shown to be greater than 90% by PAGE (section 2.3.2.5.1)(Figure 33). The extinction coefficients (at 280nm) were calculated by sequence, and the protein concentrations were measured by absorbance at 280nm (section 2.3.2.5.2.1).

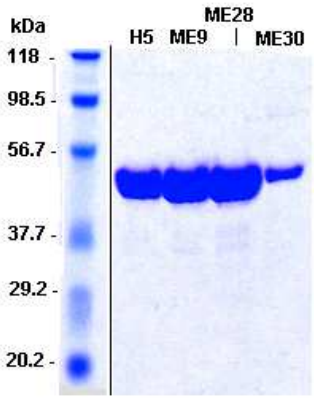

Figure 33. Metal selected variants obtained after purification process, and run on a 12% Bis-Tris SDS-PAGE gel with MES Buffer.

6.2.10 Metal binding variants k_{cat} and K_M towards Paraoxon

The kinetic parameters k_{cat} and K_M of the selected variants towards Paraoxon were measured as described in sections 2.3.2.5.3 and 3.2.2; the data obtained is compiled in Table 34.

Table 34. Kinetic properties of selected PTE metal variants for the hydrolysis of Paraoxon.

Variant	Sequence			Activity		
	K169	V170	A171	k_{cat}	K_M	k_{cat}/K_M
PTE-H5	K	V	A	22336 (±1244)	0.39 (±0.18)	5.7 x10^7
PTE-ME9	R	V	H	0.55 (±0.03)	0.14 (±0.01)	3.9 x10^3
PTE-ME28	KV	G	G	6776 (±893)	0.94 (±0.07)	7.2 x10^6
PTE-ME30	LC	A	A	1.12 (±0.9)	0.48 (±0.04)	2.3 x10^3

The PTE variants ME9 and ME30 exhibited a significant decrease in their k_{cat} against Paraoxon. In the particular case of PTE-ME9, the loss, relative to PTE-H5, was 50,000-fold. The K_M values, however, remained relatively unchanged. The variant PTE-ME28, on the other hand, showed only a 3-fold drop in its k_{cat}, and a 2-fold increase in its K_M.

6.3 Discussion

6.3.1 PTE-like family

The multiple aligment of the PTE-like family proteins revealed that its members could be classified in two groups according to which residue is used to bridge the two ions in the metal center. On the one hand, the group *K* utilises the carbamide group of the post-transcriptionally carboxylated lysine to hold both anions in place; the Phosphotriesterase of *P. diminuta* (PTE) belongs to this group. On the other hand, the group *E* utilises the carboxylate group of a glutamate as a bridge between the two metal ions; the Protein Homologue to Phosphotriesterase of *E. coli* (ePHP) belongs to this group.

The phylogenetic tree of the PTE-like family proteins reveled that this familiy is composed of at least two subfamilies. The subfamily that includes *Agrobacterium tumefaciens* PHP and all the eukaryotic Phosphotriesterase Related proteins is clearly defined by the bootstrap values obtained. All the members of this subfamily belong to the group *E*. The other subfamiliy is less well defined and includes all members of the group *K*, and could include ePHP and *B. halodurans* PHP. Given the low bootstrap values of the nodes that connect the latter two proteins with the rest of the subfamily, it is not entirely clear whether or not they belong to this subfamily.

The picture that emerged from analysing the distribution of groups *K* and *E* in the different subfamilies is that exchanges between modified lysine- and glutamate-based strategies to bridge anions in a metal center rarely (if at all) occurred in nature. It is important to mention that the sequence divergence is such that amongst the members of the subfamilies, no consensus was found at any other residue.

6.3.2 Replacement of Lys*169 by Glu

The directed replacement of Lys*-169 by a Glu preceded by a Ala or Gly yielded insoluble aggregates when expressed in *E. coli* C41 cells. Attempts to stabilise the presence of the (Ala/Gly)/Lys pairs in PTE-wt, by replacing Thr-103 for Asn and Ala-127 by Cys, were fruitless. In fact, the mutations T103N and A127C reduced the wild-type activity *in vivo* by 125- and 2-fold, respectively. Activity was detected, however, when the mutations K169GE were introduced in PTE-S5a and PTE-H5; *in vivo* these activities were approximately 10,000-fold lower than those found for their respective templates. It was not possible to purify either of the PTE-S5a(G1) or PTE-H5(G1) constructs as both readily formed aggregates upon refolding. According to the activity levels obtained *in vivo*, the fusion of Maltose Binding Protein with PTE where did not prevent the insolubility of the constructs.

6.3.3 Selection of libraries

Five libraries were designed in which the residues Lys*-169, Val-170 and Ala-171 were fully or partially randomised. Three of these libraries, *CE*, *DE* and *EE*, have an extra residue encoded in position 169; libraries *CE* and *DE* fixed in the second codon at the position 169 a Glu. Ten libraries were synthesised as both PTE-wt and PTE-H5 were used as templates.

Libraries *CE* and *DE* were screened to completion, but no positive colony was detected when either PTE-wt or PTE-H5 was used as template. Regarding libraries *BE* and *EE*, 31 clones out of the hundreds of colonies that exhibited activity were sequenced and their activity *in vivo* determined. Most of these selected clones (80%) proved to have a lysine in position 169, while mainly residues Val, Ile, Leu, Ala, Ser were recovered at positions 170 and 171. There was no consensus on the variants

with a non-lysine residue, as Glu, Arg, Gly, Val, Ser and Cys were found at position 169.

Eight mutants were selected to be expressed and purified, but only PTE-ME9 (K169R/V170V/A171H), PTE-ME28 (K169KV/V170G/A171G), and PTE-ME30 (K169LC/V170A) proved to be readily soluble under the conditions tested. When PTE-ME9 and PTE-ME30 showed a significant reduction of approximately 50,000-fold in their k_{cat} towards Paraoxon; the K_M values, however remained relatively unchanged. The variant PTE-ME28, on the other hand, showed only a 3-fold drop in its k_{cat}, and a 2-fold increase in its K_M.

The first conclusion that can be drawn from the results obtained by the combinatorial substitution of Lys*-169 is that mutations at sites 170 and 171 that rescue the activity of variants bearing a Glu-169 are unlikely to occur. Despite the insertion of an extra residue at position 169, lysine is the only residue that maintains wild-type activity levels. In the case of those mutants that presented a Lys with the extra residue inserted, the strain cause by this insertion is most likely relieved by the loop that follows the β-strand in which Lys*-169 is placed. The fact that the non-lysines showed significant reduction of activities both *in vitro* and *in vivo* simply highlights the sensitivity of the selection system employed.

Conclusions and Future Work

Conclusions

The reactivity of organophosphatases PTE and PON1 towards the fluorogenic nerve agents confirmed that these compounds are suitable substrates for both enzymes, and that despite all analogues sharing the same leaving group, their functional and structural diversity is maintained. These results, along with the *in vitro* AchE inhibition assays and the *in vivo* toxicity of the 12/Cyclosarin analogue reported elsewhere (Briseño-Roa, Hill et al. 2004), strongly suggests that the fluorogenic analogues are indeed good mimics of their nerve agent (NA) counterparts.

The combination of fluorogenic substrates, used as probes, and the partial lysis of bacterial colonies resulted in a very sensitive screening method that also provided a simple way of coupling the genotype with the phenotype. Measuring the activity *in vivo* of those clones selected in plates proved to be a good qualitative assessment of their activity and selectivity relative to the wild type enzyme. The easy implementation of the directed evolution platform developed and used here compensates for the fact that only a small number of variants can be screened relative to the number of mutations that might be needed to obtain significant improvements in activity towards NAs.

From the data obtained both *in vivo* and *in vitro*, it is clear that mutations that contribute to the improvement in the activity for NA analogues are more frequent in the Pro-R pocket than in the Pro-S and Entrance pockets.

The improvements in the activities of variants A, C, D, E and F for the 4/Paraoxon analogue derived mainly from their increase in preference for the fluorogenic coumarin as leaving group. In contrast, the improvements obtained activity towards 9/Sarin, 10/Russian-VX, 11/Soman, and 12/Cyclosarin analogue found in variants Q, S and T were due mainly to a better acceptance of phosphonates, relative to phosphate substrates. Thus, improved activities of the variants PTE-Q, S

and T towards the phosphonate NA analogues are likely to be translated to the original NAs, as these improvements are not derived solely from a better fit for the fluorescent leaving group.

One selected variant, PTE-H, exhibited significant increases both in its K_M and k_{cat} for Paraoxon, while maintaining the k_{cat}/K_M ratio relatively unchanged. Using the criteria on the evolution of maximum rate proposed by Fersht (Fersht 1974; Fersht 1999), both PTE-H and the *in vitro* evolved PTE-H5 (Griffiths and Tawfik 2003) are more efficient catalysts than the wild type enzyme for hydrolysis of Paraoxon.

The net changes in activity of the selected PTE variants, relative to PTE-wt, are a result of the combination of those mutations already present in PTE-S5a and those obtained after the randomisation of the substrate binding pockets. These observations highlight the fact that strategies that combine the generation and selection of mutations both in the active site and out of it, may be advantageous.

It can be concluded, from the values obtained both *in vivo* and *in vitro*, that changes in selectivity are necessary but not sufficient to ensure changes in activity, for mutations occurring in the active site of an enzyme. This observation suggests that an active site must relax its grip on the *wild-type* substrate, if promiscuous activities are to be evolved as high as the wild-type activity.

Regarding the case study presented, it was not possible to substitute the carboxylated lysine of PTE by any other residue without significantly interfering with its enzymatic activity. Despite Protein Homologue to Phosphotriesterase from *E. coli* (ePHP) possessing a remarkable structural congruence with PTE, constructs of the latter bearing a glutamate residue preceded by a glycine or alanine were insoluble *in vivo* and could not be refolded *in vitro*. Combining these results with the fact that it was not possible to pin-point a residue that directly stabilised the internal bulge created by alanine 124 in the ePHP structure, it seems unlikely that the PTE structure will easily utilise a functional glutamate to bridge together the ions of its metal center.

Future Work

Crystallographic studies on PTE-Q are currently being done in order to shed light on the structural and functional determinants of its improvement in selectivity and activity towards phosphonate substrates.

All NA analogues used in this work were synthesised as racemic mixtures. It is known, however, that some enantioners of NAs are significantly more toxic than others. The preparation of enantiomerically pure analogues will permit screening for PTE variants with increased activities towards the more toxic enantiomers of NAs.

It was found that mutations that enhanced NA analogue hydrolysis are more likely to occur in Pro-R than in any other region of the PTE active site. As less than 1% of the Pro-R library was screened, a more thorough screening will likely yield variants with higher activities and selectivity towards NA analogues.

In directed evolution studies, the most dramatic improvements are achieved after several rounds of variation and selection. Thus, recombination of the PTE-Q, S and T variants, may generate variants with further improvements in activity for the hydrolysis of NA analogues.

The final objective of this work was the creation of PTE variants with higher activities towards nerve agents. The determination of the kinetic properties of the selected variants PTE-Q, S and T for NAs is being carried out in the laboratory of Dr. Christopher M. Timperley at the Defence Science and Technology Laboratory (Porton Down, UK).

Supplementary Information

Table 35. Kinetics properties of selected PTE variants for the hydrolysis of Paraoxon.

	Selected PTE variants																						
	wt	**S5a**	**H5**	**A**	**B**	**C**	**D**	**E**	**F**	**G**	**H**	**I**	**J**	**K**	**L**	**M**	**N**	**O**	**P**	**Q**	**R**	**S**	**T**
k_{cat}	5954	6441	26294	7184	27.2	962	8884	2074	3431	1.2	31016	1214	113	2568	2265	2300	797	1602	3167	72 ± 2	5.2	25.4	28.0
(s^{-1})	±188	±322	±927	± 0.35	±1.7	±36	±1174	±68	±331	±0.1	±1009	±48	±4	±97	±138	±123	±39	±72	±157		±0.1	±0.9	±1.5
K_M	0.029	0.037	0.96	0.35	1.73	0.078	0.28	0.062	0.19	0.28	0.84 ±	0.31	0.72	4.28	0.70	4.12	0.16 ±	0.57	0.41	0.15	0.69	0.16	0.53
(mM)	±0.012	±0.007	±0.07	±0.09	±0.23	±0.011	±0.08	±0.007	±0.04	±0.02	0.08	±0.04	±0.07	±0.28	±0.11	±0.36	0.02	±0.08	±0.06	±0.2	±0.05	±0.02	±0.09
k_{cat}/K_M	2.1	1.75 x	2.74 x	2.05 x	1.59 x	1.23 x	3.16 x	3.37 x	1.83 x	4.42 x	3.69 x	3.91 x	1.57 x	6.00 x	3.25 x	5.51 x	4.96 x	2.83 x	7.80 x	4.66 x	7.51 x	1.62 x	5.27 x
($M^{-1}s^{-1}$)	x10^8	10^8	10^7	10^7	10^4	10^7	10^7	10^7	10^7	10^3	10^7	10^6	10^5	10^5	10^6	10^5	10^6	10^6	10^6	10^5	10^3	10^5	10^4

Grey boxes highlight k_{cat} values higher than those for S5a.

Table 36. k_{cat}/K_M values for the selected variants

	Selected PTE variants																				
Analogue of	**wt**	**S5a**	**A**	**B**	**C**	**D**	**E**	**F**	**G**	**H**	**I**	**J**	**K**	**L**	**M**	**N**	**O**	**P**	**Q**	**R**	**S**	**T**
1/Methyl-parathion	1.3 x 10^6	2.5 x 10^6	1.0 x 10^5	1.6 x 10^2	7.7 x 10^4	1.2 x 10^5	8.1 x 10^4	4.8 x 10^4	4.9 x 10^3	1.8 x 10^3	6.9 x 10^3	4.7 x 10^3	3.0 x 10^3	3.4 x 10^3	1.2 x 10^3	1.6 x 10^6	1.6 x 10^5	3.0 x 10^5	1.2 x 10^5	1.1 x 10^5	3.0 x 10^4	2.2 x 10^4
2/Parathion	2.2 x 10^7	2.3 x 10^7	1.5 x 10^6	3.1 x 10^3	3.6 x 10^6	5.4 x 10^6	7.0 x 10^6	4.6 x 10^5	1.4 x 10^5	4.4 x 10^5	8.3 x 10^4	1.2 x 10^4	3.6 x 10^4	5.2 x 10^4	1.7 x 10^4	2.6 x 10^6	1.1 x 10^6	3.0 x 10^6	2.4 x 10^4	4.6 x 10^3	7.4 x 10^4	4.6 x 10^4
3/Methyl-paraoxon	7.2 x 10^5	1.8 x 10^6	4.6 x 10^4	3.3 x 10^2	1.4 x 10^5	6.8 x 10^4	4.2 x 10^4	3.3 x 10^5	9.9 x 10^2	1.9 x 10^4	1.4 x 10^5	4.8 x 10^3	6.6 x 10^3	5.1 x 10^4	2.8 x 10^4	3.1 x 10^5	1.0 x 10^5	1.4 x 10^5	6.3 x 10^4	2.3 x 10^4	1.1 x 10^4	1.2 x 10^4
4/Paraoxon	5.3 x 10^6	1.8 x 10^6	3.1 x 10^6	4.8 x 10^3	3.9 x 10^6	5.0 x 10^6	7.5 x 10^6	3.5x 10^6	3.3 x 10^4	9.2 x 10^5	1.2 x 10^6	1.9 x 104	7.0 x 10^5	4.0 x 10^5	1.5 x 10^5	5.8 x 10^5	2.7 x 10^5	9.4 x 10^5	9.0 x 10^4	1.5 x 10^3	8.1 x 10^4	3.7 x 10^4
5/DFP	4.5 x 10^5	2.1 x 10^6	4.9 x 10^5	6.4 x 10^1	8.8 x 10^5	6.4 x 10^5	7.6 x 10^4	8.1 x 10^3	2.3 x 10^3	7.6 x 10^4	5.0 x 10^3	1.4 x 10^2	2.4 x 10^3	3.8 x 10^3	8.6 x 10^2	2.8 x 10^4	1.7 x 10^4	7.2 x 10^4	1.0 x 10^3	†	1.4 x 10^4	7.4 x 10^3
7/Tabun	2.3 x 10^3	4.6 x 10^3	1.0 x 10^2	†	5.2 x 10^2	2.8 x 10^2	1.3 x 10^2	5.2 x 10^2	†	1.3 x 10^2	3.8 x 10^2	†	†	1.6 x 10^2	†	1.3 x 10^3	1.5 x 10^2	2.8 x 10^2	5.4 x 10^1	2.5 x 10^1	3.1 x 10^1	†
8/VX	6.9 x 10^5	2.2 x 10^6	1.3 x 10^5	2.6 x 10^3	1.4 x 10^5	1.6 x 10^5	8.1 x 10^4	1.4 x 10^6	2.7 x 10^3	2.0 x 10^5	3.6 x 10^5	1.2 x 10^4	8.5 x 10^4	1.2 x 10^5	1.0 x 10^5	2.6 x 10^5	2.3 x 10^5	1.4 x 10^5	4.5 x 10^5	1.0 x 10^5	1.4 x 10^5	1.3 x 10^5
9/Sarin	5.2 x 10^5	1.3 x 10^6	9.4 x 10^4	4.4 x 10^3	1.1 x 10^5	7.7 x 10^4	4.6 x 10^4	1.2 x 10^6	4.5 x 10^3	1.7 x 10^5	6.3 x 10^5	2.6 x 10^4	1.4 x 10^5	2.2 x 10^5	1.6 x 10^5	6.7 x 10^5	4.8 x 10^5	3.0 x 10^5	1.1 x 10^6	1.9 x 10^5	4.3 x 10^5	4.9 x 10^5
10/Russian-VX	6.7 x 10^5	2.1 x 10^6	1.8 x 10^5	7.9 x 10^3	1.3 x 10^5	3.5 x 10^4	9.3 x 10^4	1.9 x 10^6	1.7 x 10^4	3.5 x 10^5	1.7 x 10^6	7.6 x 10^4	3.5 x 10^5	6.0 x 10^5	4.5 x 10^5	1.5 x 10^6	8.8 x 10^5	7.2 x 10^5	5.1 x 10^6	1.4 x 10^5	2.1 x 10^6	1.9 x 10^6
11/Soman	1.6 x 10^4	5.7 x 10^3	8.8 x 10^2	ND	9.7 x 10^2	3.0 x 10^2	1.7 x 10^2	3.4 x 10^3	†	8.1 x 10^3	6.3 x 10^5	7.1 x 10^2	1.8 x 10^3	7.2 x 10^3	1.2 x 10^3	4.9 x 10^3	2.3 x 10^3	1.5 x 10^3	7.8 x 10^4	1.9 x 10^3	1.3 x 10^4	1.3 x 10^4
12/Cyclosarin	1.1 x 10^4	4.7 x 10^5	4.4 x 10^4	1.7 x 10^3	4.6 x 10^4	2.2 x 10^4	1.1 x 10^4	4.4 x 10^5	3.1 x 10^3	1.5 x 10^5	9.7 x 10^5	5.4 x 10^4	2.0 x 10^5	3.8 x 10^5	1.3 x 10^5	2.0 x 10^5	1.9 x 10^5	2.1 x 10^5	6.9 x 10^5	2.9 x 10^4	2.3 x 10^6	2.8 x 10^6

Grey boxes highlight k_{cat} values higher than for S5a. The errors for all values are of 10% (not shown).

Table 37. Change of specificities relative to 2/Parathion analogue.

			Select PTE Variants																		
Analogue of	**wt**	**S5a**	**A**	**B**	**C**	**D**	**E**	**F**	**G**	**H**	**I**	**J**	**K**	**L**	**M**	**N**	**O**	**P**	**Q**	**R**	**S**	**T**
Paraoxon	9.5	7.6	1.7	0.66	0.43	0.75	0.62	5.0	0.004	10.8	6.1	1.7	2.1	8.1	4.1	0.2	0.3	0.3	2.5	0.2	0.3	0.1
1/Methyl-parathion	0.059	0.11	0.62	0.45	0.19	0.20	0.10	0.94	0.31	0.03	0.76	3.6	0.77	0.6	0.6	5.6	1.3	0.9	44.0	215.3	3.7	4.3
3/Methyl-paraoxon	0.033	0.08	0.37	1.3	0.47	0.15	0.07	8.7	0.08	0.54	21.3	5.0	2.3	12.1	20.6	1.5	1.2	0.6	31.9	61.4	1.9	3.1
4/Paraoxon	0.241	0.079	26.1	19.7	13.6	11.80	13.6	94.8	2.8	26.5	189.8	20.1	250.5	97.9	115.0	2.8	3.1	4.1	47.0	4.1	13.9	10.4
5/DFP	0.020	0.09	3.4	0.22	2.6	1.2	0.11	0.18	0.17	1.8	0.66	0.12	0.72	0.7	0.55	0.1	0.2	0.3	0.5	†	2.0	1.8
7/Tabun	$1x10^{-4}$	$2x10^{-4}$	0.33	†	0.70	0.25	0.08	5.5	†	1.4	22.3	†	†	15.0	†	2.4	0.7	0.5	10.9	27.0	2.0	†
8/VX	0.031	0.1	0.82	8.4	0.40	0.29	0.11	30.1	0.19	4.5	44.1	10.0	24.0	23.8	61.0	1.0	2.1	0.5	183.3	227.7	18.6	28.0
9/Sarin	0.024	0.06	1.0	23.6	0.51	0.24	0.11	43.7	0.5	6.6	129.2	37.0	68.3	70.9	156.5	4.3	7.3	1.7	746.4	683.0	99.1	182.1
10/Russian-VX	0.030	0.09	1.2	27.3	0.37	0.07	0.14	43.0	1.2	8.4	224.7	69.0	104.0	125.4	281.0	5.9	8.5	2.6	2222.0	318.8	303.0	458.0
11/Soman	0.001	$3x10^{-4}$	2.2	†	1.1	0.22	0.09	28.9	†	74.0	302.6	238.7	202.4	552.9	276.9	7.4	8.4	2.0	12712	1624.9	675.3	1178.3
12/Cyclosarin	0.005	0.02	1.4	25.8	0.60	0.19	0.07	45.8	1.0	16.5	560.5	216.3	265.9	349.4	378.9	3.7	8.3	3.4	1345.0	296.7	1487.8	2986.4

† No detection. The changes in grey tone from light to dark, indicate 10-fold increases in the selectivity values. The horizontal dashed box indicates phosphonate substrates.

Table 38. Change of specificities relative to 1/Methyl-parathion

	Selected PTE variants																				
Analogue of	**wt**	**S5a**	**A**	**B**	**C**	**D**	**E**	**F**	**G**	**H**	**I**	**J**	**K**	**L**	**M**	**N**	**O**	**P**	**Q**	**R**	**S**	**T**
Pxn	161.5	71.0	2.7	1.4	2.2	3.6	5.8	5.3	0.01	281.4	7.9	0.46	2.7	13.2	6.5	0.04	0.25	0.36	0.05	0.001	0.07	0.03
2/Parathion	16.9	9.1	1.5	2.1	5.1	4.8	9.4	1.0	3.1	25.9	1.3	0.27	1.2	1.6	1.5	0.18	0.76	1.0	0.02	0.005	0.27	0.23
3/Methyl-paraoxon	0.55	0.74	0.60	2.9	2.4	0.75	0.70	9.2	0.27	14.08	27.8	1.38	2.9	19.8	32.3	0.26	0.88	0.60	0.72	0.28	0.51	0.72
4/Paraoxon	4.0	0.72	41.6	43.0	69.5	56.9	129.4	100.3	9.2	689.1	247.8	5.48	321.7	159.1	179.9	0.50	2.3	4.3	1.0	0.01	3.7	2.4
5/DFP	0.34	0.84	5.5	0.48	13.9	6.2	1.1	0.19	0.55	48.9	0.86	0.03	0.92	1.2	0.86	0.02	0.12	0.28	0.01	†	0.55	0.41
7/Tabun	0.002	0.002	0.52	†	3.5	1.2	0.84	5.8	†	37.8	29.1	†	†	24.5	†	0.42	0.51	0.50	0.24	0.12	0.54	†
8/VX	0.53	0.91	1.3	18.3	2.0	1.4	1.1	31.8	0.60	118.0	57.6	2.7	30.8	38.9	95.4	0.18	1.6	0.51	4.1	1.0	5.0	6.4
9/Sarin	0.40	0.54	1.6	51.4	2.6	1.1	1.0	46.2	1.6	171.7	168.7	10.0	87.7	115.8	244.9	0.77	5.5	1.8	16.9	3.1	26.7	42.0
10/Russian-VX	0.51	0.85	1.9	59.6	1.9	0.33	1.3	45.4	3.9	220.0	293.4	18.7	133.6	204.8	439.5	1.0	6.5	2.7	50.5	1.4	81.7	105.8
11/Soman	0.01	0.002	3.6	†	5.4	1.0	0.93	30.6		1918.6	395.1	65.0	259.9	902.8	433.2	1.3	6.4	2.1	289.1	7.5	182.1	272.3
12/Cyclosarin	0.08	0.19	2.1	56.3	3.0	0.93	0.70	48.3	3.2	428.9	731.9	58.8	341.5	570.6	592.7	0.67	6.3	3.6	30.5	1.3	401.2	690.3

† No detection. The changes in grey tone from light to dark, indicate 10-fold increases in the selectivity values. The horizontal dashed box indicates phosphonate substrates.

Table 39. Change of specificities relative to 3/Methyl-paraoxon

	Selected PTE Variants																				
Analogue of	**wt**	**S5a**	**A**	**B**	**C**	**D**	**E**	**F**	**G**	**H**	**I**	**J**	**K**	**L**	**M**	**N**	**O**	**P**	**Q**	**R**	**S**	**T**
Paraoxon	291.6	96.3	4.5	0.49	0.91	4.8	8.7	0.58	0.6	19.9	0.28	†	0.94	0.66	0.20	0.16	0.28	0.59	0.07	0.01	0.14	0.05
1/Methyl-parathion	1.8	1.4	1.6	0.34	0.41	1.3	1.8	0.10	3.6	0.07	0.03	†	0.33	0.05	0.03	3.7	1.1	1.6	1.3	3.5	1.9	1.3
2/Parathion	30.5	12.4	2.6	0.74	2.0	6.4	13.7	0.11	11.7	1.8	0.04	†	0.43	0.08	0.04	0.67	0.86	1.5	0.03	0.01	0.52	0.31
4/Paraoxon	7.3	0.98	69.4	14.8	28.5	75.6	183.5	10.8	34.9	48.9	8.9	†	108.1	8.0	5.5	1.8	2.7	7.1	1.4	0.06	7.2	3.3
5/DFP	0.62	1.1	9.2	0.16	5.5	8.2	1.5	0.02	2.0	3.4	0.03	†	0.31	0.06	0.02	0.07	0.14	0.46	0.01	†	1.0	0.56
7/Tabun	0.003	0.003	0.87	†	1.4	1.6	1.1	0.60	†	2.6	1.7	†	†	1.2	†	1.5	0.58	0.82	0.34	0.43	1.0	†
8/VX	0.95	1.2	2.8	6.3	0.83	1.9	1.5	3.1	2.2	8.3	2.0	†	10.3	1.9	2.9	0.67	1.8	0.84	5.7	3.7	9.6	8.9
9/Sarin	0.72	0.74	2.7	17.6	1.0	1.5	1.5	4.9	6.1	12.1	6.0	†	29.4	5.8	7.5	2.8	6.3	3.0	23.4	11.1	51.4	57.9
10/Russian-VX	0.93	1.2	3.6	20.4	0.78	0.44	1.9	4.9	14.3	15.6	10.3	†	44.9	10.3	13.5	3.9	7.4	4.5	69.7	5.1	157.4	145.6
11/Soman	0.02	0.003	6.5	†	2.2	1.4	1.3	3.3	†	136.7	14.1	†	87.3	45.4	13.4	4.9	7.3	3.4	399.1	26.4	350.7	374.8
12/Cyclosarin	0.15	0.26	3.6	19.5	1.2	1.2	1.0	5.2	11.8	30.1	26.7	†	114.2	28.7	18.3	2.5	7.1	5.9	42.2	4.8	772.9	949.9

† No detection. The changes in grey tone from light to dark, indicate 10-fold increases in the selectivity values. The horizontal dashed box indicates phosphonate substrates.

Table 40. Change of substrate selectivity in PTE-H.

Substrate	Pxn	**1**/ MPthn	**2**/ Parathion	**3**/ MPxn	**4**/ Paraoxon	**5**/ DFP	**7**/ Tabun	**8**/ VX	**9**/ Sarin	**10**/ RussianVX	**11**/ Soman	**12**/ Cyclosarin
Paraoxon	1	281.41	10.86	19.98	0.41	5.75	7.44	2.38	1.64	1.28	0.15	0.66
1/Methyl-parathion	4×10^{-3}	1	0.04	0.07	1×10^{-3}	0.02	0.03	0.01	0.01	5×10^{-3}	5×10^{-4}	$2. \times 10^{-3}$
2/Parathion	0.09	25.91	1	1.84	0.04	0.53	0.68	0.22	0.15	0.12	0.01	0.06
3/Methyl-paraoxon	0.05	14.09	0.54	1	0.02	0.29	0.37	0.12	0.08	0.06	0.01	0.03
4/Paraoxon	2.45	689.13	26.60	48.92	1	14.07	18.21	5.84	4.01	3.13	0.36	1.61
5/DFP	0.17	48.97	1.89	3.48	0.07	1	1.29	0.41	0.29	0.22	0.03	0.11
7/Tabun	0.13	37.85	1.46	2.69	0.05	0.77	1	0.32	0.22	0.17	0.02	0.09
8/VX	0.42	118.09	4.56	8.38	0.17	2.41	3.12	1	0.69	0.54	0.06	0.28
9/Sarin	0.61	171.76	6.63	12.19	0.25	3.51	4.54	1.45	1	0.78	0.09	0.40
10/Russian-VX	0.78	220.03	8.49	15.62	0.32	4.49	5.81	1.86	1.28	1	0.11	0.51
11/Soman	6.82	1918.69	74.06	136.22	2.78	39.18	50.69	16.25	11.17	8.72	1	4.47
12/Cyclosarin	1.52	428.91	16.56	30.45	0.62	8.76	11.33	3.63	2.50	1.95	0.22	1

† No detection. The changes in grey tone from light to dark, indicate 10-fold increases in the selectivity values. The horizontal dashed box indicates phosphonate substrates.

Table 41. Change of specificities in PTE-E relative to S5a.

Substrate	*Pxn*	**1**/ MPthn	**2**/ Parathion	**3**/ MPxn	**4**/ Paraoxon	**5**/ DFP	**7**/ Tabun	**8**/ VX	**9**/ Sarin	**10**/ RussianVX	**11**/ Soman	**12**/ Cyclosarin
Paraoxon	1	5.8	0.62	8.3	0.04	5.2	6.9	5.3	5.5	4.3	6.3	8.1
1/Methyl-parathion	0.17	1	0.10	1.4	0.00	0.89	1.1	0.90	0.94	0.74	1.0	1.4
2/Parathion	1.6	9.4	1	13.4	0.07	8.4	11.2	8.5	8.9	7.0	10.1	13.3
3/Methyl-paraoxon	0.12	0.70	0.07	1	0.005	0.63	0.8	0.63	0.66	0.52	0.75	0.9
4/Paraoxon	21.9	129.4	13.6	183.5	1	116.0	153.5	117.2	121.9	96.2	138.7	182.9
5/DFP	0.18	1.1	0.11	1.5	0.009	1	1.3	1.0	1.0	0.82	1.1	1.5
7/Tabun	0.14	0.84	0.08	1.1	0.007	0.75	1	0.76	0.79	0.62	0.90	1.1
8/VX	0.18	1.1	0.11	1.5	0.009	0.99	1.3	1	1.0	0.82	1.1	1.5
9/Sarin	0.18	1.0	0.11	1.5	0.008	0.95	1.2	0.96	1	0.78	1.1	1.5
10/Russian-VX	0.22	1.3	0.14	1.9	0.01	1.2	1.5	1.2	1.2	1	1.4	1.9
11/Soman	0.15	0.93	0.09	1.3	0.007	0.83	1.1	0.84	0.8	0.69	1	1.3
12/Cyclosarin	0.12	0.70	0.07	1.0	0.005	0.63	0.8	0.64	0.66	0.52	0.75	1

† No detection. The changes in grey tone from light to dark, indicate 10-fold increases in the selectivity values. The horizontal dashed box indicates phosphonate substrates..

Table 42. Change of substrate selectivity in PTE-Q.

Substrate	Pxn	**1**/ MPthn	**2**/ Parathion	**3**/ MPxn	**4**/ Paraoxon	**5**/ DFP	**7**/ Tabun	**8**/ VX	**9**/ Sarin	**10**/ RussianVX	**11**/ Soman	**12**/ Cyclosarin
Paraoxon	1	0.056	2.4	0.07	0.05	5.2	0.22	0.01	0.003	0.001	1.9E-04	0.002
1/Methyl-parathion	17.8	1	43.3	1.3	0.93	94.4	4.0	0.24	0.05	0.02	0.003	0.03
2/Parathion	0.40	0.023	1	0.03	0.02	2.1	0.09	0.005	0.001	4.5×10^{-4}	7.9E-05	0.001
3/Methyl-paraoxon	12.9	0.724	31.8	1	0.67	68.4	2.9	0.17	0.04	0.01	0.003	0.02
4/Paraoxon	19.0	1.068	46.9	1.4	1	100.9	4.3	0.25	0.06	0.02	0.004	0.03
5/DFP	0.18	0.011	0.46	0.01	0.01	1	0.04	0.00	0.001	2.1×10^{-4}	3.7×10^{-5}	3.5×10^{-4}
7/Tabun	4.4	0.247	10.8	0.34	0.23	23.3	1	0.05	0.01	0.005	0.001	0.00
8/VX	74.4	4.16	183.2	5.7	3.9	393.7	16.8	1	0.24	0.08	0.014	0.13
9/Sarin	303.3	16.9	746.3	23.4	15.8	1603.8	68.7	4.0	1	0.33	0.05	0.55
10/Russian-VX	903.2	50.5	2222.0	69.7	47.3	4774.7	204.7	12.1	2.9	1	0.17	1.6
11/Soman	5167.3	289.1	12712.1	399.1	270.6	27316.1	1171.3	69.3	17.0	5.7	1	9.4
12/Cyclosarin	546.7	30.5	1345.0	42.2	28.6	2890.2	123.9	7.3	1.8	0.60	0.1	1

† No detection. The changes in grey tone from light to dark, indicate 10-fold increases in the selectivity values. The horizontal dashed box indicates phosphonate substrates.

References

(1970). "IUPAC-IUB Combined Commission on Biochemical Nomenclature; Abbreviations and Symbols for Chemical Names of Special Interest in Biological Chemistry; Revised Tentative Rules (1965)." Arch Biochem Biophys **136**(1): 1-12.

Aharoni, A., L. Gaidukov, et al. (2005). "The 'evolvability' of promiscuous protein functions." Nat Genet **37**(1): 73-6.

Aharoni, A., L. Gaidukov, et al. (2004). "Directed evolution of mammalian paraoxonases PON1 and PON3 for bacterial expression and catalytic specialization." Proc Natl Acad Sci U S A **101**(2): 482-7.

Arnold, F. H. (1998). "When blind is better: protein design by evolution." Nat Biotechnol **16**(7): 617-8.

Arnold, F. H., P. L. Wintrode, et al. (2001). "How enzymes adapt: lessons from directed evolution." Trends Biochem Sci **26**(2): 100-6.

ATSDR, A. f. T. S. a. D. R. (2002). Managing Hazardous Materials Incidents. Volume III - Medical Management Guidelines for Acute Chemical Exposures: Nerve Agents (GA, GB, GD, VX). Atlanta, GA. U.S., Department of Health and Human Services, Public Health Service.

Aubert, S. D., Y. Li, et al. (2004). "Mechanism for the hydrolysis of organophosphates by the bacterial phosphotriesterase." Biochemistry **43**(19): 5707-15.

Bajgar, J. (2004). "Organophosphates/nerve agent poisoning: mechanism of action, diagnosis, prophylaxis, and treatment." Adv Clin Chem **38**: 151-216.

Bajgar, J. (2004). "Prophylaxis against organophosphorus poisoning." J Med Chem Def **1**: 1-16.

Bell, A. J., J. Murrell, et al. (2001). "Fragmentation and reactions of two isomeric O-alkyl S-(2-dialkylamino)ethyl methylphosphonothiolates studied by electrospray ionization/ion trap mass spectrometry." J Am Soc Mass Spectrom **12**(8): 902-10.

Benning, M. M., S. B. Hong, et al. (2000). "The binding of substrate analogs to phosphotriesterase." J Biol Chem **275**(39): 30556-60.

Benning, M. M., J. M. Kuo, et al. (1994). "Three-dimensional structure of phosphotriesterase: an enzyme capable of detoxifying organophosphate nerve agents." Biochemistry **33**(50): 15001-7.

Benning, M. M., J. M. Kuo, et al. (1995). "Three-dimensional structure of the binuclear metal center of phosphotriesterase." Biochemistry **34**(25): 7973-8.

Benning, M. M., H. Shim, et al. (2001). "High resolution X-ray structures of different metal-substituted forms of phosphotriesterase from Pseudomonas diminuta." Biochemistry **40**(9): 2712-22.

Bernath, K., M. Hai, et al. (2004). "In vitro compartmentalization by double emulsions: sorting and gene enrichment by fluorescence activated cell sorting." Anal Biochem **325**(1): 151-7.

Billecke, S., D. Draganov, et al. (2000). "Human serum paraoxonase (PON1) isozymes Q and R hydrolyze lactone and cyclic carbonate esters." Drug Metab Dispos **28**: 1335-1342.

Bittker, J. A., B. V. Le, et al. (2004). "Directed evolution of protein enzymes using nonhomologous random recombination." Proc Natl Acad Sci U S A **101**(18): 7011-6.

Black, R. M. and J. M. Harrison, Eds. (1996). The Chemistry of Organophosphorus Chemical Warfare Agents. The Chemistry of Organophosphorus Compounds. Chichester, Jonh Wiley & Sons.

Branden, C. and J. Tooze (1991). Introduction to Protein Structure. New York and London, Garland Publishing, Inc.

Briggs, G. E. and J. B. S. Haldane (1925). "A note on the kinetics of enzyme action." Biochem J **19**: 338-.

Briseño-Roa, L., J. Hill, et al. (2004). "Analogues with fluorescent leaving groups for screening and selection of enzymes which efficiently hydrolyse organophosphorus nerve agents." In preparation.

Brown, A. J. (1892). "Influence of oxygen and concentration on alcohol fermentation." J. Chem. Soc. **61**: 369-385.

Brown, A. J. (1902). "Enzyme action." J. Chem. Soc. **81**: 373-386.

Buchbinder, J. L., R. C. Stephenson, et al. (1998). "Biochemical characterization and crystallographic structure of an Escherichia coli protein from the phosphotriesterase gene family." Biochemistry **37**(15): 5096-106.

Bullock, W. O., J. M. Fernandez, et al. (1987). "XL1-Blue: A high efficiency plasmid transforming recA Escherichia coli strain with beta-galactosidase selection." Biotechniques **5**: 376-378.

Cadwell, R. C. and G. F. Joyce (1994). "Mutagenic PCR." PCR Methods Appl **3**(6): S136-40.

Caldwell, S. R., J. R. Newcomb, et al. (1991). "Limits of diffusion in the hydrolysis of substrates by the phosphotriesterase from Pseudomonas diminuta." Biochemistry **30**(30): 7438-44.

Casadaban, M. J. and S. N. Cohen (1980). "Analysis of gene control signals by DNA fusion and cloning in Escherichia coli." J Mol Biol **138**(2): 179-207.

Castle, L. A., D. L. Siehl, et al. (2004). "Discovery and directed evolution of a glyphosate tolerance gene." Science **304**: 1151-1154.

Chae, M. Y., G. A. Omburo, et al. (1995). "Utilization of copper as a paramagnetic probe for the binuclear metal center of phosphotriesterase." Arch Biochem Biophys **316**(2): 765-72.

Chang, F. C., B. E. Hoffman, et al. (2002). "Pharmacological antagonism of lethal effects induced by O-isobutyl S-[2-(diethylamino)ethyl]methylphosphonothioate." Drug Chem Toxicol **25**(3): 321-37.

Chaudry, G. R., A. N. Ali, et al. (1988). "Isolation of a methyl parathion-degrading Pseudomonas sp that possesses DNA homologous to the opd gene from a Flavobacterium sp." Appl Environ Microbiol **54**(288-293).

Chen-Goodspeed, M., M. A. Sogorb, et al. (2001). "Structural determinants of the substrate and stereochemical specificity of phosphotriesterase." Biochemistry **40**(5): 1325-31.

Chen-Goodspeed, M., M. A. Sogorb, et al. (2001). "Enhancement, relaxation, and reversal of the stereoselectivity for phosphotriesterase by rational evolution of active site residues." Biochemistry **40**(5): 1332-9.

Chiang, C. M. and R. G. Roeder (1993). "Expression and purification of general transcription factors by FLAG epitope-tagging and peptide elution." Pept Res **6**(2): 62-4.

Chin, J. W. and T. J. Magliery (in preparation). Protein Expression by Expansion of the Genetic Code.

Copley, R. R. and P. Bork (2000). "Homology among (betaalpha)(8) barrels: implications for the evolution of metabolic pathways." J Mol Biol **303**(4): 627-41.

Copley, S. D. (2003). "Enzymes with extra talents: moonlighting functions and catalytic promiscuity." Curr Opin Chem Biol **7**(2): 265-72.

Dave, K. I., C. Lauriano, et al. (1994). "Expression of organophosphate hydrolase in the filamentous fungus Gliocladium virens." Appl Microbiol Biotechnol **41**(3): 352-8.

Davies, H. G., R. J. Richter, et al. (1996). "The effect of the human serum paraoxonase polymorphism is reversed with diazoxon, soman and sarin." Nat Genet **14**(3): 334-6.

Dear, P. H. (1999). Codon Controller. Cambridge.

DeFrank, J. J. and T. C. Cheng (1991). "Purification and properties of an organophosphorus acid anhydrase from a halophilic bacterial isolate." J Bacteriol **173**(6): 1938-43.

Delano, W. L. (2004). The PyMOL Molecular Graphics System. San Carlos, CA, USA, DeLano Scientific LLC.

diSioudi, B., J. K. Grimsley, et al. (1999). "Modification of near active site residues in organophosphorus hydrolase reduces metal stoichiometry and alters substrate specificity." Biochemistry **38**(10): 2866-72.

Dodd, R. B., M. D. Allen, et al. (2004). "Solution structure of the kaposi's sarcoma-associated herpesvirus K3 N-terminal domain reveals a novel E2-binding C4HC3-type RING domain." J Biol Chem.

Draganov, D. and B. N. La Du (2004). "Pharmacogenetics of paraoxonases: a brief review." Naunyn-Schmiedeberg's Arch Pharmacol **369**: 78-88.

Dumas, D. P., S. R. Caldwell, et al. (1989). "Purification and properties of the phosphotriesterase from Pseudomonas diminuta." J Biol Chem **264**(33): 19659-65.

Dumas, D. P., H. D. Durst, et al. (1990). "Inactivation of organophosphorus nerve agents by the phosphotriesterase from Pseudomonas diminuta." Arch Biochem Biophys **277**(1): 155-9.

Duncan, E. J., A. Brown, et al. (2002). "Site-specific percutaneous absorption of methyl salicylate and VX in domestic swine." J Appl Toxicol **22**(3): 141-8.

Durrington, P. N., B. Mackness, et al. (2001). "Paraoxonase and Atherosclerosis." Arterioscler Thromb Vasc Biol **21**: 473-480.

Estelle, M., J. Hanks, et al. (1985). "Site-specific mutagenesis of ribulose-1,5-bisphosphate carboxylase/oxygenase. Evidence that carbamate formation at Lys 191 is required for catalytic activity." J Biol Chem **260**(17): 9523-6.

Farber, G. K. and G. A. Petsko (1990). "The evolution of alpha/beta barrel enzymes." Trends Biochem Sci **15**(6): 228-34.

Fernandez, A., D. Tawfik, et al. (2005). "Protein promiscuity: drug resistance and native functions -- HIV-1 case." J Biomol Struct Dyn **22**(6): 615-624.

Fersht, A. (1974). "Catalysis, binding and enzyme-substrate complementarity." Proc R Soc **B187**: 397-401.

Fersht, A. (1999). Structure and mechanism in protein science. New York, W.H. Freeman and Company.

Fest, C. and K. J. Schmidt (1973). The Chemistry of Organophosphorus Pesticides. Berlin/Heidelberg/NY, Springer-Verlag.

Fiedler, S. and R. Wirth (1988). "Transformation of bacteria with plasmid DNA by electroporation." Anal Biochem **170**(1): 38-44.

Field, J., J. Nikawa, et al. (1988). "Purification of a RAS-responsive adenylyl cyclase complex from Saccharomyces cerevisiae by use of an epitope addition method." Mol Cell Biol **8**(5): 2159-65.

Galtier, N. and M. Gouy Phylo_Win. A Graphic Tool for Phylogenetic Inference. Lyon, Montpellier.

Gerlt, J. A. and F. M. Raushel (2003). "Evolution of function in (beta/alpha)8-barrel enzymes." Curr Opin Chem Biol **7**(2): 252-64.

Gill, I. and A. Ballesteros (2000). "Degradation of organophosphorous nerve agents by enzyme-polymer nanocomposites: efficient biocatalytic materials for personal protection and large-scale detoxification." Biotechnol Bioeng **70**(4): 400-10.

Glieder, A., E. T. Farinas, et al. (2002). "Laboratory evolution of a soluble, self-sufficient, highly active alkane hydroxylase." Nat Biotechnol **20**(11): 1135-9.

Gonzalez-Blasco, G., J. Sanz-Aparicio, et al. (2000). "Directed evolution of beta -glucosidase A from Paenibacillus polymyxa to thermal resistance." J Biol Chem **275**(18): 13708-12.

Gopal, S., V. Rastogi, et al. (2000). "Mutagenesis of organophosphorus hydrolase to enhance hydrolysis of the nerve agent VX." Biochem Biophys Res Commun **279**(2): 516-9.

Gould, S. M. and D. Tawfik (2005). "Directed evolution of the promiscuous esterase activity of carbonic anhydrase II." Biochemistry **44**(14): 54444-54452.

Griffiths, A. D. and D. S. Tawfik (2003). "Directed evolution of an extremely fast phosphotriesterase by in vitro compartmentalization." Embo J **22**(1): 24-35.

Griffths, A. D. and D. S. Tawfik (2000). "Man-made enzymes - from design to in vitro compartamentalisation." Curr Opin Biotechnol **11**: 338-353.

Guex, N., M. C. Peitsch, et al. (2001). Deep View / Swiss-Pdb Viewer, GlaxoSmithKline.

Gunderson, C. H., C. R. Lehmann, et al. (1992). "Nerve agents: a review." Neurology **42**(5): 946-50.

Hall, T. (1999). "BioEdit: a user-friendly biological sequence aligment editor and analysis program for Windows 95/98/NT." Nucleic Acids Symp Ser **41**: 95-98.

Hardin, C. C. e. a. (2001). Cloning, Gene Expression and Protein Purification: Experimental Procedures and Process Rationale, Oxford University Press.

Harel, M., A. Aharoni, et al. (2004). "Structure and evolution of the serum paraoxonase family of detoxifying and anti-atherosclerotic enzymes." Nat Struct Mol Biol **11**(5): 412-9.

Harel, M., I. Schalk, et al. (1993). "Quaternary ligand binding to aromatic residues in the active-site gorge of acetylcholinesterase." Proc Natl Acad Sci U S A **90**(19): 9031-5.

Harper, L. L., C. S. McDaniel, et al. (1988). "Dissimilar plasmids isolated from Pseudomonas diminuta MG and a Flavobacterium sp. (ATCC 27551) contain identical opd genes." Appl Environ Microbiol **54**(10): 2586-9.

Hegyi, H. and M. Gerstein (1999). "The relationship between protein structure and function: a comprehensive survey with application to the yeast genome." J Mol Biol **288**(1): 147-64.

Hermes, J. D., S. M. Parekh, et al. (1989). "A reliable method for random mutagenesis: the generation of mutant libraries using spiked oligodeoxyribonucleotide primers." Gene **84**(1): 143-51.

Higgins, S. J. and B. D. Hames, Eds. (1999). Protein Expression: A Practical Approach. Practical Approach Series, Oxford University Press.

Hill, C. M., W.-S. Li, et al. (2003). "Enhanced degradation of chemical warfare agents through molecular engieering of the phosphotriesterase active site." J. Am. Chem. Soc. **125**: 8990-8991.

Hiraga, K. and F. H. Arnold (2003). "General method for sequence-independent site-directed chimeragenesis." J Mol Biol **330**(2): 287-96.

Holm, L. and C. Sander (1997). "An evolutionary treasure: unification of a broad set of amidohydrolases related to urease." Proteins **28**(1): 72-82.

Hong, S. B., J. M. Kuo, et al. (1995). "CO2 is required for the assembly of the binuclear metal center of Phosphotriesterase." J Am Chem Soc **117**: 7580-7581.

Hong, S. B. and F. M. Raushel (1999). "Stereochemical constraints on the substrate specificity of phosphotriesterase." Biochemistry **38**(4): 1159-65.

Horne, I., T. D. Sutherland, et al. (2002). "Cloning and expression of the phosphotriesterase gene hocA from Pseudomonas monteilii C11." Microbiology **148**(Pt 9): 2687-95.

Jabri, E., M. B. Carr, et al. (1995). "The crystal structure of urease from Klebsiella aerogenes." Science **268**(5213): 998-1004.

James, L. C. and D. S. Tawfik (2001). "Catalytic and binding poly-reactivities shared by two unrelated proteins: The potential role of promiscuity in enzyme evolution." Protein Sci **10**(12): 2600-7.

James, L. C. and D. S. Tawfik (2003). "Conformational diversity and protein evolution--a 60-year-old hypothesis revisited." Trends Biochem Sci **28**(7): 361-8.

Jensen, R. A. (1976). "Enzyme recruitment in evolution of new function." Annu Rev Microbiol **30**: 409-25.

Jeyaratnam, J. (1990). "Acute pesticide poisoning: a major global health problem." World Health Stat Q **43**(3): 139-44.

Joerger, A. C., S. Mayer, et al. (2003). "Mimicking natural evolution in vitro: an N-acetylneuraminate lyase mutant with an increased dihydrodipicolinate synthase activity." Proc Natl Acad Sci U S A **100**(10): 5694-9.

Josse, D., O. Lockridge, et al. (2001). "The active site of human paraoxonase (PON1)." J Appl Toxicol **21 Suppl 1**: S7-11.

Kapust, R. B. and D. S. Waugh (1999). "Escherichia coli maltose-binding protein is uncommonly effective at promoting the solubility of polypeptides to which it is fused." Protein Sci **8**(8): 1668-74.

Kazlauskas, R. J. (2005). "Enhancing catalytic promiscuity for biocatalysis." Curr Opin Chem Biol **9**(2): 195-201.

Kegler-Ebo, D. M., C. M. Docktor, et al. (1994). "Codon cassette mutagenesis: a general method to insert or replace individual codons by using universal mutagenic cassettes." Nucleic Acids Res **22**(9): 1593-9.

Kent, S. (2004). "Novel forms of chemical protein diversity -- in nature and in the laboratory." Curr Opin Biotechnol **15**(6): 607-14.

Khersonsky, O. and D. Tawfik (2005). "Structure-reactivity studies of serum paraoxonase PON1 suggest that its native activity is lactonase." Biochemistry **44**(16): 6371-6382.

Kuo, J. M., M. Y. Chae, et al. (1997). "Perturbations to the active site of phosphotriesterase." Biochemistry **36**(8): 1982-8.

La Du, B. N. (1992). Human serum paraoxonase/arylesterase. Genetic factors influencing the metabolism of foreign compounds. W. Kallow. New York, Pergamon Press.

Laidler, K. J. (1997). A brief history of enzyme kinetics. New Beer in an Old Bottle: Eduard Buchner and the Growth of Biochemical Knowledge. A. Cornish-Bowden. Valencia, Spain, Univsersitat de Valencia**:** 127-133.

Lang, D., R. Thoma, et al. (2000). "Structural evidence for evolution of the beta/alpha barrel scaffold by gene duplication and fusion." Science **289**(5484): 1546-50.

LeJeune, K. E., A. J. Mesiano, et al. (1997). "Dramatically stabilized phosphotriesterase - polymers for nerve agent degradation." Biotechnol Bioeng **54**: 105-114.

LeJeune, K. E., J. R. Wild, et al. (1998). "Nerve agents degraded by enzymatic foams." Nature **395**(6697): 27-8.

Lewis, V. E., W. J. Donarski, et al. (1988). "Mechanism and stereochemical course at phosphorus of the reaction catalyzed by a bacterial phosphotriesterase." Biochemistry **27**(5): 1591-7.

Li, W., K. T. Lum, et al. (2001). "Stereoselective detoxification of chiral sarin and soman analogues by phosphotriesterase." Bioorg Med Chem **9**(8): 2083-91.

Lloyd, D. (1999). "MICROBIAL ECOLOGY:How to Avoid Oxygen." Science **286**: 249.

Lockridge, O., R. M. Blong, et al. (1997). "A single amino acid substitution, Gly117His, confers phosphotriesterase (organophosphorus acid anhydride hydrolase) activity on human butyrylcholinesterase." Biochemistry **36**(4): 786-95.

Lorimer, G. H. and H. M. Miziorko (1980). "Carbamate formation on the epsilon-amino group of a lysyl residue as the basis for the activation of ribulosebisphosphate carboxylase by CO2 and Mg2+." Biochemistry **19**(23): 5321-8.

Love, A. H., A. L. Vance, et al. (2004). "Investigating the affinities and persistence of VX nerve agent in environmental matrices." Chemosphere **57**(10): 1257-64.

Luger, K., U. Hommel, et al. (1989). "Correct folding of circularly permuted variants of a beta alpha barrel enzyme in vivo." Science **243**(4888): 206-10.

Lundy, P. (2004). "Clinical aspects of percutaneous poisoning by the chemical warfare agent VX: effects of applicaiton site and decontamination." Mil Med **11**: 856-862.

Lusis, A. J. (2000). "Atherosclerosis." Nature **407**(6801): 233-41.

Mackness, B., P. N. Durrington, et al. (1998). "Human serum paraoxonase." Gen Pharmacol **31**(3): 329-36.

Mainfroid, V., K. Goraj, et al. (1993). "Replacing the (beta alpha)-unit 8 of E.coli TIM with its chicken homologue leads to a stable and active hybrid enzyme." Protein Eng **6**(8): 893-900.

Martineau, P., P. Jones, et al. (1998). "Expression of an antibody frament at high levels in the bacterial cytoplasm." J Mol Biol **280**: 117-127.

Matsumura, I. and A. D. Ellington (2001). "In vitro evolution of beta-glucuronidase into a beta-galactosidase proceeds through non-specific intermediates." J Mol Biol **305**(2): 331-9.

May, O., P. T. Nguyen, et al. (2000). "Inverting enantioselectivity by directed evolution of hydantoinase for improved production of L-methionine." Nat Biotechnol **18**(3): 317-20.

McDaniel, C. S., L. L. Harper, et al. (1988). "Cloning and sequencing of a plasmid-borne gene (opd) encoding a phosphotriesterase." J Bacteriol **170**(5): 2306-11.

Merz, A., M. C. Yee, et al. (2000). "Improving the catalytic activity of a thermophilic enzyme at low temperatures." Biochemistry **39**(5): 880-9.

Meyer, A., A. Schmid, et al. (2002). "Changing the substrate reactivity of 2-hydroxybiphenyl 3-monooxygenase from Pseudomonas azelaica HBP1 by directed evolution." J Biol Chem **277**(7): 5575-82.

Michaelis, L. and M. L. Menten (1913). "Kinetik der Invertinwirkung." Biochem. Z. **49**: 333-369.

Microsoft (1999). MIcrosoft Excel 2000, Microsoft Corporation.

Miroux, B. and J. E. Walker (1996). "Over-production of proteins in Escherichia coli: mutant hosts that allow synthesis of some membrane proteins and globular proteins at high levels." J Mol Biol **260**(3): 289-98.

Morita, H., N. Yanagisawa, et al. (1995). "Sarin poisoning in Matsumoto, Japan." Lancet **346**(8970): 290-3.

Mulbry, W. W. and J. S. Karns (1989). "Parathion hydrolase specified by the Flavobacterium opd gene: relationship between the gene and protein." J Bacteriol **171**(12): 6740-6.

Mulbry, W. W., J. S. Karns, et al. (1986). "Identification of a plasmid-borne parathion hydrolase gene from Flavobacterium sp. by southern hybridization with opd from Pseudomonas diminuta." Appl Environ Microbiol **51**(5): 926-30.

Mulchandani, A., W. Chen, et al. (2001). "Biosensors for direct determination of organophosphate pesticides." Biosens Bioelectron **16**(4-5): 225-30.

Munnecke, D. M. (1976). "Enzymatic hydrolysis of organophosphate insecticides, a possible pesticide disposal method." Appl Environ Microbiol **32**: 7-13.

Murzin, A. G., S. E. Brenner, et al. (1995). "SCOP: a structural classification of proteins database for the investigation of sequences and structures." J Mol Biol **247**(4): 536-40.

Nagao, M., T. Takatori, et al. (1997). "Definitive evidence for the acute sarin poisoning diagnosis in the Tokyo subway." Toxicol Appl Pharmacol **144**(1): 198-203.

Naki, D., C. Paech, et al. (1998). "Selection of a subtilisin-hyperproducing Bacillus in highly structured environment." Appl Microbiol Biotechnol **49**: 290-294.

O'Brien, P. J. and D. Herschlag (1999). "Catalytic promiscuity and the evolution of new enzymatic activities." Chem Biol **6**(4): R91-R105.

Okudera, H. (2002). "Clinical features on nerve gas terrorism in Matsumoto." J Clin Neurosci **9**(1): 17-21.

Omburo, G. A., J. M. Kuo, et al. (1992). "Characterization of the zinc binding site of bacterial phosphotriesterase." J Biol Chem **267**(19): 13278-83.

Omburo, G. A., L. S. Mullins, et al. (1993). "Structural characterization of the divalent cation sites of bacterial phosphotriesterase by 113Cd NMR spectroscopy." Biochemistry **32**(35): 9148-55.

OPCW (2005). "Chemical Disarmament - March."

Pace, C. N., F. Vajdos, et al. (1995). "How to measure and predict the molar absorption coefficient of a protein." Protein Sci **4**(11): 2411-23.

Patrick, W. M., A. E. Firth, et al. (2003). "User-friendly algorithms for estimating completeness and diversity in randomized protein-encoding libraries." Protein Eng **16**(6): 451-7.

Phillips, J. P., J. H. Xin, et al. (1990). "Transfer and expression of an organophosphate insecticide-degrading gene from Pseudomonas in Drosophila melanogaster." Proc Natl Acad Sci U S A **87**(20): 8155-9.

Polayes, D. A., A. Goldstein, et al. (1994). "Tev Protease, Recombinant: A Site-Specific Protease For Efficient Cleavage Of Affinity Tags From Expressed Proteins." FOCUS **16**: 1-4.

Proba, K., A. Worn, et al. (1998). "Antibody scFV fragments without disulfide bonds made by molecular evolution." J Mol Biol **275**: 245-253.

Rader, C. and C. F. Barbas, 3rd (1997). "Phage display of combinatorial antibody libraries." Curr Opin Biotechnol **8**(4): 503-8.

Rastogi, V. K., J. J. DeFrank, et al. (1997). "Enzymatic hydrolysis of Russian-VX by organophosphorus hydrolase." Biochem Biophys Res Commun **241**(2): 294-6.

Raushel, F. M. and H. M. Holden (2000). "Phosphotriesterase: an enzyme in search of its natural substrate." Adv Enzymol Relat Areas Mol Biol **74**: 51-93.

Raychaudhuri, S., F. Younas, et al. (1997). "Backbone makes a significant contribution to the electrostatics of alpha/beta-barrel proteins." Protein Sci **6**(9): 1849-57.

Reardon, D. and G. K. Farber (1995). "The structure and evolution of alpha/beta barrel proteins." Faseb J **9**(7): 497-503.

Richins, R. D., A. Mulchandani, et al. (2000). "Expression, immobilization, and enzymatic characterization of cellulose-binding domain-organophosphorus hydrolase fusion enzymes." Biotechnol Bioeng **69**(6): 591-6.

Roodveldt, C. and D. S. Tawfik (2005). "Directed evolution of phosphotriesterase from Pseudomonas diminuta for heterologous expression in Escherichia coli results in stabilization of the metal-free state." Protein Eng Des Sel **18**(1): 51-8.

Russell, R. J., J. M. Ferguson, et al. (1997). "The crystal structure of citrate synthase from the hyperthermophilic archaeon pyrococcus furiosus at 1.9 A resolution." Biochemistry **36**(33): 9983-94.

Russell, R. J., U. Gerike, et al. (1998). "Structural adaptations of the cold-active citrate synthase from an Antarctic bacterium." Structure **6**(3): 351-61.

Sayle, R. (1995). RasWin Molecular Graphics.

Sethunathan, N. and T. Yoshida (1973). "A flavobacterium that degrades diazinon and parathion." Can J Microbiol **19**: 873-875.

Shim, H., S. B. Hong, et al. (1998). "Hydrolysis of phosphodiesters through transformation of the bacterial phosphotriesterase." J Biol Chem **273**(28): 17445-50.

Silverman, J. A., R. Balakrishnan, et al. (2001). "Reverse engineering the (beta/alpha)8 barrel fold." Proc Natl Acad Sci U S A **98**(6): 3092-7.

Smith, A. D. e. a., Ed. (2000). Oxford Dictionary of Biochemistry and Molecular Biology. Oxford, Oxford University Press.

Smith, P. K., R. I. Krohn, et al. (1985). "Measurement of protein using bicinchoninic acid." Anal Biochem **150**(1): 76-85.

Smolen, A., H. W. Eckerson, et al. (1991). "Characteristics of the genetically determined allozymic forms of human serum paraoxonase/arylesterase." Drug Metab Dispos **19**: 107-112.

Stemmer, W. P. (1994). "DNA shuffling by random fragmentation and reassembly: in vitro recombination for molecular evolution." Proc Natl Acad Sci U S A **91**(22): 10747-51.

Studier, F. W., A. H. Rosenberg, et al. (1990). "Use of T7 RNA polymerase to direct expression of cloned genes." Methods Enzymol **185**: 60-89.

Sultatos, L. G. (1994). "Mammalian toxicology of organophosphorus pesticides." J Toxicol Environ Health **43**(3): 271-89.

Taddei, F., M. Radman, et al. (1997). "Role of mutator alleles in adaptive evolution." Nature **387**(6634): 700-2.

Tanaka, T., H. Kimura, et al. (1994). "Characteristics of a de novo designed protein." Protein Sci **3**(3): 419-27.

Taverna, D. M. and R. A. Goldstein (2002). "Why are proteins marginally stable?" Proteins **46**(1): 105-9.

Tawfik, D. S. and A. D. Griffiths (1998). "Man-made cell-like compartments for molecular evolution." Nat Biotechnol **16**(7): 652-6.

Thoden, J. B., G. N. Phillips, Jr., et al. (2001). "Molecular structure of dihydroorotase: a paradigm for catalysis through the use of a binuclear metal center." Biochemistry **40**(24): 6989-97.

Timperley, C. M., Ed. (2000). Highly-Toxic Fluorine Compounds. Fluorine Chemistry at The Millennium - Fascinated by Fluorine. Oxford, Elsevier.

Timperley, C. M., D. J. Sellers, et al. (2001). "Fluorinated phosphorus compounds. Part 4. A lack of anticholinesterase activity for four tris(fluoroalkyl) phosphates." J. Fluorine Chem **107**: 155-158.

Tompa, P. (2002). "Intrinsically unstructured proteins." Trends Biochem Sci **27**(10): 527-33.

Tõugu, V. (2001). "Acetylcholinesterase: Mechanism of catalysis and inhibition." Curr. Med. Chem. – CNSA **1**(2): 155-170.

Vanhooke, J. L., M. M. Benning, et al. (1996). "Three-dimensional structure of the zinc-containing phosphotriesterase with the bound substrate analog diethyl 4-methylbenzylphosphonate." Biochemistry **35**(19): 6020-5.

Vilanova, E. and M. A. Sogorb (1999). "The role of phosphotriesterases in the detoxication of organophosphorus compounds." Critical Reviews In Toxicology **29**(1): 21-57.

Voigt, C. A., C. Martinez, et al. (2002). "Protein building blocks preserved by recombination." Nat Struct Biol **9**(7): 553-8.

Watkins, L. M., H. J. Mahoney, et al. (1997). "Augmented hydrolysis of diisopropyl fluorophosphate in engineered mutants of phosphotriesterase." J Biol Chem **272**(41): 25596-601.

Wierenga, R. K. (2001). "The TIM-barrel fold: a versatile framework for efficient enzymes." FEBS Lett **492**(3): 193-8.

Wilson, D. K., F. B. Rudolph, et al. (1991). "Atomic structure of adenosine deaminase complexed with a transition-state analog: understanding catalysis and immunodeficiency mutations." Science **252**(5010): 1278-84.

Yang, Y. (1999). "Chemical Detoxification of Nerve Agent VX." Acc Chem Res **32**: 109-115.

Yang, Y. C., J. A. Baker, et al. (1992). "Decontamination of Chemical Warfare Agents." Chem Rev **92**(1729-1743).

Yang, Y. C., F. J. Berg, et al. (1997). "Peroxyhydrolysis of nerve agent VX and model compounds and related nucleophilic reactions." J Chem Soc, Perkin Trans **2**: 607-613.

Zaccolo, M., D. M. Williams, et al. (1996). "An approach to random mutagenesis of DNA using mixtures of triphosphate derivatives of nucleoside analogues." J Mol Biol **255**(4): 589-603.

Zhao, H. and F. H. Arnold (1997). "Combinatorial protein design: strategies for screening protein libraries." Curr Opin Struct Biol **7**(4): 480-5.

Mi padre no me aguantaba,
decía muy aburrido:
“¿Qué hacemos con este crío?
¿Lo mandamos a otra tierra?”
Y allá fui yo a Inglaterra
con veintitrés años de nacido.